Summer 8-14-2015

The Role of Glutaminase 1 in HIV-1 Associated Neurocognitive Disorders and in Brain Development

Yi Wang
University of Nebraska Medical Center

The Role of Glutaminase 1 in HIV-1 Associated Neurocognitive Disorders and in Brain Development

By

Yi Wang

A DISSERTATION

Presented to the Faculty of

The Graduate College in the University of Nebraska

In Partial Fulfillment of the Requirements

For the Degree of Doctor of Philosophy

Department of

Pharmacology and Experimental Neuroscience

Under the Supervision of Dr. Jialin Zheng

Medical Center

Omaha, Nebraska

July, 2015

The Role of Glutaminase 1 in HIV-1 Associated Neurocognitive Disorders and in Brain Development

Yi Wang, Ph.D.

University of Nebraska, 2015

Advisor: Jialin Zheng, M.D.

Glutaminase is the enzyme that converts glutamine into glutamate, which serves as a key excitatory neurotransmitter and one of the energy providers for cellular metabolism. Glutamate is essential for proper brain functioning but at excess levels, it is neurotoxic and has a key role in the pathogenesis of various neurodegenerative diseases, including HIV-1 associated neurocognitive disorders (HAND). However, the detailed mechanism of glutamate-mediated neurotoxicity remains unclear. In part I, we identified the regulation of glutaminase 1 (GLS1) in the central nervous system (CNS) of HAND animal models including HIV-Tat transgenic (Tg) mouse and HIVE-SCID mouse, since GLS1 is the dominant isoform of glutaminase in mammalian brains. Interestingly, examinations of both animals revealed an upregulation of GLS1 in correlation with the increase of brain inflammation and cognitive impairment. As our previous data revealed an upregulation of glutaminase C (GAC) in the postmortem brain tissues of patients with HIV dementia by protein analysis, suggesting a critical role of GAC in the instigation of primary dysfunction and subsequent neuronal damage in HAND, thus in part II we hypothesize that GAC dysregulation in brain is sufficient to induce brain inflammation and dementia in relevance to HAND.

Using a brain GAC overexpression mouse model (which has the overexpression of GAC confined in the brain), we found that the expressions of the marker for brain inflammation, the glial fibrillary acidic protein (GFAP), were increased in the brains of GAC-overexpression mice, suggesting increased reactive astrogliosis. To study the functional impact of GAC overexpression, we performed Morris Water Maze (MWM) test and Contextual Fear Conditioning (CFC) test to determine the learning and memory of mice. GAC-overexpression mice perfomed poorer in both tests, indicating that overexpressing GAC in mouse brain impaired the learning and memory of the animals. Moreover, pathological and physiologial examinations revealed synaptic damage and increased apoptosis in Nestin-GAC mouse brain. Together, these data suggest that dysregulated GAC has a causal relationship with prolonged inflammation and dementia relevant to HAND. In part III, we evaluated the feasibility of genetically knocking down GLS1 in CNS to treat HAND using human primary neural progenitor cell (NPC) culture. However, we have found that GLS1 is essential for the survival, proliferation and differentiation of human NPC. This suggests that more-advanced genetic methods capable of targeting GLS1 in specific cell types of CNS ought to be developed for the therapeutic purpose.

In summary, we report that GLS1 is dysregulated in the brains of HAND murine models in correlation with increased brain inflammation and cognitive impairment. Moreover, overexpressed GAC in mouse brains has a causal relationship to prolonged brain inflammation and dementia of these animals,

suggesting a pathologenic role of dysregulated brain GLS1 in relevance to HAND.

TABLE OF CONTENTS

List of Tables and Figures

Abbreviations

Human immunodeficiency virus (HIV)

HIV-1 associated neurocognitive disorders (HAND)

HIV-1 associated dementia (HAD)

Mild neurocognitive disorders (MND)

Asymptomatic neurocognitive impairment (ANI)

Highly active antiretroviral therapy (HAART)

Blood brain barrier (BBB)

HIV-1 encephalitis (HIVE)

Monocyte-derived Macrophages (MDM)

Central nervous system (CNS)

Tumor necrosis factor-α (TNF-α)

Interleukin-1 β (IL-1β)

Glycoprotein 120 (gp120)

HIV *trans* activator of transcription (HIV-Tat)

N-Methyl-D-aspartic acid (NMDA)

Glutaminase 1 (GLS1)

Glutaminase C (GAC)

Kidney-type glutaminase (KGA)

Tricarboxylic acid (TCA)

α-amino-3-hydroxy-5-methyl-4-isoxazolepropionic acid (AMPA)

Macrophage-conditioned medium (MCM)

Transgenic (Tg)

Severe combined immunodeficient (SCID)

Simian immunodeficiency virus (SIV)

Combined antiretroviral therapy (cART)

Cerebrospinal fluid (CSF)

Glial fibrillary acidic protein (GFAP)

Institutional Animal Care and Use Committee (IACUC)

Dulbecco's modified Eagles medium (DMEM)

Macrophage colony stimulating factor (M-CSF)

Morris-Water-Maze (MWM)

Sodium dodecyl sulfate-polyacrylamide gel electrophoresis (SDS-PAGE)

Polyvinyldifluoridene (PVDF)

Analysis of variance (ANOVA)

Wide-type (WT)

Contextual fear conditioning (CFC)

Standard error (SEM)

Green fluorescent protein (GFP)

Polymerase chain reaction (PCR)

Phosphate-buffered saline (PBS)

Paraformaldehyde (PFA)

Terminal deoxynucleotidyl transferase dUTP Nick-end labeling (TUNEL)

Artifical cerebrospinal fluid (ACSF)

Field excitatory postsynaptic potentials (fEPSPs)

Long-term potentiation (LTP)

High-frequency stimulus (HFS)

Reverse transcription polymerase chain reaction (RT-PCR)

Poly ADP ribose polymerase (PARP)

Chapter 1

Introduction

1.1 HIV-1 associated neurocognitive disorders

1.1.1 Clinical manifestations

HIV infection continues to cause substantial morbidities worldwide. Till 2013, 35 million people are living with HIV around the world. HIV-1 infection accounts for more than 90% of the global HIV pandemic, with the fact that fewer than 3 million of the 35 million infections are caused by HIV-2 [1].

HIV-1 associated neurocognitive disorders (HAND) represent a spectrum of cognitive disorders caused by HIV infection. These disorders are characterized by cognitive deteriorations, behavioral disorders and potential progressive motor impairments as a consequence of neuronal damage [2]. These disorders affect up to 50% of HIV-1 infected individuals [3]. HAND comprise three categories based on standardized measures of dysfunction: HIV-1 associated dementia (HAD), mild neurocognitive disorder (MND), and asymptomatic neurocognitive impairment (ANI) [4]. With the effective treatment by highly active antiretroviral therapy (HAART), the occurrence of HAD, the most severe and devastating form of HAND, has dramatically fallen [5]. However, even the incidence of moderate or severe form of HAND, MND and HAD, has largely declined since the introdction of HAART in 1996, the prevalence of HAND remains high (15-50%) [5, 6] with the increase of the life span of HIV-infected individuals [7], emergence of drug-resistant viral mutants [8, 9], compromised blood-brain barrier (BBB) penetration of HAART [10], and sustained HIV infection and virus production in mononuclear phagocytes (macrophages and microglia) of the brain [5, 11]. The high prevalence of the

milder forms of HAND is still significant because cognitive impairment continues to be a commonplace and interferes with everday functioning like employment, finance management, driving, housekeeping and adherence to medications of HIV-infected individuals.

1.1.2 Pathobiology of HAND

The most severe form of HAND, HAD, is a synonym of HIV encephalopathy or AIDS dementia complex [5]. Its pathological correlate is termed HIV-1 encephalitis (HIVE). The pathological characteristics of HIVE include progressive infection within perivascular monocyte-derived macrophages (MDM), the infiltration of MDM into the brain, and often the formation of multinucleated giant cells due to the fusion of HIV-infected MDM [12, 13]. Other pathological features include reactive astrogliosis, diffuse rarefaction of white matter, BBB breakdown, simplification and decrease of synaptic dendrites, and neuronal loss [14-16].

Cognitive impairment in HAND is a consequence of synaptic network damage in basal ganglia, cerebral cortex and hippocampus of HAND patients. Morphometric studies have revealed approximately 40% decreases in the densities of neurons in the frontotemporal cortex [14, 17], and 50% - 90% decreases of neuronal densities in hippocampus [18] before the HAART era. Previous studies with *in situ* hybridization have confirmed that productive HIV-1 infections occur almost exclusively in perivascular MDM [19]. Brain microglia are infected by HIV-1 to a lesser degree while astrocytes are only non-productively

or restrictively infected due to the fact that CD4 is not present on them [20-25]. Neurons are not infected by HIV-1 [20]. Since neurons have the lowest susceptibility to HIV infection among all cells in the central nervous system (CNS), their dysfucntion largely results from HIV infection of nerboring cells. Initially, HIV-infected perivascular macrophages enter into CNS via the broken BBB, bringing HIV that has the ability to infect brain macrophages and microglia. Infection of macrophages and microglia results in production of viral proteins and neurotoxins [26-29] that start to damage synapses, thus disrupt the connections of neuronal network and neurotransmission at first stage. HIV-infected macrophages and microglia can serve as long-lived reservior for the virus production in the brain, leading to progressive neuronal damage [14, 30]. And importantly, those viral proteins released by infected macrophages and microglia activate uninfected macrophages, microglial and astrocytes, resulting in the production of more viral proteins, a variety of proinflammatory molecules and neurotoxins [28, 29, 31, 32], leading to prolonged brain inflammation and further damage to neurons at the second stage [33-37]. Studies have shown that the severity of HAND is significantly associated with the densities of activated brain macrophages, microglia, and astrocytes, and with the expression levels of the neurotoxins secreted by those activated brain cells [38].

1.2 Excitotoxicity

Chronic neuroinflammation is a hallmark of HAND and a constitutive component of the pathogenesis of neurodegenerative diseases including HAND,

multiple sclerosis, amyotrophic lateral sclerosis, Parkinson's disease and Alzheimer's disease [33-35]. Literature have suggested a close link between brain inflammation and neuronal injury [36, 39]. HIV-infected and activated microglia and macrophages instigate brain inflammation and induce neuronal injury through the production and release of various soluble neurotoxic factors including viral proteins [30], platelet activating factor [40-43], proinflammatory cytokines and chemokines [37, 44-47], nitric oxide [48, 49], and excess glutamate [32, 50-52]. Apart from brain macrophages, microglia and astrocytes, neurons play a critical role in the progress of brain inflammation as well. Specifically, proinflammatory cytokines TNF-α and IL-1β, which are typically elevated during neurodegenerative diseases, induced neuronal loss via the production and release of excess glutamate in neuronal culture [53].

Glutamate is the most important excitatory neurotransmitter in mammalian CNS [54, 55]. It is essential for vital physiologic processes including neural development, synaptic plasticity, learning and memory [55-57]. However at excess levels, glutamate has the potential to induce extensive neuronal injury, which is termed excitotoxicity. Excess glutamate causes neuronal damage via overactivation of glutamate receptors. Studies of the neurotoxic effects of viral proteins like HIV-1 coat protein glycoprotein 120 (Gp120) and HIV *trans*-acting protein Tat have revealed that viral proteins induced modification of the kinectics of NMDA receptors located on postsynaptic neruons via stimulating the release of arachidonic acid from infected glial cells [58]. The combination of the increased pool of extracellular glutamate and overactivated NMDA receptors

results in calcium overload within neurons [59]. Calcium is one the most important second messagers in neural signal transduction. Deregulated calcium leads to oxidative stress including production of free radicals and disruption of redox balance, and results in mitochondrial dysfunction, caspase activation and cellular death [60]. Besides, lipid imbalance in neurons has also been associated with calcium overload-induced neuronal dysfunction or death in HAND [59, 61]. The moderate-affinity glutamate receptor antagonist memantine has been reported to have successfully reversed HIV viral protein-induced calcium overload in neurons and substantially protected neurons from apoptosis [62-64].

Therefore, elevated glutamate has been linked to the pathogenic processes of various CNS disorders [65-68] and neurodegenerative diseases including HAND [50, 69, 70].

1.3 Glutaminase 1

In mammalian CNS, glutamate is typically derived from glutamine by the action of an phosphate-activated amidohydrolase named glutaminase (EC 3.5.1.2) [71]. Two different kinds of glutaminase are found in mammals. The predominant glutamine-utilizing and glutamate-producing enzyme in CNS is glutaminase 1 (GLS1), a mitochondrial hetero-tetramer localized on the inner membrane of mitochondria, whereas the isozyme glutaminase 2 (GLS2) is expressed at lower levels [72] in the brain.

GLS1 and GLS2 are encoded by separate genes on different chromosomes [73]. The human *Gls1* gene is on chromosome 2 [74] and has several isoforms due to tissue-specific alternative splicing. Two splice variants of GLS1, glutaminase C (GAC) and kidney-type glutaminase (KGA), are found in mammalian brain tissues [75]. GAC shares the same functional region of KGA and possesses a unique C-terminal [76]. Glutaminase catalyzes the following reaction: Glutamine + H_2O → Glutamate + NH_3. Glutamate is subsequently converted to α-ketoglutarate with the catalysis by glutamate dehydrogenase. The end-product α-ketoglutarate enters into the tricarboxylic acid (TCA) cycle that maintains the energy generation. Therefore, GLS1 plays an essential role in generating neurotransmitter and brain bioenergetics.

In the brain under physiological conditions, GLS1 is expressing at highest levels in neurons and to relatively lesser extents in astrocytes, microglia and macrophages. The expression profile of GLS1 in different cells of the brain is in agreement with the compartmentation of the glutamate-glutamine cycle that is critial for neural signal transmission in CNS.

1.4 Glutamate - glutamine cycle in the brain

There is not a clearly-defined starting point of the glutamate-glutamine cycle. We begin with events that occurred in the presynaptic neurons. In presynaptic neurons, glutamine is converted to glutamate by GLS1 and the newly-produced glutamate is packaged into presynaptic vesicles. The glutamate-filled vesicles are recruited and docked to specialized release sites

that are dense electron regions termed the active zones of presynaptic neurons [77]. Intracellular calcium influxes trigger the release of glutamate-containing vesicles from presynaptic nerve terminals into synaptic cleft via exocytosis [77, 78]. Afterwards, glutamate diffuses across the synaptic cleft and binds to glutamate receptors located on postsynaptic neurons. The binding of glutamate with its receptors alters membrane potential of the postsynaptic neurons and triggers downstream signal transduction cascades. There are two major types of glutamate receptors: the ionotropic glutamate receptors that are ligand-gated ion channels including AMPA, NMDA, kainate and Delta receptors [79]; and the metabotropic glutamate receptors that are G protein-coupled receptors including metaotropic glutamate receptor 1-8 [80].

Glutamate that resides in the synaptic cleft is utilized or removed rapidly via three major ways. First, glutamate is uptaken by postsynaptic neurons for neural signal transmission. Second, some glutamate is reuptaken by presynaptic neurons via glutamate transporters located on neurons. Third, a substantial amount of extra glutamate in synaptic cleft is transported to neighboring astrocytes by glutamate transporters located on astrocytes. As the resting membrane potential of astrocytes is relatively low compared to that of neurons, extracellular glutamate is favorably efficiently uptaken by astrocytes through a sodium-dependent mechanism [81]. Within astrocytes, where the enzyme glutamine synthase is expressing at high levels, the majority of glutamate is converted back to glutamine [82]. The newly-synthesized glutamine is released extracellularly and transported back to neurons by glutamine

transporters [83]. Then in neurons, glutamine is converted to glutamate. With the regeneration of glutamate in neurons, the glutamate-glutamine cycle has "closed".

Importantly, the reaction of deaminating glutamine to produce glutamate by GLS1 is energetically favorable. So GLS1 must be tightly regulated to prevent excess glutamate generation and excitotoxicity [73].

1.5 The possible pathological role of GLS1 in HAND

Although the exact way in which HIV causes HAND remains incompletely understood, GLS1 has been reported to have a crucial role in mediating excitotoxicity. In the past decade our laboratory and others have helped with defining the excitotoxic profile of brain macrophages and microglia. We have developed molecular and chemical tools with explicit intent to understand HAND pathogenesis and to find an effective treatment for HAND. Along with others, we identified that human macrophages and microglia infected by HIV-1 were substantially involved in the generation of excess extracellular glutamate [50, 84]. This generation of excess glutamate represents a major component of macrophage –, or microglia – mediated neurotoxicity [85]. Notably, we have demonstrated that the neuroinflammatory and neurotoxic events of macrophages and microglia infected by HIV-1 are augmented by GLS1 *in vitro* [71, 84, 86]. And importantly, we have determined that GLS1 dysregulation is a key event in neuroinflammation required for excess glutamate generation in

HIV-1 infection – induced neurotoxicity [87, 88]. And interestingly, GLS1 release is involved in extracellular glutamate production [85, 89, 90].

So together we have documented roles of GLS1 in microglia and macrophages in brain injury, infection and inflammation [50, 86, 90] and more recently the regulation and function of GLS1 in neurons under inflammation [53].

1.5.1 Pathogenic role of macrophage GLS1 in HAND

HIV-1-infected macrophages have been reported to be a critial cellular source of extracellular glutamate. In the past decade, we have reported an HIV-1-mediated increase of glutamate generation by MDM [50]. The examination of GLS1 regulation in HIV-1-infected MDM has revealed an isoform-specific upregulation of GAC expression, while the expression of KGA remains largely unchanged. The siRNA targeting GAC in HIV-1-infected MDM has substantially decreased the production of glutamate [90]. In addition, rat cortical neurons treated by macrophage-conditioned medium (MCM) from HIV-1-infected MDM have shown significant toxicity, which, can be largely reversed by removing glutamine from the MCM, antagonizing NMDA receptor, inhibiting GLS1 activity with pharmacological inhibitors, or targeting GAC with siRNA [85]. Together, these studies demonstrate a pathogenic role of macrophage GAC in mediating excitotoxicity and disease progressions of HAND [90].

1.5.2 Pathogenic role of microglial GLS1 in HAND

Microglia are the main cellular targets of HIV-1 infection in CNS. The HIV-1-infected- or immune-activated microglia have been reported to play an important pathogenic role in HAND. Specifically, our laboratory has demonstrated that HIV-1-infected microglia have substantially-increased glutamate production and are largely more neurotoxic than uninfected microglia using a human microglia primary culture system. Consistent with the findings in HIV-1-infected MDM, the examinations of GLS1 RNA and protein levels in HIV-1-infected microglia have revealed an isoform-specific upregulation of GAC. And importantly, targeting GAC by siRNA and inhibiting GLS1 using pharmacological inhibitors have successfully reversed the excess glutamate production and the neurotoxic effects of HIV-1-infected microglia [84]. Again, these findings support that glutaminase as an important component of the pathogenic process of HAND.

1.5.3 Pathogenic role of neuronal GLS1 in HAND

Despite the fact that neurons having the highest expression levels of GLS1 in CNS, little is known about the role of neuronal GLS1 in mediating excitotoxcity of HAND until recently. In 2013, our laboratory has reported that both human and rat primary neurons treated by two proinflammatory cytokines that are typically elevated in neurodegenerative conditions, interleukin-1β (IL-1β) and tumor necrosis factor-α (TNF-α), produce substantially-increased intracellular and extracellular glutamate. The increase in glutamate production by those neurons under inflammation has induced toxic effects as the viability of

other neurons treated by the conditioned medium from inflammtory cytokines-treated neurons is largely decreased. GLS1 isoform KGA has been found to be significantly upregulated in both human and rat primary neurons under inflammation. And importantly, the neurotoxic effects are reversed by inhibiting GLS1 activity with pharmacological inhibitors or by antagolizing NMDA receptors [53]. Taken together, these results demonstrate a critical role of dysregulated GLS1 in neurons in mediating the progresses of brain inflammation and excitotoxicity in HAND.

1.6 Conclusion

Excitotoxicity mediated by excess glutamate production and overactivation of NMDA receptor is a basic componenet of various neurodegenerative disorders [50, 69, 70]. Specifically in HAND, excess glutamate generation seems to be a critical contributor although a number of factors clearly affect the pathogenesis of HAND. Glutamine, the substrate for the production of glutamate by GLS1 in the brain, is abundantly available at the millimolar range. In CNS, GLS1 catalyzes the deamination of glutamine to produce glutamate in an energetically favorable process. It is important to identify the specific cell type accounting for excess glutamate generation and understand the underlying mechanisms. With explicit effort, our laboratory with others have demonstrated that increased glutamate generation and release, decreased glutamate reuptake by presynaptic neurons, and reduced glutamate uptake by astrocytes all contribute to excess extracellular level of glutamate [91-

93]. We have documented the ciritcal roles of GLS1 dysregulation in brain macrophages, microglia, and inflammatory neurons, in excess glutamate production and augmentation of brain inflammation and neurotoxicity *in vitro* [50, 86, 90] [53].

To verify the clinical relevance of these findings, we investigated the expression levels of GLS1 in the postmortem brain tissues of HIV-1-infected patients with dementia. Importantly, we have identified an isoform-specific upregulation of GAC levels in the postmortem brain tissue of HAND patients comparing with that of HIV serum-negative controls, and the increased levels of GAC are correlated with elevated concentrations of glutamate in HAND patients' postmortem brain tissues [84, 90].

These results suggest that in a disease involving progressive neuroinflammation and excitoxicity as HAND, the aberrantly upregulated or released GLS1 plays a pathogenic role. Even more importantly, the findings that by targeting the dysregulated GLS1 with pharmacological inhibitors or siRNA reversed neuroinflammation or neurotoxicity strongly indicate that GLS1 can be a potentially valuable therapeutic target for treating HAND.

In order to further determine the pathogenic role of aberrantly regulated GLS1 and further investigate GLS1 as a new therapeutic target for HAND, we have started to utilize integral animal models to study the role of aberrantly regulated GLS1 in HAND pathogenesis and the underlying mechanisms *in vivo*. We hypothesize that there is strong association between GLS1 dysregulation and brain inflammation or cognitive impairment of HAND animals, and the brain-

specific overexpression of GLS1 will have a causal effect on inducing neurotoxicity.

1.7 Figures

Figure 1.1 Proposed model for the pathogenic role of dysregulated GLS1 in HAND. Previous studies revealed that GLS1 levels are increased in the HIV-1-infected macrophages and microglia. Viral proteins and neurotoxins secreted by infected brain macrophages and microglia activate uninfected microglia, macrophages, and astrocytes. Activated microglia, macrophages, and astrocytes release more neurotoxins and inflammatory molecules that damage neurons via overactivation of NMDA receptors. Neurons treated by proinflammatory cytokines have increased levels of GLS1. Inflammatory neurons secrete excess glutamate extracellularly and cause further damage to neurons.

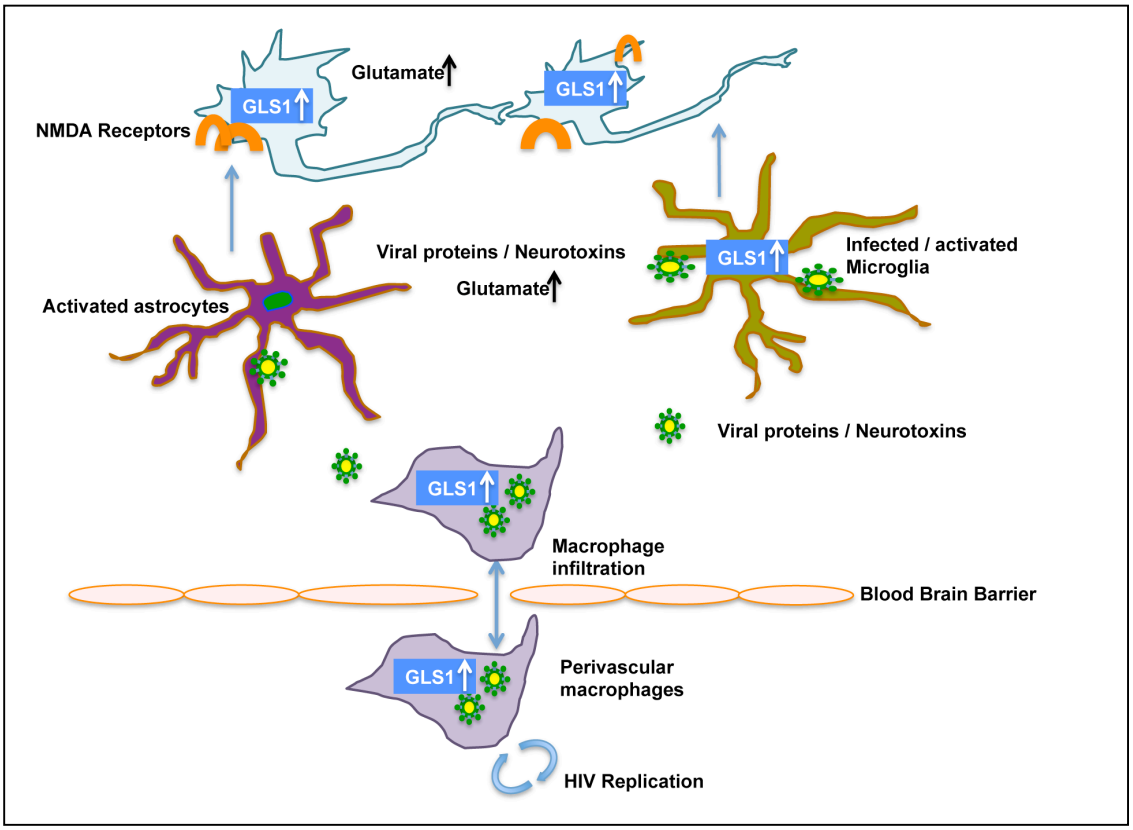
Glutamate
GLS1
GLS1
NMDA Receptors
Viral proteins / Neurotoxins
Glutamate
GLS1
Infected / activated
Microglia
Activated astrocytes
Viral proteins / Neurotoxins
GLS1
Macrophage
infiltration
Blood Brain Barrier
GLS1
Perivascular
macrophages
HIV Replication

CHAPTER 2

Glutaminase 1 is Aberrantly Upregulated in CNS of HAND murine models and is Associated with Brain Inflammation and Cognitive Impairment

2.1 Abstract

Glutaminase is the enzyme that converts glutamine into glutamate, which serves as a key excitatory neurotransmitter and one of the energy providers for cellular metabolism. Glutamate is essential for proper brain functioning but at excess levels, it is neurotoxic and has a key role in the pathogenesis of various neurodegenerative diseases, including HIV-1 associated neurocognitive disorders (HAND). However, the detailed mechanism of glutamate-mediated neurotoxicity remains incompletely understood. Our previous data revealed that GLS1 dysregulation is a key event in neuroinflammation and excess glutamate production in HIV-1-infected macrophages and microglia, and in neurons treated by inflammatory cytokines *in vitro*. But the regulation of GLS1 and its association with the progressions of neuroinflammation and neurotoxicity *in vivo* remains unknown. Using the well-established HAND murine models, the HIV trans-activator of transcription (HIV-Tat) transgenic (Tg) mouse and HIVE-severe combined immunodeficient (SCID) mouse, we identified that GLS1 isoforms were upregulated in whole brain tissues of HIV-Tat Tg mouse and in the neuroinflammatory areas of HIVE-SCID mouse brains. The elevated GLS1 expression levels were correlated with increased CNS astrogliosis and impaired spatial learning and memory of HIV-Tat Tg mouse, suggesting that GLS1 dysregulation is strongly associated with the pathogenesis of HAND. Together, these data imply a pathogenic role of GLS1 dysregulation for HAND *in vivo.*

2.2 Introduction

Non-human primates infected by the simian immunodeficiency virus (SIV) or by chimeric SIV/HIV viruses best mimic human HIV disease among all animal models. However, murine models possess notable advantages in consideration of advanced and easy-to-handle genetic methods for mouse genome manipulation, comparably low cost of maintaining animals and less difficulty of handling animals.

Given the fact that HIV is not infectious to murine species, generating small animal models to mimic the human pathology of HAND is a very challeging job. To date, the well-established and accepted murine models for HAND include: HIV-1 glycoprotien 120 (gp120) Tg mouse, HIV-Tat Tg mouse, the humanized mouse, and HIVE-SCID mouse [94]. HIV-Tat Tg mouse and HIVE-SCID mouse represnet two major different approaches of making murine models for HAND.

Generating Tg mouse models was among the very first endeavors for the study of HAND pathology *in vivo*. But it was not until recently that HIV-Tat Tg mouse has been well-accepted and extensively used as a HAND murine model. Tat is the first protein produced by HIV-1-infected cells. Upon secreted, Tat can invade and enter into most cell types of the human body via its arginie-rich domain. Importantly, Tat production is not significantly affected by the combined antiretroviral therapy (cART) as recent studies demonstrate that Tat is present in the cerebrospinal fluid (CSF) of HIV-1-infected individuals virologically controlled under cART [95]. This makes HIV-Tat Tg mouse the most popular HAND Tg

murine model in the post-HAART era [96, 97] because although gp120 is the most prominent viral antigen found in the lysates of HIV-1-infected cells [98] and gp120 can be shed by infected macrophages and activated astrocytes in CNS to cause neuronal damage, its production is largely reduced by sustained cART. Several HIV-Tat Tg mouse models have been created to understand the contribution of Tat protein to HAND progressions [96, 99-101], among which, the brain-specific HIV Tat Tg mouse under the control of the *GFAP* promoter with doxycycline-inducible system (GFAP-Tat) is one of the best characterized and most widely used [96, 101]. In this study, we utilized the GFAP-Tat Tg mouse. This line of mouse will be referred to as HIV-Tat Tg mouse in the rest of text.

Besides Tg mouse, another major approach for generating HAND murine models is by transplanting human cells or tissues into genetically modified immunodeficient mice. The HIVE-SCID mouse is created by implanting HIV-1-infected macrophages directly into the basil ganglia of SCID mice [102]. These mice persistently express HIV p24 antigen in the brain and can survive up to 5 weeks following cell implantation [103].

Neuroinflammation, excitotoxicity, synaptic damage and cognitive impairments have been found in both HIV-Tat Tg mouse and HIVE-SCID mouse. However, the regulation of GLS1 in CNS of these animals and the asssociation of GLS1 regulation with brain inflammation and neuronal damage remains unknown. In this chapter, we report that the GLS1 isoforms were upregulated in whole brain tissues of HIV-Tat Tg mouse and in the neuroinflammatory areas of HIVE-SCID mouse brains. The elevated GLS1

expression levels were correlated with increased CNS astrogliosis and impaired spatial learning and memory of HIV-Tat Tg mouse.

2.3 Materials and methods

Animals

C.B.-17-SCID mice of four weeks of age were purchased from Jackson Laboratory (Bar Harbor, ME). The GFAP-Tat Tg mice were generously provided to us by Dr. Kurt Hauser from Virginia Commonwealth University. The GFAP-Tat Tg mouse model was originally developed by Dr. Avindra Nath. Distribution of this model was allowed by Dr. Nath. All animals were housed and bred in the Comparative Medicine facilities of the University of Nebraska Medical Center. All procedures were conducted according to protocols approved by the Institutional Animal Care and Use Committee (IACUC) of the University of Nebraska Medical Center. All Tg mice were genotyped through PCR reactions. DNA of embryonic tissue or adult mouse-tail tissue was extracted with phenol/chloroform, and purified by isopropanol and ethanol for PCR reactions. The primers used for genotyping are listed in Table 2.1.

MDM isolation, culture, HIV-1 infection and implantation to SCID mice

Human monocytes recovered from peripheral blood mononuclear cells of healthy donors (HIV-1, 2 and hepatitis B seronegative donors) after leukopheresis and counter current centrifugal elutration [104] were cultured as adherent monolayers at the density of 1.1 x 10^6 cells / well in the 24-well plates for 7 days. The medium for cultivating monocytes is Dulbecco's modified Eagles medium (DMEM, GIBCO Invitrogen Corp, Carlsbad, CA) with 10% heat-inactivated pooled human serum (Cambrex Bio Science, Walkersville, MD), 50 μg/ml gentamicin, 10 μg/ml ciprofloxacin (Sigma-Aldrich, St. Louis, IL) and 1000

U/ml highly purified recombinant human macrophage colony stimulating factor (M-CSF) (Generously provided to us by Wyeth Institute, Cambridge, MA).

One week after being plated, MDM were infected by the laboratory HIV-1_{ADA} strain at a multiplicity of infection (MOI) of 0.1 virus per cell. On day after infection, HIV-1_{ADA}-infected MDM (5 x 10^5 cells in 5 μl per mouse) were intracranially injected into the basil ganglia of SCID mice by stereotactic methods [103]. Duplicate SCID mice receiving intracranial injections of uninfected MDM (5 x 10^5 cells in 5 μl per mouse) served as controls.

Morris-Water-Maze (MWM) Test

One week after the intracranial injection of MDM, HIVE-SCID mice were subjected to MWM test for behavior characterization. MWM test consists two parts, the training phase and probe test. Mice were introduced into a circular, water-filled tank, 91 cm in diameter and 110 cm in height. The tank was equally divided into four quadrants. Visual cues were placed around the pool in plain sight of the mouse to flag the submerged platform (10 cm in diameter). Various parameters of mouse movement were recorded, including the time spent in each quadrant of the pool, the time taken to reach the platform (escape latency), and the total distance traveled. For each trial, the mouse was allowed no more than 60 seconds to find the submerged platform before they were guided to the platform, removed from water, towel dried and returned to their cage. Each mouse will complete 4 trials per day during the 5-day training phase. Immediately after the training, the probe test was conducted. For the probe test, the platform was removed and each mouse was still given 60 seconds to swim

in the water. The swimming was videotaped analyzed by Ethovision XT (Noldus, Netherlands). The same test was done in HIV-Tat mice.

Brain-tissue protein extraction and Western-blot

After behavior tests, a set of animals were sacrificed and the whole brains were removed. The dissected tissues were homogenized by M-PER Protein Extraction Buffer (Pierce, Rockford, IL) containing 1× protease inhibitor cocktail (Roche Diagnostics, Indianapolis, IN). Protein concentrations were determined using a BCA Protein Assay Kit (Pierce). Proteins (5-10 μg) from tissue lysates were separated by sodium dodecyl sulfate-polyacrylamide gel electrophoresis (SDS-PAGE). After electrophoretic transfer to polyvinyldifluoridene (PVDF) membranes (Millipore and Bio-Rad), proteins were treated with purified primary antibodies for KGA (rabbit, Dr. N. Curthoys, Colorado State University, 1:1000), GAC (rabbit, Dr. N. Curthoys, Colorado State University, 1:500), GFAP (mouse, cat#3670S, cell signaling, 1:1000), or β-actin (mouse, Sigma-Aldrich, 1:10,000) overnight at 4 ^{o}C followed by a horseradish peroxidase-linked secondary anti-rabbit or anti-mouse antibody (Cell Signaling Technologies, 1:10,000). Antigen-antibody complexes were visualized by Pierce ECL Western Blotting Substrate (Pierce). For data quantification, films were scanned with a CanonScan 9950F scanner; the acquired images were then analyzed on a Macintosh computer using the public domain NIH Image J program (at http://rsb.info.nih.gov/nih-image/).

Analyses of glutamate concentrations

The intracellular glutamate levels in whole brain lysates of mice were determined by Amplex Red Glutamic acid / Gutamate oxidase Assay Kit (invitrogen) based on the manufacturer's instruction. Brain tissue lysates were diluted to the same protein concentration before entering the assay.

Statistical analyses

Data were analyzed as means ± SEM. The data were evaluated statistically by the analysis of variance (ANOVA) followed by Tukey-test for pairwise comparisons by using GraphPad Prism software. The two-tailed Student's t test was used to compare means of two groups. Correlations were determined by Spearman correlation. Significance was considered when $P < 0.05$. All experiments were performed with at least three mice in each group to account for any individual animal-specific differences. Assays were performed at least three times in triplicate or quadruplicate.

2.4 Results

GLS1 isoforms are upregulated in HIV-Tat Tg mice brains

Our previous data revealed an upregulation of GLS1 in the neuroinflammatory areas of HIVE-SCID mouse brain [53]. To validate and further study the upregulation of GLS1 isoforms in CNS of HAND murine models, we examined the expression levels of GLS1 isoforms KGA and GAC in the whole brain tissue lysates of HIV-Tat Tg mice. In agreement of the upregulation of GLS1 in HIVE-SCID mouse brains, protein analyses by Western-blot revealed that the protein levels of both KGA and GAC were elevated in HIV-Tat Tg mice brains compared to that in wide-type (WT) littermate controls (Figure 2.1A-B). In parallel with the upregulation of GLS1 isoforms KGA and GAC, analysis of glutamate levels in the whole brain tissue lysates revealed a significant increase of glutamate production in HIV-Tat Tg mice brains (Figure 2.1C). Together, these data demonstrate that GLS1 isoforms were aberrantly upregulated in CNS of HIV-Tat mice and the upregulated GLS1 produced more glutamate.

HIV-Tat Tg mice have increased astrogliosis in correlation with the elevated GLS1 isoform expression levels and brain glutamate levels

Protein analysis by Western-blot confirmed a significant increase of GFAP expression levels in HIV-Tat Tg mice brain tissue lysates, demonstrating for an increased ongoing astrogliosis in these animals (Figure 2.2A-B). Importantly, the elevations of KGA protein levels and glutamate levels in the whole brain tissue lysates of HIV-Tat Tg mice were significantly correlated with

the increase of the expression levels of GFAP (Figure 2.2C,E), and the elevations of GAC protein levels is marginally correlated (P = 0.09) with the increase of the expression levels of GFAP (Figure 2.2D). Together, these data suggest a significant association between GLS1 dysregulation and increased brain inflammation.

HIV-Tat Tg mice and HIVE-SCID mice displayed impairments in spatial learning and memory

Previous studies have reported behavior deficits in learning and memory of HAND patients and animals. To behaviorally characterize and validate the cognitive deficits of HIV-Tat Tg mouse and HIVE-SCID mouse, we carried out the MWM test to determine the spatial learning and memory of these animals.

During the training phase of MWM test, HIV-Tat Tg mice displayed longer escape latency (time spent to reach the submerged platform) (Figure 2.3A) and travelled longer distance to escape (Figure 2.3B), indicating that HIV-Tat mice had impaired capabilities in learning to escape from water. Meanwhile, HIV-Tat Tg mice had similar swimming velocities comparing with that of WT control littermates (Figure 2.3C). This demonstrates that the impairment of learning in HIV-Tat Tg mice is not due to deficits in motor functions. Likewise, HIV-Tat Tg mice spent significantly less time in the target quadrant (Q2, where the escape platform was during the training phase) in the probe test than that spent by WT control littermates (Figure 2.3D). These results indicate that Nestin-GAC mice are impaired in spatial learning and memory.

Importantly, HIVE-SCID mice also exhibited longer escape latency during the training phase (Figure 2.4A) and had significantly less time spent in the target quadrant Q2 in the probe test (Figure 2.4B) comparing to SCID mice injected with infected MDM. Together, these results demonstrate that HIV-Tat Tg mice and HIVE-SCID have deficits in learning and memory related to hippocampal and cortical functions.

Elevations of the expression levels of GLS1 isoforms and brain glutamate levels are in correlation with the behavior impairments in spatial learning and memory of HIV-Tat Tg mice

Correlation analyses were made to determine the associations between GLS1 dysregulation and behavior deficits in spatial learning and memory of HIV-Tat Tg mice. Correlation analyses revealed that GAC protein levels and brain glutamate levels were positively correlated with the escape latencies on the last day of MWM training phase (Figure 2.5B-C), and KGA protein levels were marginally positively correlated with the escape latencies (Figure 2.5A). Also, the elevation of brain glutamate levels was negatively correlated with the times that animals spent in the target quadrant Q2 of MWM probe test (Figure 2.5D). Therefore, these data indicate a strong association between GLS1 dysregulation and the spatial learning and memory impairments of HIV-Tat Tg mice.

2.5 Discussion

Understanding the regulation GLS1 and its association with brain inflammation, neurotoxicity, and cognitive impairments in HAND animal models will give the first clue towards the identifcation of whether GLS1 dysregulation has a pathogenic role and whether GLS1 can be a potential therapeutic target for HAND. In this chapter, we studied the regulation of GLS1 isoforms and the production of glutamate by GLS1 in HAND murine models. We report that the GLS1 isoforms were upregulated in the whole brain tissues of HIV-Tat Tg mouse and in the neuroinflammatory areas of HIVE-SCID mouse brains. The elevated GLS1 expression levels were correlated with increased CNS astrogliosis and impaired spatial learning and memory of HIV-Tat Tg mouse. These data support our central hypothesis that GLS1 dysregulation contributes to HAND pathogenesis via mediating brain inflammation and excitotoxicity.

Aberrant GLS1 upregulation and excess glutamate production in HIV-1-infected macrophages [73, 85, 86, 90], microglia [84-86] and in neurons under inflammation [53] has been well-characterized *in vitro*, and increased glutamate and upregulated GLS1 levels were found in HAND patients [84, 105]. The current study is the first to report an aberrant upregulation of GLS1 isoforms in the well-accepted and widely used HAND murine model, HIV-Tat Tg mouse; and the first to link GLS1 dysreuglation with neuroinflammation and cognitive impairments of HAND animals *in vivo*.

At current stage, we have determined the aberrant upregulation of GLS1 isoforms KGA and GAC in the whole brain tissues of HIV-Tat Tg mice. It will be

interesting and important to document the expression profiles of KGA and GAC in different areas of HIV-Tat Tg mice brains. Unlike HIVE-SCID mice which have the HIV-1-infected MDM injected into the basil ganglia thus displaying most of the neuroinflammatory and neurotoxic responses there, HIV-Tat Tg mice carry the expression of Tat almost globally in CNS [96, 97]. Therefore, the spatial pattern of GLS1 dysregulation in HIV-Tat Tg mouse CNS is expected to be different from that in HIVE-SCID mouse CNS. Our previous data revealed that the majority of GLS1 aberrant upregulation in HIVE-SCID mouse CNS was found in neurons of the inflammatory area [53]. One study reported that the neuronal damage is largely localized in the cerebellum and cortex of HIV-Tat Tg mouse [101]. Other studies reported relatively subtle neural damages including reductions in spine density and malformations of dendrites of neurons [106]. It is important to locate the specific cell type and possibly the specific brain area that has the majority of GLS1 dysregulation in HIV-Tat Tg mouse.

Besides the spatial profile of GLS1 dysregulation, to know the temporal regulation profile of GLS1 in HIV-Tat Tg mouse is equally important. This will help to determine the sequence of inflammatory and neurotoxic events occuring in HIV-Tat Tg mouse brain. It is interesting to know whether the aberrant upregulation of GLS1 occurs prior to brain inflammatory responses. This will be critical to determine the pathogenic role of GLS1 dysregulation in HAND. It could be challenging to distinguish sequence of events as multiple events could have occurred within a very short time frame thus making it difficult for investigators to tell them apart. In consideration of this, using genetical tools to modify GLS1

regulation in mouse CNS will be a helpful approach towards the determination of the cause-effect relationship.

2.6 Tables and Figures

TAT 1	GCGGATCCATGGAGCCAGTAGATCCTAG
TAT 2	GCGAATTCTCATTGCTTTGATAGAGAAACTTG
RTTA 1	AATCGAAGGTTTAACCCG
RTTA 2	TTGATCTTCCAATACGCAACC

Table 2.1 Primers used for the genotyping of HIV-Tat Tg mouse. Two sets of primers were used to determine the genotype of HIV-Tat Tg mouse. TAT 1 and TAT 2 were used to determine the presence of *Tat* gene. RTTA 1 and RTTA 2 were used to determine the presence of the doxycyline-inducible control of the promoter.

Figure 2.1 HIV-Tat Tg mice had upregulated GLS1 isoforms KGA and GAC in the brain. A-B). Whole brain lysates from HIV-Tat Tg and their WT control littermates were collected and the expression levels of KGA and GAC were determined by Western blot. Representative blots of GAC expression are shown (A). Quantification data were normalized to beta-actin and presented as fold changes compared to control mice (B). C). Intracellular glutamate levels of whole brain lysates were determined using the Amplex Red Glutamic acid / Gutamate oxidase Assay Kit. Data are shown as the means ± SEM. * $P < 0.05$, compared with control mice, N = 6 for WT controls and HIV-Tat Tg mice.

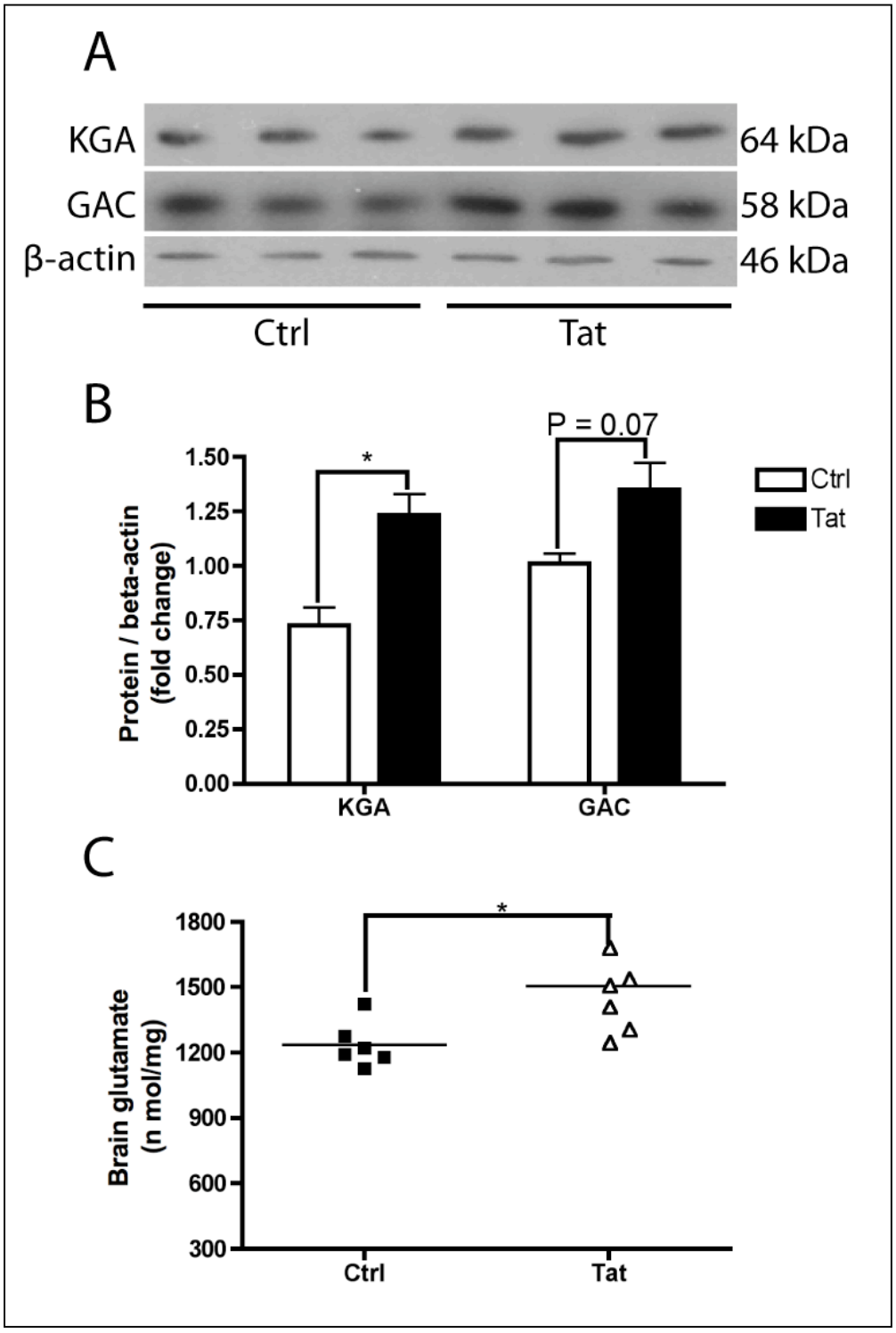
A
KGA
GAC
β-actin
64 kDa
58 kDa
46 kDa
Ctrl
Tat
B
P = 0.07
*
Protein / beta-actin (fold change)
1.50
1.25
1.00
0.75
0.50
0.25
0.00
Ctrl
Tat
KGA
GAC
C
*
Brain glutamate (n mol/mg)
1800
1500
1200
900
600
300
Ctrl
Tat

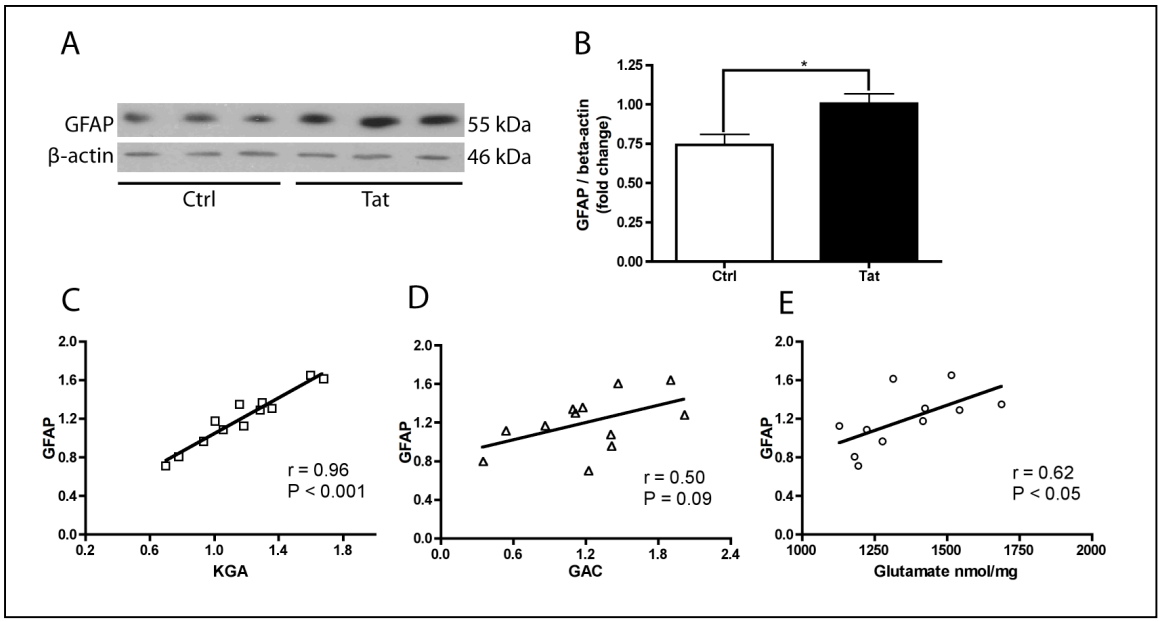

Figure 2.2 HIV-Tat Tg mice had increased astrogliosis in correlation with the upregulation of GLS1 and elevation of brain glutamate. A-B). Whole brain lysates from HIV-Tat Tg and their WT control littermates were collected and the expression levels of GFAP were determined by Western blot. Representative blots of GFAP expression are shown (A). Quantification data were normalized to beta-actin and presented as fold changes compared to control mice (B). C-E). Correlations of KGA protein levels (C), GAC protein levels (D), brain glutamate levels (E) with GFAP protein levels were determined by Spearman correlation.

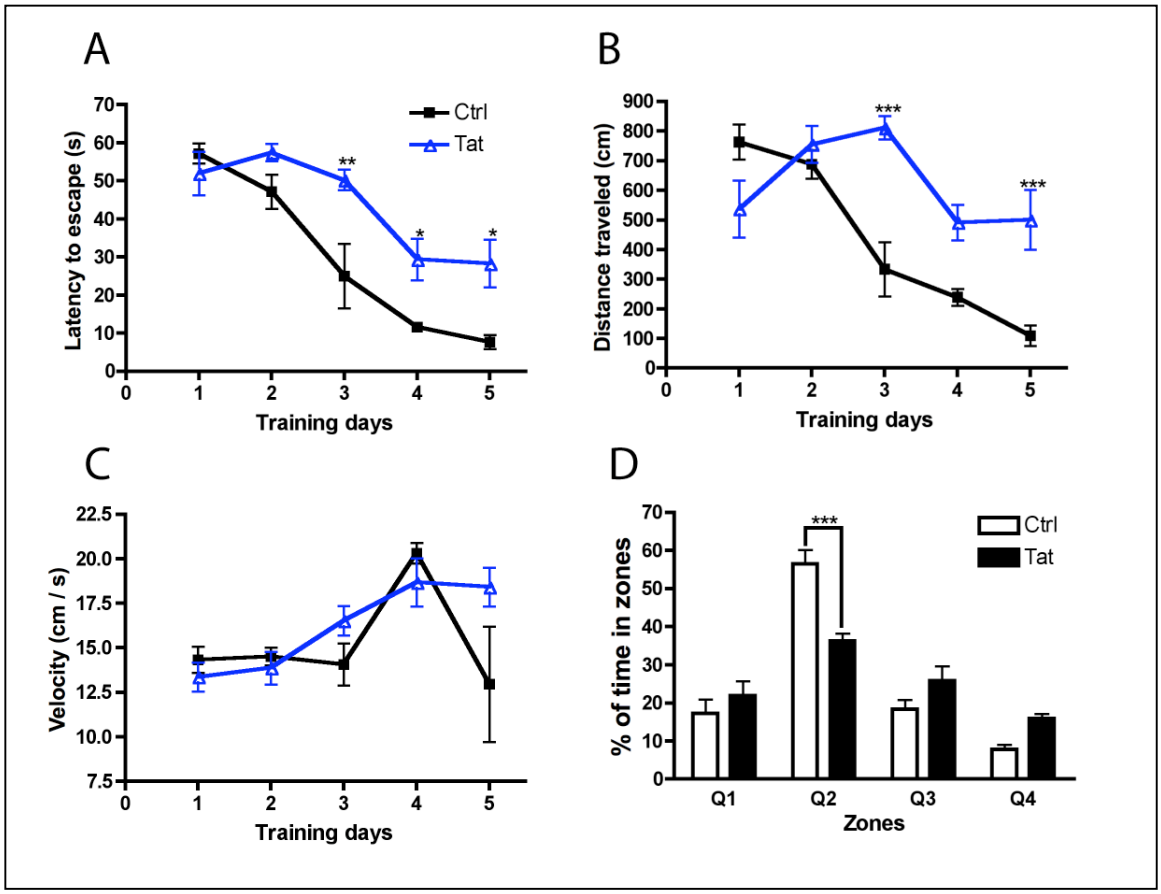

Figure 2.3 HIV-Tat Tg mice exhibited impairment in spatial learning and memory. A-D). Morris-Water-Maze test was utilized to examine the spatial learning of memory of HIV-Tat Tg mice. During the training phase, HIV-Tat Tg mice exhibited longer escape latency (A), travelled longer distance to reach platform (B), but exhibited similar swimming velocities (C). During probe test, HIV-Tat Tg mice spent less time in the target quadrant (D). Data are shown as the means ± SEM. * $P < 0.05$, *** $P < 0.001$, compared with control mice, N = 6 for WT controls and HIV-Tat Tg mice.

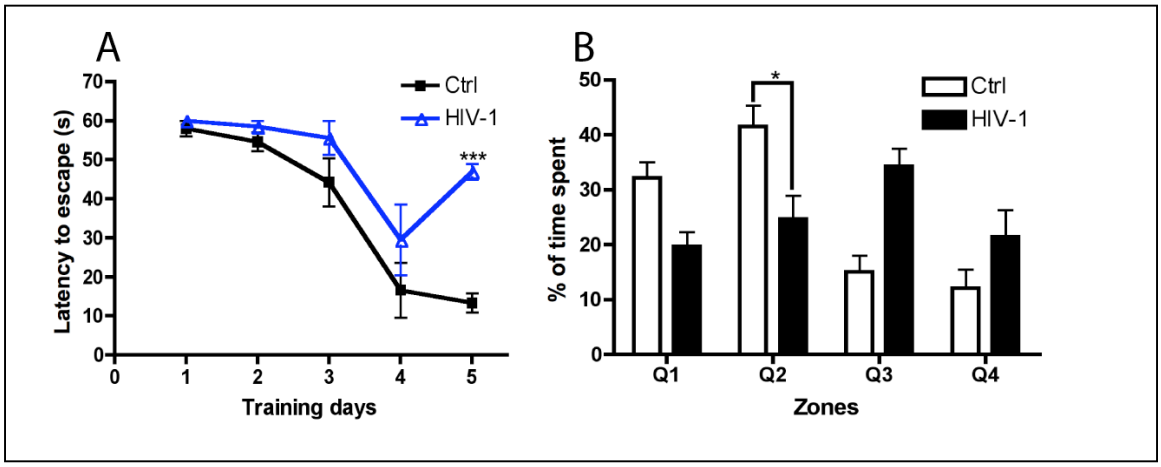

Figure 2.4 HIVE-SCID mice exhibited impairment in spatial learning and memory. A-B). Morris-Water-Maze test was utilized to examine the spatial learning of memory of HIVE-SCID mice. During the training phase, HIVE-SCID mice exhibited longer escape latency (A). During probe test, HIVE-SCID mice spent significantly less time in the target quadrant (B). Data are shown as the means ± SEM. * $P < 0.05$, *** $P < 0.001$, compared with control mice, N = 6 for uninfected-MDM controls and HIVE-SCID mice.

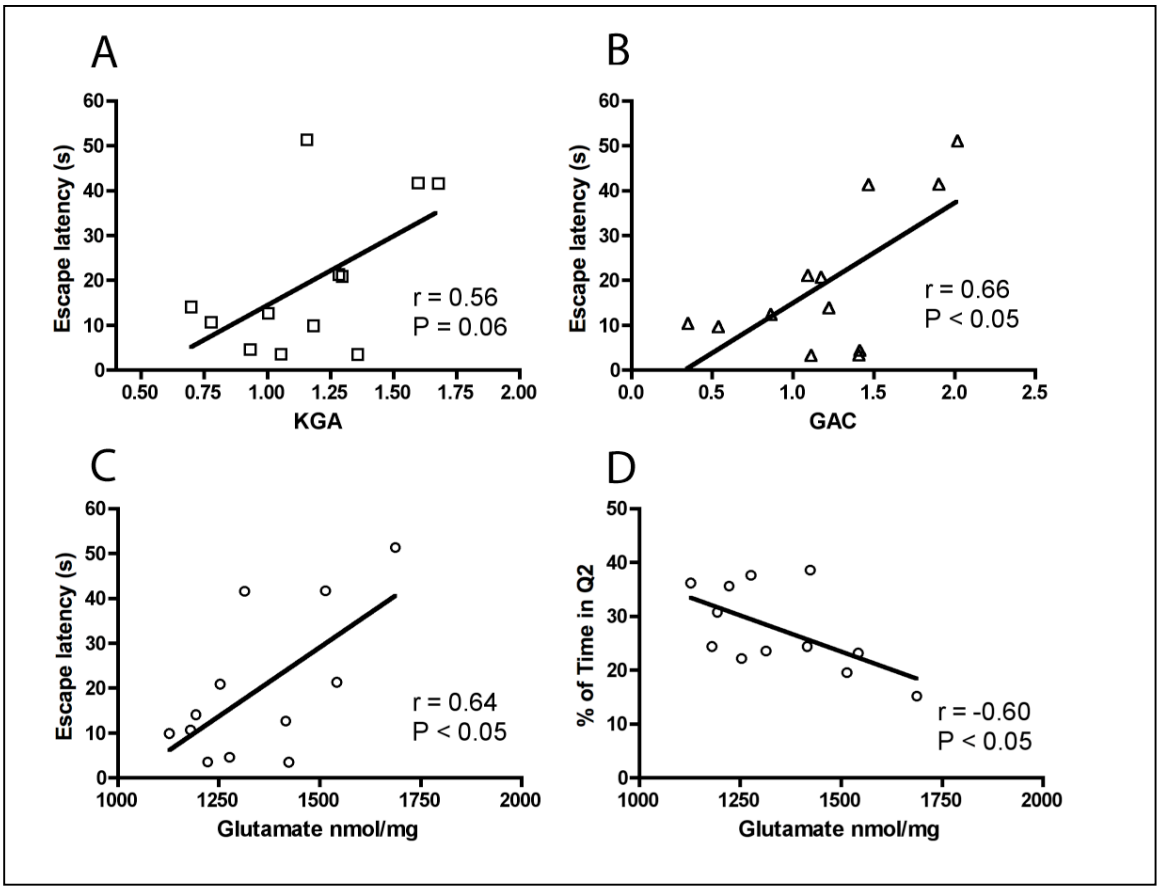

Figure 2.5 GLS1 and glutamate levels were in correlation with MWM performances of HIV-Tat Tg mice. A-D). Correlations of KGA protein levels (A), GAC protein levels (B), brain glutamate levels (C) with the escape latencies (A-C) on the last day of MWM training phase and the times that mice spent in Q2 (D) of MWM probe test were determined by Spearman correlation. Levels of significance are indicated in the figure.

CHAPTER 3

Brain-specific Overexpression of Glutaminase C Induces Neuroinflammation, Synaptic Damage and Dementia in Mice: Relevance to HAND

3.1 Abstract

Glutaminase is the enzyme that converts glutamine into glutamate, which serves as a key excitatory neurotransmitter and one of the energy providers for cellular metabolism. Glutamate is essential for proper brain functioning but at excess levels, it is neurotoxic and has a key role in the pathogenesis of various neurodegenerative diseases, including HIV-1 associated neurocognitive disorders (HAND). However, the detailed mechanism of glutamate-mediated neurotoxicity remains unclear. Our previous data revealed upregulation of glutaminase C (GAC) in the postmortem brain tissues of patients with HIV dementia by protein analysis, suggesting a critical role of GAC in the instigation of primary dysfunction and subsequent neuronal damage in HAND. Therefore, we hypothesize that GAC dysregulation in brain is sufficient to induce brain inflammation and dementia in relevance to HAND. Using a brain GAC overexpression mouse model (which has the overexpression of GAC confined in the brain), we found that the expression of the marker for brain inflammation, the glial fibrillary acidic protein (GFAP), was increased in the brains of GAC-overexpression mice, suggesting increased reactive astrogliosis. To study the functional impact of GAC overexpression, we performed Morris Water Maze (MWM) test and Contextual Fear Conditioning (CFC) test to determine the learning and memory of mice. GAC-overexpression mice exhibited longer escape latency during the training and lower percentage of time spent in the target quadrant during the probe test, indicating that overexpressing GAC in mouse brain impaired the learning and memory of the animals. Together, these

data suggest that dysregulated GAC in mouse brain causes prolonged inflammation and dementia.

3.2 Introduction

Neurological disorders develop during progressive HIV-1 infection and are characterized by cognitive deteriorations, behavioral disorders and potential progressive motor impairments as a consequence of neuronal damage [107]. These disorders affect up to 50% of HIV-1 infected individuals and are termed as HIV-1 associated neurocognitive disorders (HAND) [3]. HAND comprise three categories based on standardized measures of dysfunction [2]: HIV-1 associated dementia (HAD), minor cognitive motor disorder (MCMD), and asymptomatic neurocognitive impairment (ANI) [2]. With the effective treatment by highly active antiretroviral therapy (HAART), the occurrence of HAD, the most severe and devastating form of HAND, has dramatically fallen [4]. However, HAART fails to prevent the milder neurocognitive disorders, thus cognitive impairment continues to be a commonplace associated with HIV-1 infection. It is critical to develop new therapeutic approaches to prevent neurocognitive impairment, as it is affecting the everyday life of patients including driving, employment and medication management.

Chronic neuroinflammation is a hallmark of HAND and a constitutive component of the pathogenesis of neurodegenerative diseases including HAND, multiple sclerosis, amyotrophic lateral sclerosis, Parkinson's disease and Alzheimer's disease [33-35]. Literature have suggested a close link between brain inflammation and neuronal injury [36, 39]. HIV-infected and activated microglia or macrophages instigate brain inflammation and induce neuronal injury through the production and release of various soluble neurotoxic factors

including glutamate [51, 52, 108]. Apart from glia cells, neurons play a role in the progress of brain inflammation as well. Specifically, proinflammatory cytokines TNF-α and IL-1β, which are typically elevated during neurodegenerative diseases, induced neuronal loss via the production and release of glutamate in neuronal culture [53].

Glutamate is the most abundant neurotransmitter in CNS [55]. It is essential for vital physiologic processes including neural development, synaptic plasticity, learning and memory [56, 57]. However at excess levels, glutamate has the potential to induce extensive neuronal injury, which is termed excitotoxicity. Therefore, elevated glutamate has been linked to the pathogenic processes of various CNS disorders [65-68] and neurodegenerative diseases including HAND [50, 69, 70]. In CNS, glutamate is typically derived from glutamine by the action of mitochondrial enzyme glutaminase. The predominant glutamine-utilizing and glutamate-producing enzyme in CNS is glutaminase 1 (GLS1), whereas the isozyme glutaminase 2 is expressed at lower levels [72]. Furthermore, GLS1 has two alternative splicing isoforms, which include glutaminase C (GAC) and kidney-type glutaminase (KGA). GAC shares the same functional region of KGA and possesses a unique C-terminal [76]. Glutaminase catalyzes the following reaction: Glutamine + H_2O → Glutamate + NH_3. This reaction is energetically favorable so glutaminase must be tightly regulated to prevent excess glutamate generation and excitotoxicity [73]. In the past decade our laboratory developed molecular and chemical tools with explicit intent to understand glutaminase activity and functions in the brain. Along with

others, we have documented roles of GLS1 in microglia and macrophages in brain injury, infection and inflammation [50, 84, 85] and more recently the regulation and function of GLS1 in neurons [53]. Importantly, we have identified a specific upregulation of GAC levels in the postmortem brain tissue of HAND patients [84, 90], suggesting that GAC might play a pathogenic role in HAND.

The currently available murine models for HAND include: HIV-1 glycoprotien 120 (gp120) transgenic mouse, HIV-Tat transgenic mouse, the humanized mouse, and the HIV-1 encephalitis (HIVE) mouse [94]. While all these models contribute to revealing the neuropathology of HAND, none of them study the role of glutaminase. In order to unravel it, we generated a brain GAC overexpression mouse model (which has the GAC overexpression confined in the brain) and found prolonged brain inflammation and dementia in brain-specific GAC overexpression animals.

3.3 Materials and methods

Generation of CAG-loxp-GAC and Nestin-GAC mice

The mouse *Gac* gene was cloned from a C57 mouse cDNA library and was inserted into the pCAG-Loxp-STOP-Loxp-IRES-LacZ plasmid at restriction enzyme site XhoI. The constructed plasmid was sequenced to ensure that only plasmids with *Gac* forwardly inserted. The selected plasmid was linearized and the linearized plasmid was microinjected into the fertilized egg for implantation into a pseudopregnant female to create CAG-loxp-GAC mouse in the Mouse Genome Engineering Core Facility of UNMC. GFP expressions in the brains of CAG-loxp-GAC mice were examined to ensure the stable expressions of the constructed plasmid. The CAG-loxp-GAC mice were then mated with a *nestin* promoter-driven *cre* transgenic mouse (Nestin-Cre mouse) line (in which the *cre* activity is confined to CNS) [109] to produce Nestin-GAC mice (Figure 3.1).

Animals

Nestin-Cre mice of four weeks of age were purchased from Jackson Laboratory (Bar Harbor, ME). All mice were housed and bred in the Comparative Medicine facilities of the University of Nebraska Medical Center. All procedures were conducted according to protocols approved by the Institutional Animal Care and Use Committee of the University of Nebraska Medical Center. All transgenic mice were genotyped through PCR reactions. DNA of embryonic tissue or adult mouse-tail tissue was extracted with phenol/chloroform, and purified by isopropanol and ethanol for PCR reactions. The primers used for genotyping are listed in Table 3.1.

Morris Water Maze (MWM) test

MWM test consists two parts, the training phase and probe test. Mice were introduced into a circular, water-filled tank, 91 cm in diameter and 110 cm in height. The tank was equally divided into four quadrants. Visual cues were placed around the pool in plain sight of the mouse to flag the submerged platform (10 cm in diameter). Various parameters of mouse movement were recorded, including the time spent in each quadrant of the pool, the time taken to reach the platform (escape latency), and the total distance traveled. For each trial, the mouse was allowed no more than 60 seconds to find the submerged platform before they were guided to the platform, removed from water, towel dried and returned to their cage. Each mouse will complete 4 trials per day during the 5-day training phase. Immediately after the training, the probe test was conducted. For the probe test, the platform was removed and each mouse was still given 60 seconds to swim in the water. The swimming was videotaped analyzed by Ethovision XT (Noldus, Netherlands).

Contextual Fear Conditioning (CFC) Test

Fear conditioning was performed following standard procedures in the light- and sound-attenuated chambers for mouse (Coulbourn Tru Scan Activity Monitoring System for mouse). Mouse behavior was evaluated under ambient illumination (room light) and was recorded by a SAMSUNG digital videocamera set above the mouse arena chamber. The recorded behavior videos were analyzed by Ethovision XT (Noldus), which assesses the time of freezing by measuring changes in pixel intensities of video frames. The fear conditioning

procedure was conducted over 3 days. On 1st day, mice were given 300 seconds to be habituated to the arena chamber and no shock was administered. The mouse chamber was cleaned with 70% ethanol before the introduction of each mouse to the arena chamber. On 2nd day, the mouse chamber was scented with 0.1% acetic acid and the mice were given two electric shocks at 170 s and 290 s during the 300 s through the automated Tru Scan Stimulus. Chamber was cleaned with a non-alcohol disinfectant. On 3rd day, the chamber was also scented with 0.1% acetic acid but no shock was given. Mice in the mouse chamber were recorded for 180 s on the third day. The mouse chamber was cleaned with a non-alcohol disinfectant. The freezing behavior was analyzed by Ethovision XT (Noldus) and the percent of freezing was calculated for each day.

Tissue protein extraction and Western-blot

The animals were sacrificed and the brains were removed. The hippocampi, cortices, striatum, and kidneys were dissected free. The dissected tissues were homogenized by M-PER Protein Extraction Buffer (Pierce, Rockford, IL) containing 1× protease inhibitor cocktail (Roche). Protein concentrations were determined using a BCA Protein Assay Kit (Pierce). Proteins (5-10 μg) from tissue lysates were separated by sodium dodecyl sulfate-polyacrylamide gel electrophoresis (SDS-PAGE). After electrophoretic transfer to polyvinyldifluoridene (PVDF) membranes (Millipore and Bio-Rad), proteins were treated with purified primary antibodies for MAP-2 (mouse, cat#MAB3418, Millipore, 1:1000), GAC (rabbit, Dr. N. Curthoys, Colorado State

University, 1:500), Synaptophysin (rabbit, cat#ab32127, Abcam, 1:25,000), GFAP (mouse, cat#3670S, cell signaling, 1:1000), PARP (rabbit, cat# 9542s, Cell Signaling Technologies, Beverly, MA, 1:1000), Caspase 3 (rabbit, cat#9662s, Cell Signaling, 1:1000) or β-actin (Sigma-Aldrich) overnight at 4 ^{o}C followed by a horseradish peroxidase-linked secondary anti-rabbit or anti-mouse antibody (Cell Signaling Technologies, 1:10,000). Antigen-antibody complexes were visualized by Pierce ECL Western Blotting Substrate (Pierce). For data quantification, films were scanned with a CanonScan 9950F scanner; the acquired images were then analyzed on a Macintosh computer using the public domain NIH Image J program (at http://rsb.info.nih.gov/nih-image/).

Free-floating immunohischemistry and image analyses

Animals were sacrificed and perfused with phosphate-buffered saline (PBS) and then with depolymerized 4% paraformaldehyde (PFA). The brains were rapidly removed and immersed in freshly depolymerized 4% PFA for 48 hours and then cryoprotected by 30% sucrose for 48 hours. The fixed, cryoprotected brains were frozen and sectioned in the coronal plane at 30 μM using a Cryostat (Leica Microsystems Inc., Bannockburn, IL), with sections collected serially in PBS as previously described [110]. Brain sections were then incubated overnight at 4 ^{o}C with primary antibodies, followed by goat anti-mouse IgG Alexa Fluor 488 secondary antibodies (Molecular Probes, Eugene, OR, 1:1000) for 1 hour at 25 ^{o}C. Primary antibodies included rabbit GLS1 (Dr. N. Curthoys, Colorado State University, 1:500), rabbit Synaptophysin (Abcam, cat#ab32127, 1:500), and rabbit GFAP (Dako, Carpinteria CA, 1: 2000). All

antibodies were diluted in 0.1% Triton X-100, 5% goat serum in PBS. Cells were counterstained with DAPI (Sigma-Aldrich, 1:1000) to identify nuclei. Images were taken using a Zeiss Meta 710 confocal microscope (Carl Zeiss MicroImaging, LLC) (20X object, tile scan 4X4 mode). Eight brain section images from three mice were imported into Image-ProPlus, version 7.0 (Media Cybernetics, Silver Spring, MD) for quantifying levels of either GFAP / DAPI, or Synaptophysin / DAPI double positive staining.

In situ TUNEL assay

Brain sections were stained with an *in situ* TUNEL assay (Roche Diagnostics, Indianapolis, IN) according to the manufacturer's protocol. The fluorescence intensity of TUNEL was quantified after acquiring random images from immunostained fields using a Nikon Eclipse TE2000E microscope. Eight brain section images from four mice were imported into Image-ProPlus, version 7.0 (Media Cybernetics, Silver spring, MD) for quantifying levels of fluorescence intensity.

Hippocampal electrophysiology

Mouse hippocampal electrophysiology was perfomed as previously described [111, 112]. mouse hippocampi were dissected free and live sagittal hippocampal slices (300 μM in thickness) were prepared using a tissue chopper. The hippocampal slices were incubated in the artificial cerebrospinal fluid (ACSF, containing 124mM NaCl, 26mM $NaHCO_3$, 1.25 mM NaH_2PO_4, 2.5 mM KCl, 2 mM $CaCl_2$, 2 mM $MgCl_2$, and 10 mM glucose equilibrated with 95% O_2 and 5% CO_2, pH 7.3-7.4). The temperature of the perfusate was maintained at

30 $\pm$ 1 ^{o}C with an automatic temperature controller (Warner Instrument, Hamden, CT). The slices were incubated in the ACSF for 1-2 hours, and then transferred to a recording chamber mounted on the stage of a dissection microscope. Field excitatory postsynaptic potentials (fEPSPs) were evoked by a low-frequency orthodromic stimulation (0.05 Hz) with constant current of Schaffer collateral / Schaffer collateral commissural axons using an insulated (excluding the tip) bipolar tungsten electrode. The intensity of stimulation was selected to generate nearly 50% of a maximal response. The elicited fEPSPs were recorded with an Axopatch-1D amplifier (Axon Instruments, CA) in the CA1 dendrites area (stratum radiatum). The recording microelectrodes were made from borosiliacate glass capillaries with inner filaments enabling quick backfilling. The diameter of the tip of the microelectrode was 5.0 μm with a resistance of 1-5 MΩ when filled by ACSF.

The frequency facilitation tests were performed at 50% maximal fEPSP for each hippocampal slice. A stimulation burst consisting 10 pulses was applied to the slice after a 20 minute acclimation. The responses were recorded. Then the slice was given a 20 minute recovery time before another stimulation burst was given. The initial slopes of the recorded fEPSPs were measured and analyzed as the percent of the first pulse (taking the first as 100%). Recordings from the same group at the same time were averaged.

The ability of the high-frequency stimulation (HFS: 100 Hz, 500msec X 2) to induce long-term potentiation (LTP) in CA1 of hippocampus was studied. The high-frequency stimulus (HFS) was delivered to each hippocampal slical after

the 30 minute baseline recording and LTP was evoked. The initial slopes of fEPSPs were measured and expressed as a percent of the baseline. LTP were determined at 45-55 minutes after HFS.

Analyses of glutamate concentrations

The intracellular glutamate levels in brain lysates of mice were determined by Amplex Red Glutamic acid / Gutamate oxidase Assay Kit (invitrogen) based on the manufacturer's instruction. Brain tissue lysates were diluted to the same protein concentration before entering the assay.

Statistical analyses

Data were analyzed as means ± SEM. The data were evaluated statistically by the analysis of variance (ANOVA) followed by Tukey-test for pairwise comparisons by using GraphPad Prism software. The two-tailed Student's t test was used to compare means of two groups. Correlations were determined by Spearman correlation. Significance was considered when $P < 0.05$. All experiments were performed with at least three mice in each group to account for any individual animal-specific differences. Assays were performed at least three times in triplicate or quadruplicate.

3.4 Results

GAC overexpression is specific to brains of Nestin-GAC mice

Lysates from the whole brain and kidney of both Nestin-GAC mice and their wide-type (WT) control mice littermates prepared. Total protein was extracted from either the whole brain lysates or kidney lysates. The gene expression levels of GAC were determined by Western-blot and were found to be higher in the whole brain lysate of Nestin-GAC mice than that of WT control littermates (Figure 3.2A-B). Meanwhile, the total amount of intracellular glutamate in the whole brain lysates was measured. In parallel to the increase of GAC protein levels in the whole brain lysates of Nestin-GAC mice, the glutamate levels were found to be higher in Nestin-GAC mice brains than that in WT control littermates brains (Figure 3.2C), indicating higher enzymatic activity of glutaminase in Nestin-GAC mouse brains. In contrast to the differences of GAC protein levels in the whole brain lysates, Nestin-GAC mice and their WT control littermates were found to have similar protein expression levels of GAC in the kidney lysates (Figure 3.2D-E). Likewise, Nestin-GAC mice and their WT control littermates had similar amount of glutamate in the kidney lysates (Figure 3.2F). Therefore, these results demonstrate that the overexpression of GAC is specific to brains in Nestin-GAC mice.

GAC overexpression is confirmed in different areas of Nestin-GAC mouse brain

Whole brains of Nestin-GAC mice and their WT control littermates were dissected and protein lysates were prepared from the hippocampi, cortices,

midbrains and cerebellums. The expression levels of GAC in different areas of mouse brains were determined by Western-blot. Nestin-GAC mice had higher expression levels of GAC in hippocampal, cortical, midbrain and cerebellar lysates than that in lysates of WT control littermates (Figure 3.3A-B). In parallel to the increase of GAC protein levels in different areas of Nestin-GAC mouse brains, the amount of glutamate was found to be higher in hippocampal, cortical, midbrain and cerebellar lysates (Figure 3.3C), indicating increased glutaminase enzymatic activity in these brain areas of Nestin-GAC mice. To visualize the increase of glutaminase protein levels in hippocampi of Nestin-GAC mouse brains, we applied the anti-GLS1 antibody to brain slices of Nestin-GAC mice and their WT control littermates. The fluorescence intensities of GLS1 were quantified. Nestin-GAC mouse brain slices clearly had higher expression levels of GLS1 in hippocampi (Figure 3.3D-E). These results confirm that GAC is overexpressed in different areas of Nestin-GAC mouse brains.

Nestin-GAC mice exhibited deficits in learning and memory

To study the functional impact of the brain-specific GAC overexpression, we utilized MWM test and CFC test to study the learning and memory of Nestin-GAC mice and their WT control littermates. During the training phase of MWM test, Nestin-GAC mice displayed longer escape latency (time spent to reach the escape platform) (Figure 3.4A) and travelled longer distance to escape (Figure 3.4B), indicating that Nestin-GAC mice had impaired capabilities in learning to escape from water. Meanwhile, Nestin-GAC mice had similar swimming velocities comparing with that of WT control littermates (Figure 3.4C). This

demonstrates that the impairment of learning in Nestin-GAC mice is not due to deficits in motor functions. Likewise, Nestin-GAC mice spent significantly less time in the target quadrant (Q2, where the escape platform was during the training phase) in the probe test than that spent by WT control littermates (Figure 3.4D), and Nestin-GAC mice had significantly fewer times of crossings through the platform area (Figure 3.4E). These results indicate that Nestin-GAC mice are impaired in spatial learning and memory. Importantly, Nestin-GAC mice apparently had lower percentage of freezing than that of WT control littermates on the last day of CFC test (Figure 3.4F), indicating again that these mice are impaired in hippocampus-related memory. Together, these results demonstrate that Nestin-GAC mice have deficits in learning and memory related to hippocampal and cortical functions.

Brain-specific overexpression of GAC leads to synaptic damage in mice

To identify ongoing changes in the hippocampi and cortices relating to memory impairment of Nestin-GAC mice, we examined the synaptic network in the brains of these animals. The expression levels of synapses marker, Synaptophysin, were determined by Western blot in the hippocampal and cortical lysates of Nestin-GAC mice and their WT control littermates. Interestingly, the expression levels of Synaptophysin were found to be dramatically decreased in the hippocampal (Figure 3.5A-B) and cortical (Figure 3.5C-D) lysates of Nestin-GAC mouse brains compared to that of WT control littermates. This dramatic decrease indicates synaptic damage in the hippocampal and cortical neuronal network of Nestin-GAC mouse brains. To

visualize the changes of the expression levels of Synaptophysin, we applied the anti-Synaptophysin antibody to brain slices of Nestin-GAC mice and WT control littermates. The fluorescence intensity of Synaptophysin was quantified. Apparently, Nestin-GAC mice had lower expression levels of Synatophysin in hippocampus as implied by lower fluorescence intensity (Figure 3.5E-F). Together, these results suggest that the brain-specific GAC overexpression leads to hippocampal and cortical synaptic damage in mice.

To determine whether synaptic injury leads to loss of hippocampal synaptic function, we recorded long-term potentiation (LTP) in the CA1 region of hippocampal brain slices. Nestin-GAC Tg mice exhibited diminished initiation and maintenance of LTP (Figure. 3.6A-B), indicating GAC overexpression leads to marked impairment of hippocampal synaptic transmission *in vivo*.

Brain-specific GAC overexpression leads to increased apoptosis in mouse brains.

To explore of the specific reasons that cause the synaptic network damage, we examined the expression levels of important proteins in the apoptosis cascade. The expression levels of activated Caspase 3 (cleaved-Caspase 3) and cleaved-PARP were determined by Western blot. Interestingly, both the expression levels of cleaved-Caspase 3 and cleaved-PARP were found to be dramatically increased in the hippocampal (Figure 3.7A-B) and cortical (Figure 3.7C-D) lysates of Nestin-GAC mice compared to that of WT control littermates. This indicates that there is increased apoptosis ongoing in Nestin-GAC mouse brains. Importantly, the number of TUNEL positive cells in the

hippocampus was found to be increased as well in brain slices of Nestin-GAC mice compared to WT control littermates as revealed by the *in-situ* TUNEL assay (Figure 3.7E-F). These results together suggest that there is increased ongoing apoptosis in the Nestin-GAC mouse hippocampi and cortices that may account for the synaptic network damage in these animals.

Brain-specific GAC overexpression leads to reactive astrogliosis in mouse brains.

Brain inflammation is a hallmark of HAND and a constitutive component in the pathogenesis of HAND. To identify whether there is existing brain inflammation of Nestin-GAC mice, we examined the expression levels of the astrogliosis marker, glial fibrillary acidic protein (GFAP), by western blot and immunohistochemistry. We found a significant increase of GFAP protein expressions in the hippocampal (Figure 3.8A-B) and cortical (Figure 3.8C-D) lysates of Nestin-GAC mice compared with that of WT control littermates. Consistently, the fluorescence intensity of GFAP was found to be significantly higher in hippocampi of Nestin-GAC mouse brain slices than that of WT control littermate brain slices (Figure 3.8E-F). These results suggest ongoing reactive astrogliosis in the Nestin-GAC mouse brains which implies prolonged brain inflammation of Nestin-GAC mice.

3.5 Discussion

Despite the encouraging progresses made by HAART, HAND is still significantly affecting the quality of life of HIV-1-infected individuals [3]. Identification of the key pathogenic components and understanding the mechanisms underlying the development of neurological disorders during HIV-1 infection will largely contribute to the allevation, treatment or even prevention of cognitive deteriorations and behavioral disorders [107]. Despite the important discovery of the specific upregulation of GAC in the post mortem brain tissues of HAND patients and the implied association of GAC with the pathogenesis of HAND, the causal relationship of GAC upregulation and the disease progressions of HAND remains to be identified. In this chapter, we generate the Nestin-GAC transgenic mouse which has GAC overexpression confined in brain. We report that the brain-specific GAC overexpression results in learning and memory impairment in mice. Furthermore, we report that the brain-specific overexpression of GAC leads to hippocampal and cortical synaptic network damage, increased apoptosis and reactive astrogliosis in the hippocampi and cortices of mice. Importantly, we have observed impairment of LTP in Nestin-GAC mice, further demonstrating for the synaptic damage in hippocampi of these animals. Together, these results suggest for the first time that the overexpressed GAC in brain has a causal relationship with prolonged brain inflammation and increased apoptosis, which, lead to neural network damage and finally result in the impairment of cognitive functions of animals.

The identification of the pathogenic role of GAC in HAND has an important clinical implication. Glutaminase dysregulation has long been implicated in the pathogenesis or pathology of HAND. However, this is the first time that we show that the dysregulation of the specific isoform of glutaminase 1, GAC, in the brain may be one of the major components that cause HAND disease progressions through prolonged brain inflammation and increased apoptosis that then result in synaptic network damage. Hippocampal – cortical synaptic networking is well known to be essential for proper cognitive functions like learning and memory [113-121]. Hippocampal and hippocampal-cortical signaling has been studied for decades because of its crucial role in memory [121-131]. Among that, glutamate signaling is well known to affect synaptic plasticity [121, 127, 130, 132-134]. Specifically, a strong association between the memory loss due to aging or disease and the disruption of NMDA receptor-mediated neurotransmission has been revealed [127, 130, 134]. Glutamate is an essential and vital neurotransmitter, but it is neurotoxic at excess levels. Because the reaction of deamination of glutamine to produce glutamate is energetically favorable, glutaminase as the primary enzyme catalyzing this reaction ought to be finely regulated to prevent excess production of glutamate. Although neighboring astrocytes of neurons are able to take up extra glutamate by glutamate transporters and convert it back to glutamine with the catalysis by glutamine synthase [81, 82], the present study suggests that the neural network damage caused by dysregulated GAC in the brain cannot be overcome.

Whether there are alterations or dysregulations of glutamate receptors in Nestin-GAC mouse brains is an interesting and important question to be answered. Excitotoxicity common to various neurodegenerative diseases including HAND involves overactivation of NMDA receptors. High-affinity NMDA receptor antagonist MK801 has successfully blocked the toxicity from neurons treated by inflammatory cytokines TNF-α and IL-1β [53]. More importantly, a low-to-moderate-affinity NMDA receptor antagonist memantine has substantially abrogated neurotoxicity and largely recovered the impaired synaptic transmission and LTP [111]. Determining whether or not the neurotoxicity observed in Nestin-GAC mouse brains is via the overactivation of NMDA receptors will greatly help to further validate the resemblance of Nestin-GAC mouse as a novel HAND murine model.

Apart from glutamate receptors, to study whether there are alterations or dysregulations of glutamate transporters in Nestin-GAC mouse is of equal importance. Glutamate transporters are of prominence for glutamate uptake and regulating glutamate homeostasis [135]. Therefore, they serve as critical buffer against excitotoxicity in the brain. Previous studies have revealed that deregulation or loss of function of glutamate transporters EAAT1 and EAAT2 located on astrocytes augments neural inflammation and neurotoxicity [136, 137]. Enhancing EAAT1 activity is able to diminish neural damage and recover cognitive impairment [138, 139].

Taken together, the study in this chapter suggests that dysregulated glutaminase under pathological conditions can be an important novel

therapeutic target for reversing HAND progressions and HAND-related complications. Because of that, to develop glutaminase inhibitors that target specific isoform of the enzyme and target specific cell types are one of the promising approaches for next step. Likewise, genetic approaches aiming to knock down the expression levels of glutaminase in specific types of cells have also been proposed as a promising therapeutic approach.

3.6 Tables and Figures

GAC c	GCTGTTAATGACCTGGGAACTG
GAC d	GTACCTCGAGCATCTCTAGCTCCTCTCCC
Cre F	GCGGTCTGGCAGTAAAAACTATC
Cre R	GTGAAACAGCATTGCTGTCACTT

Table 3.1 Primers used for the genotyping of Nestin-GAC mouse. Two sets of primers were used to determine the genotype of Nestin-GAC mouse. GAC c and GAC d were used to determine the presence of *Gac* gene. Cre F and Cre R were used to determine the presence of *Cre*.

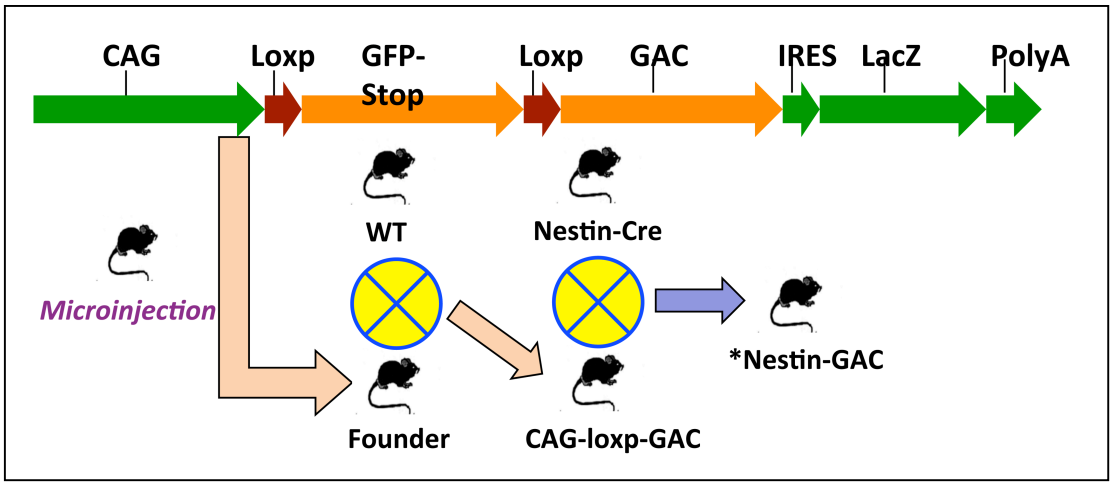

Figure 3.1 Schematic picture of Nestin-GAC mouse generation. The mouse *Gac* gene was cloned from a C57 mouse cDNA library and was inserted into the pCAG-Loxp-STOP-Loxp-IRES-LacZ plasmid at restriction enzyme site XhoI. The constructed plasmid was sequenced to ensure that only plasmids with *Gac* forwardly inserted. The selected plasmid was linearized and the linearized plasmid was microinjected into the fertilized egg for implantation into a pseudopregnant female to create CAG-loxp-GAC mouse in the Mouse Genome Engineering Core Facility of UNMC. GFP expressions in the brains of CAG-loxp-GAC mice were examined to ensure the stable expressions of the constructed plasmid. The CAG-loxp-GAC mice were then mated with a *nestin* promoter-driven *cre* transgenic mouse (Nestin-Cre mouse) line (in which the *cre* activity is confined to CNS) to produce Nestin-GAC mice.

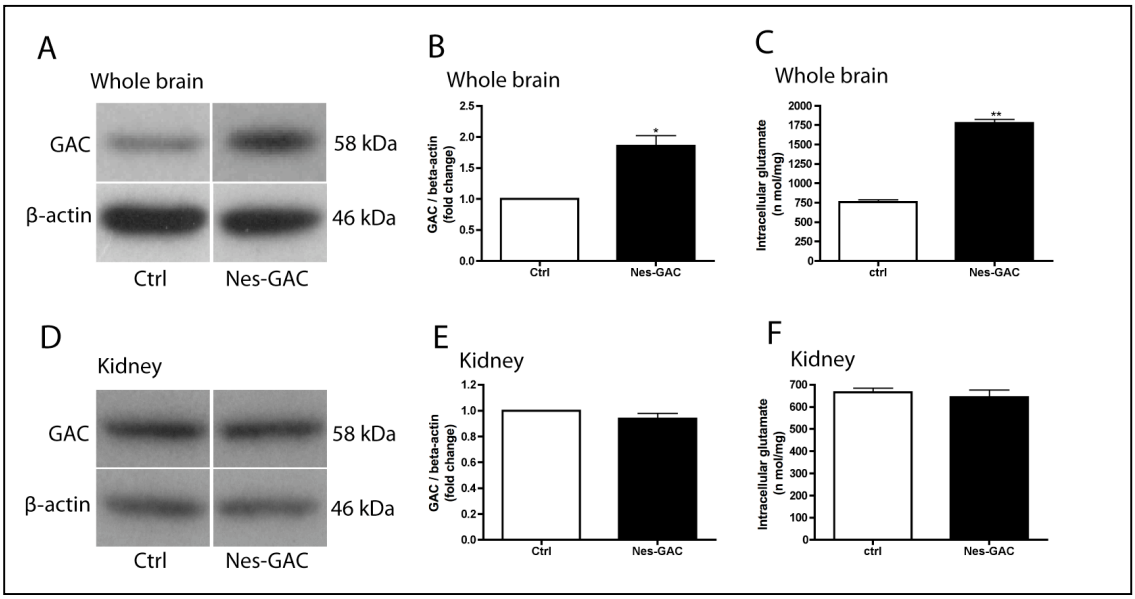

Figure 3.2 GAC overexpression was specific to brain in Nestin-GAC mice. A-B). Whole brain lysates from Nestin-GAC and their control littermates were collected and the expression levels of GAC were determined by Western blot. Representative blots of GAC expression are shown (A). Quantification data were normalized to beta-actin and presented as fold changes compared to control mice (B). C). Intracellular glutamate levels of whole brain lysates were determined using the Amplex Red Glutamic acid / Gutamate oxidase Assay Kit. D-E). Protein lysates from kidneys were collected and the expressions of GAC were determined by Western blot. Representative blots of kidney GAC expressions are shown (D). Quantification data were normalized to beta-actin and presented as fold changes compared to control mice (E). F). Intracellular glutamate levels of kidney lysates were tested using the Amplex Red Glutamic acid / Gutamate oxidase Assay Kit. Data are shown as the means ± SEM. * $P < 0.05$, ** $P < 0.01$, compared with control mice, N = 4.

Figure 3.3 GAC overexpression was confirmed in different areas of Nestin-GAC mouse brain. A-B). Proteins lysates were prepared from different areas of mice brains and the expression levels of GAC were determined by Western blot. Representative blots are shown (A). Quantification data were normalized to beta-actin and presented as fold changes compared to control mice (B). C). Intracellular glutamate levels of dissected brain tissues were tested using the Amplex Red Glutamic acid / Gutamate oxidase Assay Kit. D-E). The expression levels of GLS1 in hippocampi were visualized by immunofluorescence. Representative pictures are shown (D) and the GLS1 fluorescence intensities were quantified (E). Data are shown as the means ± SEM. * $P < 0.05$, ** $P < 0.01$, *** $P < 0.001$ compared with control mice, N = 4 for Nestin-GAC and control mice.

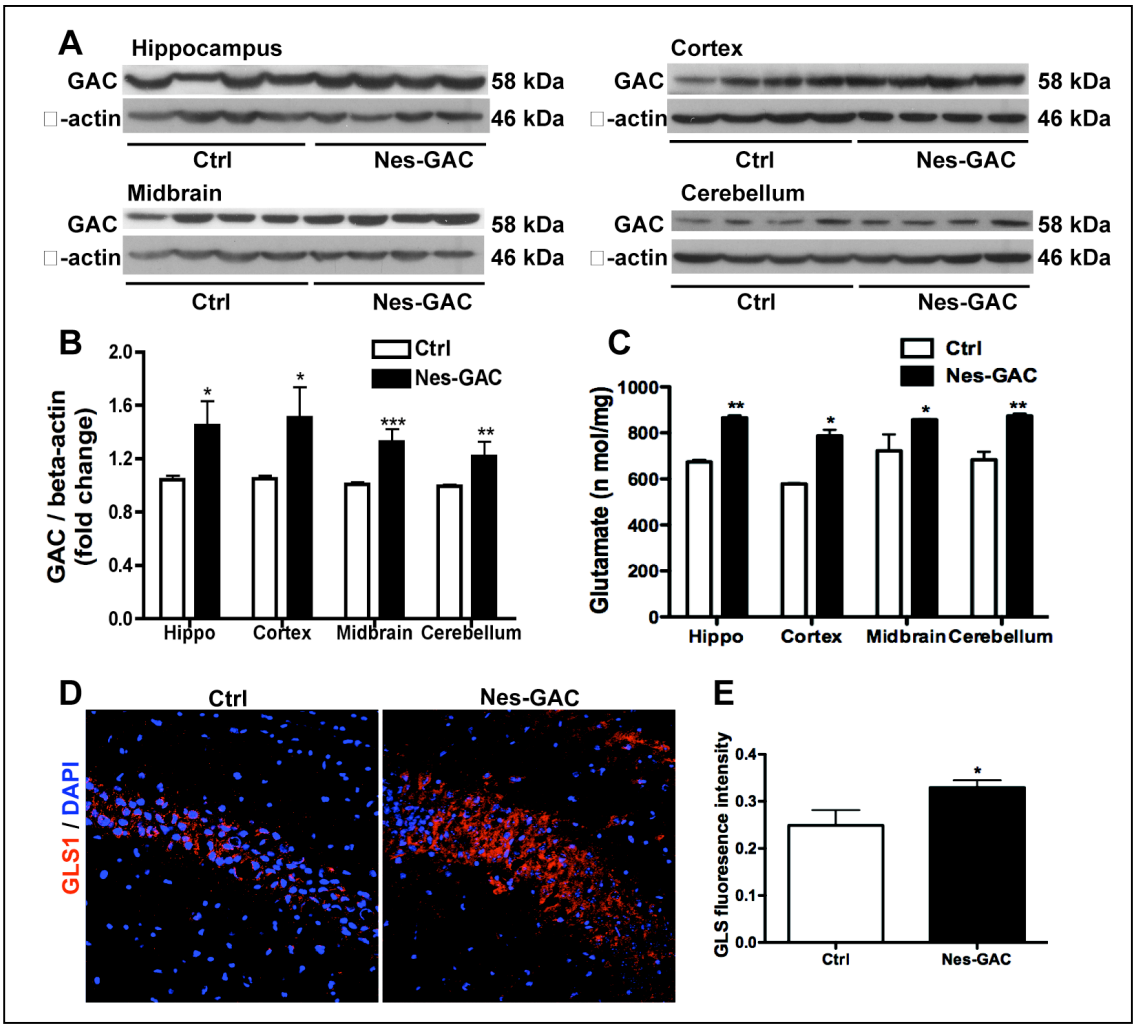
A
Hippocampus
GAC
58 kDa
-actin
46 kDa
Ctrl
Nes-GAC
Cortex
GAC
58 kDa
-actin
46 kDa
Ctrl
Nes-GAC
Midbrain
GAC
58 kDa
-actin
46 kDa
Ctrl
Nes-GAC
Cerebellum
GAC
58 kDa
-actin
46 kDa
Ctrl
Nes-GAC
B
GAC / beta-actin (fold change)
2.0
1.6
1.2
0.8
0.4
0.0
Ctrl
Nes-GAC
*
*
***
**
Hippo
Cortex
Midbrain
Cerebellum
C
Glutamate (n mol/mg)
1000
800
600
400
200
0
Ctrl
Nes-GAC
**
*
*
**
Hippo
Cortex
Midbrain
Cerebellum
D
Ctrl
Nes-GAC
GLS1 / DAPI
E
GLS fluoresence intensity
0.4
0.3
0.2
0.1
0.0
*
Ctrl
Nes-GAC

Figure 3.4 Nestin-GAC mice exhibited impairments in learning and memory. A-E). Morris-Water-Maze test was utilized to examine the spatial learning of memory of Nestin-GAC mice. During the training phase, Nestin-GAC mice exhibited longer escape latency (A), travelled longer distance to reach platform (B), but exhibited similar swimming velocities (C). During probe test, Nestin-GAC mice spent less time in the target quadrant (D) and had fewer crossings of the target place (E). F). Cued-Fear-Conditioning test was utilized to examine memory of Nestin-GAC mice. Nestin-GAC mice displayed lower percentages of freezing on last day of the test. Data are shown as the means ± SEM. * $P < 0.05$, ** $P < 0.01$, *** $P < 0.001$, compared with control mice, N = 9 for control, N = 7 for Nestin-GAC.

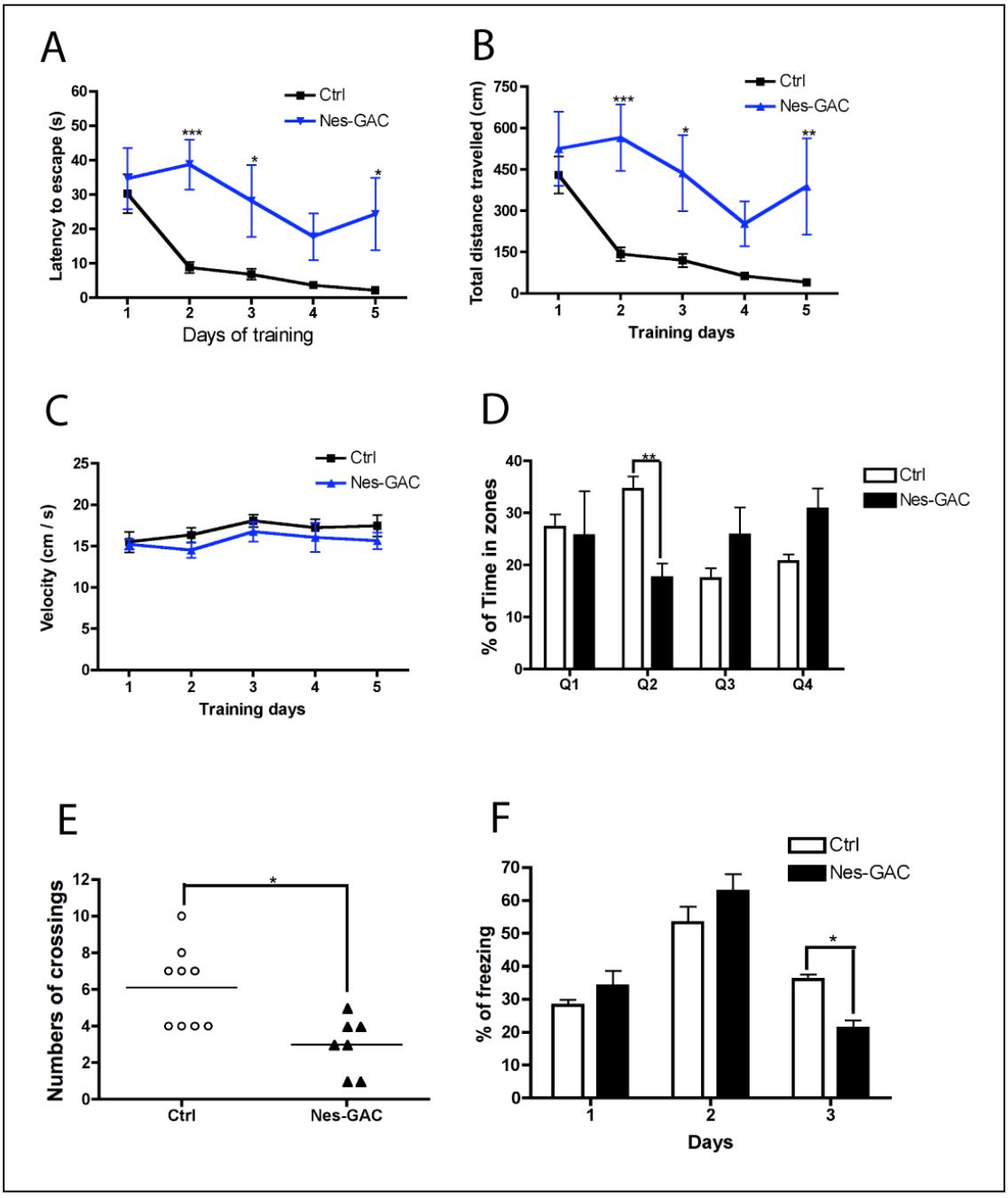
A
Latency to escape (s)
Ctrl
Nes-GAC
Days of training
B
Total distance travelled (cm)
Training days
C
Velocity (cm / s)
Training days
D
% of Time in zones
Q1
Q2
Q3
Q4
E
Numbers of crossings
Ctrl
Nes-GAC
F
% of freezing
Days

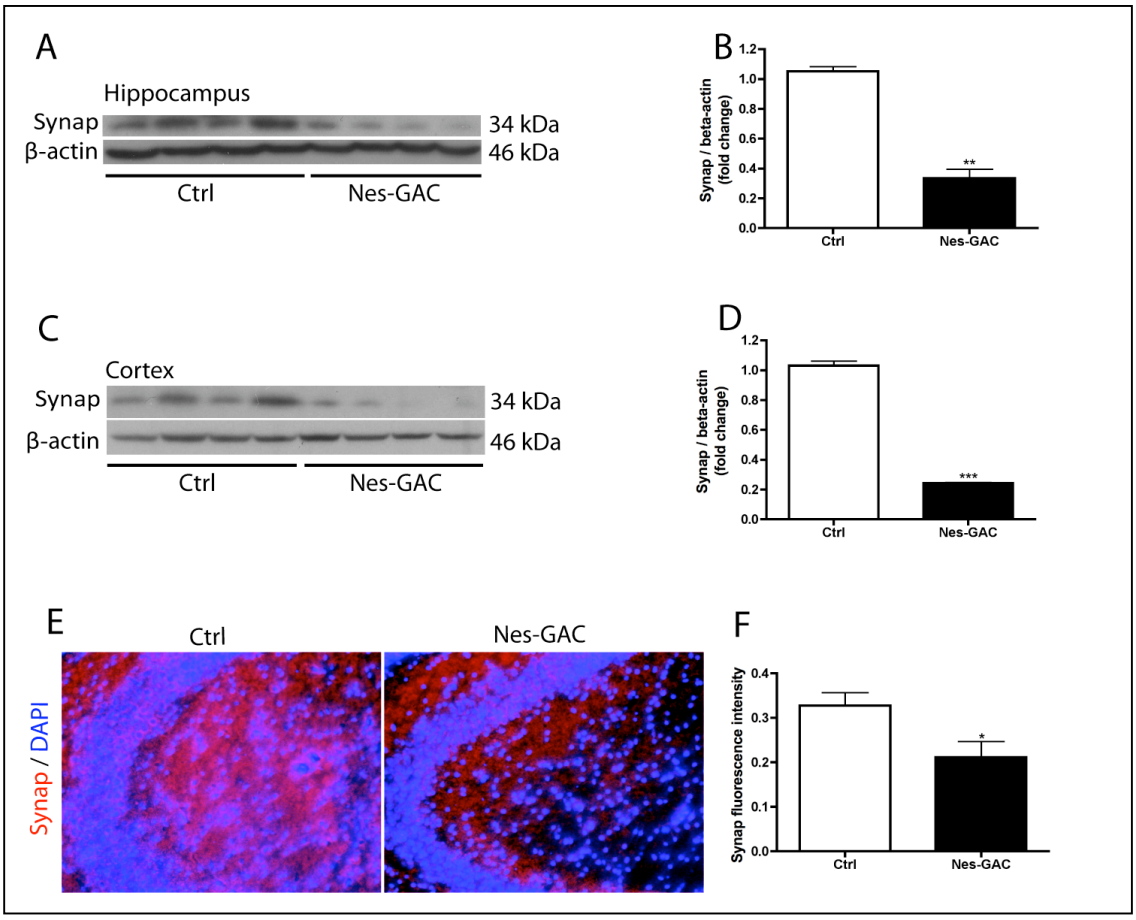

Figure 3.5 Brain-specific GAC overexpression led to synaptic damage in mice. A-D). Expression levels of synaptic marker Synaptophysin (Synap) were determined by Western blot. Nestin-GAC mice exhibited decreased protein levels of Synap in hippocampus (A, B) and in cortex (C, D). E-F). Expression levels of Synaptophysin in hippocampus were visualized and analyzed by immunofluorescence. Representative pictures are shown (E) and the fluorescence intensities of Synaptophysin were quantified (F). Data are shown as means ± SEM of 3 brain slices in each of the 4 control or Nestin-GAC mice. * $P < 0.05$, ** $P < 0.01$, *** $P < 0.001$, compared with control mice, N = 4 for both Nestin-GAC and control mice.

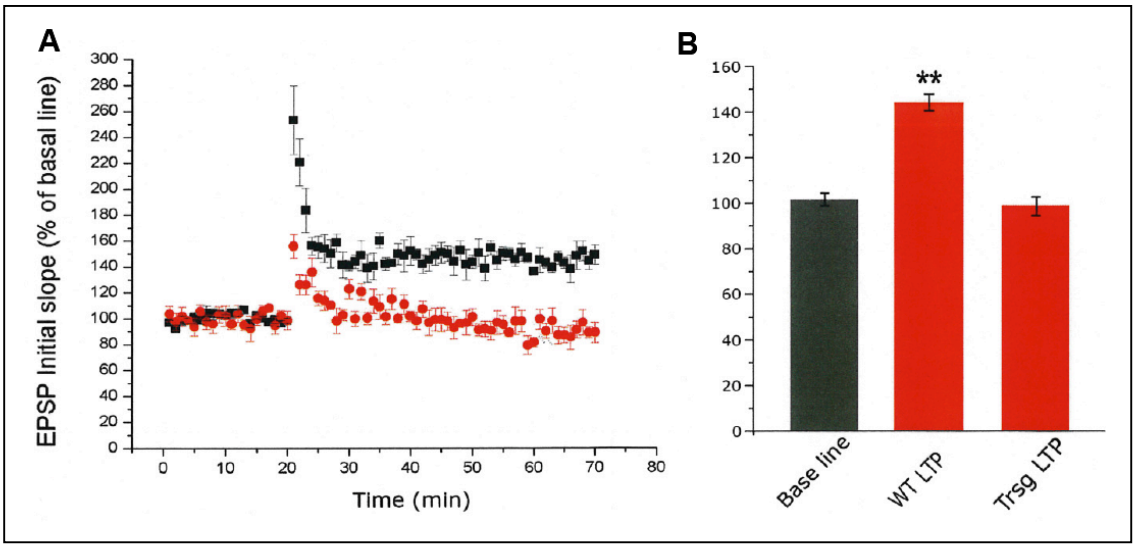

Figure 3.6 Nestin-GAC mice showed marked reduction in LTP. A-B). Hippocampi of Nestin-GAC mice were recorded for evoked fEPSPs by stimulus bursts and fEPSPs evoked by HFS. Data points represent means ± SEM of 10 brain slices. **, $P < 0.01$, compared with that of control mice.

Figure 3.7 Brain-specific GAC overexpression increased apoptosis in mouse brain. A-F). Expression levels of apoptosis marker cleaved-PARP (c-PARP) and cleaved Caspase 3 (c-Cas) were determined by Western blot. Nestin-GAC mice exhibited increased protein levels of c-PARP and c-Cas in hippocampus (A, B, C) and in cortex (D, E, F). G-H). TUNEL positive cells in mice hippocampi were visualized and analyzed. Representative pictures are shown (G) and the fluorescence intensities of TUNEL were quantified (H). Data are shown as the means ± SEM of 3 brain slices in each of the 4 control or Nestin-GAC mice. * $P < 0.05$, ** $P < 0.01$, *** $P < 0.001$, compared with control mice, N = 4 for both Nestin-GAC and control mice.

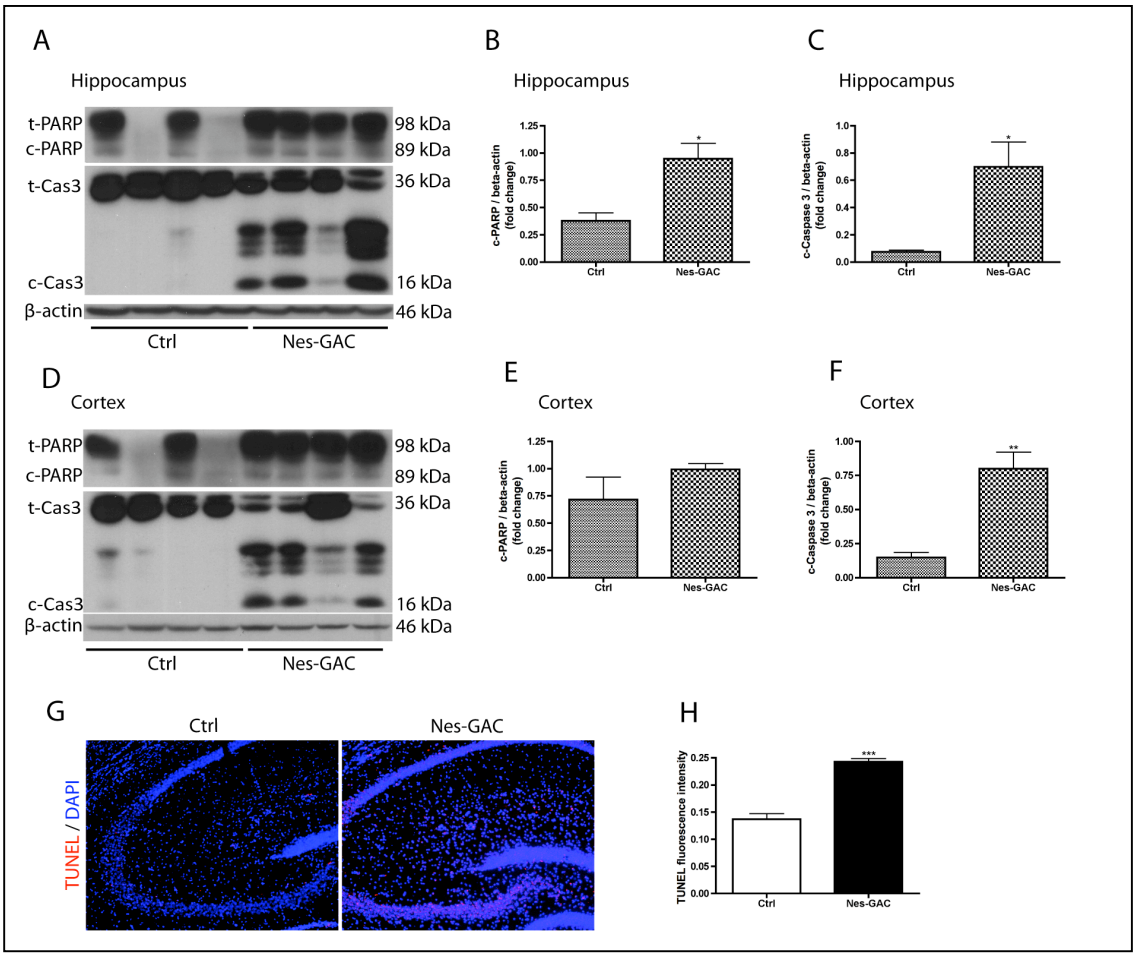
A
Hippocampus
t-PARP
c-PARP
t-Cas3
c-Cas3
β-actin
98 kDa
89 kDa
36 kDa
16 kDa
46 kDa
Ctrl
Nes-GAC
B
Hippocampus
c-PARP / beta-actin (fold change)
C
Hippocampus
c-Caspase 3 / beta-actin (fold change)
D
Cortex
E
Cortex
F
Cortex
G
Ctrl
Nes-GAC
TUNEL / DAPI
H
TUNEL fluorescence intensity

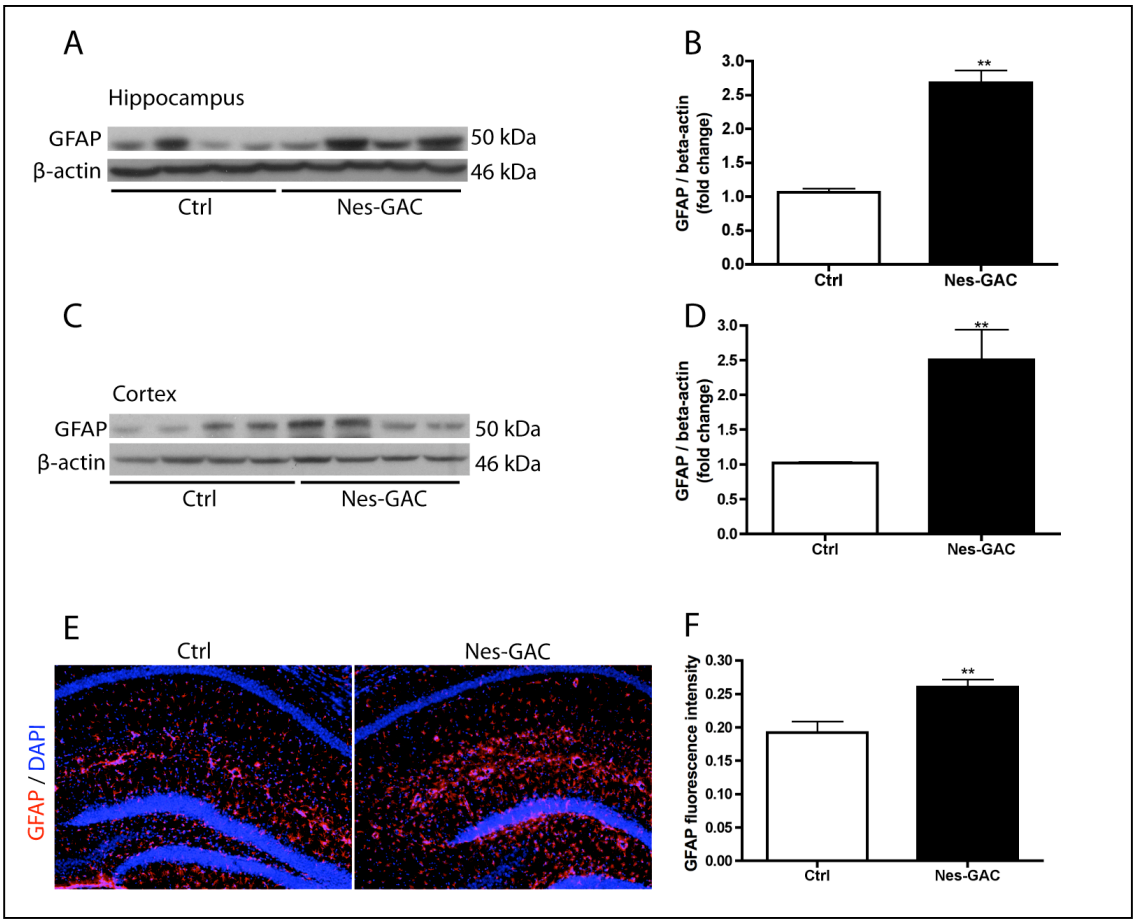

Figure 3.8 Brain-specific GAC overexpression led to reactive astrogliosis in mice. A-D). Expression levels of astrocyte marker GFAP were analyzed by Western blot. Nestin-GAC mice exhibited increased levels of GFAP in hippocampus (A, B) and in cortex (C, D). E-F). The expressions of GFAP in mice hippocampi were visualized and analyzed by immunofluorescence. Representative pictures are shown (E) and the fluorescence intensities of GFAP were quantified (F). Data are shown as the means ± SEM of 3 brain slices in each of the 4 control or Nestin-GAC mice. * $P < 0.05$, ** $P < 0.01$, compared with control mice, N = 4.

Chapter 4

GLS1 is Essential for the Differentiation, Survival and Proliferation of Human Neural Progenitor Cells

Portions of this chapter are excerpted from STEM CELLS AND DEVELOPMENT, Nov. 15, 2014, pp. 2782-2790

4.1 Abstract

Glutaminase is the enzyme that converts glutamine into glutamate, which serves as a key excitatory neurotransmitter and one of the energy providers for cellular metabolism. Previous studies have revealed that dysregulation of glutaminase 1 (GLS1), the dominant isoform in brain and kidney, has a causal effect on brain inflammation, neurotoxicity, and cognitive impairment. Therefore, we hypothesize that knocking down GLS1 will reduce toxicity and moderate the pathogenic progress. Using a human neural progenitor cell (NPC) model, we found that both GLS1 isotypes, kidney-type glutaminase (KGA) and glutaminase C (GAC), were upregulated during neuronal differentiation, which were correlated with the expression of neuronal marker microtubule-associated protein 2 (MAP-2). To study the functional impact of GLS1, we used small interference RNA targeting GLS1 and determined the expressions of neuronal genes by Western blot, Real-time PCR and immunocytochemistry. However, siRNA silencing of GLS1 significantly reduced the expression of MAP-2, indicating that GLS1 is essential for neurogenesis. To unravel the specific process(es) of neurogenesis being affected, we further studied the proliferation and survival of NPCs *in vitro*. siRNA silencing of GLS1 significantly reduced the $Ki67^+$ and increased the $TUNEL^+$ cells, suggesting a critical roles of GLS1 for the proliferation and survival of NPCs. Together, these data suggest that GLS1 is critical for proper functions of NPC, including neuronal differentiation, proliferation, and survival, thus complete knockdown of GLS1 in CNS to reduce toxicity is not applicable.

4.2 Introduction

Neural stem/progenitor cells (NPCs) are multipotent self-renewal cells with the capabilities of differentiation into neurons, astrocytes, and oligodendrocytes [140]. Neurogenesis, the process by which new neurons are generated, is a coordination of NPC self-renewal, survival, migration, proliferation, cell fate commitment, neuronal differentiation, and finally the integration of the newborn neurons into the existing networks [141, 142]. Neurogenesis is vigorous throughout embryonic brain but confined to specific brain areas in adulthood [142-144]. Attenuated neurogenesis leads to brain malformations, disruption of neural signal transduction and cognitive impairment [145-147]. This suggests that neurogenesis is indispensable to brain development, homeostasis and activity. Restricted neurogenesis in the adult brain has posted a big challenge for the brain regeneration after injuries, damage and diseases [148-153]. Therefore, extensive research is being conducted to identify endogenous factor(s) involved in neurogenesis.

Glutaminase 1 (GLS1) is an enzyme that catalyzes the deamination of glutamine to produce glutamate [154]. In the central nervous system (CNS), glutaminase 1 (GLS1) is expressed at predominant levels, especially in neurons [74] when compared with GLS2 [72]. In mouse, GLS1 begins to express at embryonic day 11.5 (E11.5) revealed by *in situ hybridization* (http://developingmouse.brain-map.org/gene/show/14436). The expression of GLS1 gose higher during brain development and reaches the plateau before birth (at E18.5). GLS1's expression remains high in postnatal mouse brain.

Kidney-type glutaminase (KGA) and glutaminase C (GAC) are two splice variants of GLS1 [76].

The product of glutaminase-modulated glutamine deamination is glutamate, a classical and the most abundantly used excitatory neurotransmitter. Glutamate has long been implicated in the generation and maturation of neurons [155-158]. Particularly, *in vitro* study on NPC has revealed the crucial role of glutamate in neuronal differentiation via the mediation of AMPA receptors [157]. However, the *in vivo* effect of glutamate on neurogenesis remains incompletely understood. Glutamate has been indicated to be beneficial for neurogenesis [159, 160], but studies on different anatomical areas in mammalian brain and using different experimental approaches yielded discrepant results [155]: moderate dose of glutamate (50 μM) applied to mouse brain slice cultures increased cellular proliferation in the ventricular zone but decreased NPC proliferation in the subventricular zone [158]. However, high dose of glutamate (300 μM) applied to brain slice culture decreased cellular proliferation and survival in the ventricular zone [159].

Our previous data revealed a pathogenic role of overexpressed brain GLS1 in brain inflammation, neurotoxicity and cognitive impairment. Thus we hypothesize that by knocking down GLS1 in the brain cells we will be able to reduce brain inflammation and reduce neurotoxicity. However in this study, we report that GLS1 is an essential enzyme for the neuronal differentiation, proliferation, and survival of human neural progenitor cells *in vitro*, thus complete knockdown of GLS1 in the brain is not applicable.

4.3 Materials and methods

Culture of human NPC

Human fetal brain tissue (12-16 weeks post-conception) was obtained from elective abortions done at the University of Washington in complete compliance with National Institute of Health (NIH), University of Nebraska Medical Center (UNMC) and University of Washington ethical guidelines. Human cortical NPCs were isolated from human fetal brain tissue as previously described [161]. Briefly, isolated NPCs were cultured in substrate-free tissue culture flasks and grown to neurospheres in the neurosphere initiation medium (NPIM), which is composed of X-Vivo 15 (BioWhittaker, Walkersville, ME) with N2 supplement (Gibco BRL, Carlsbad, CA), neural cell survival factor-1 (NSF-1, Bio Whittaker), basic fibroblast growth factor (bFGF, 20 ng/ml, Sigma-Aldrich, St. Louis, MO), epidermal growth factor (EGF, 20 ng/ml, Sigma-Aldrich), leukemia inhibitory factor (LIF, 10 ng/ml, EMD Millipore Corporation, Billerica, MA), and 60 ng/ml N-acetylcysteine (Sigma-Aldrich). Cells were passaged every two weeks as previously described [161].

Neuronal differentiation of NPC

Differentiation of NPCs to neurons was performed according to the standard procotol as previously described [161]. Briefly, mechanically- and trypsin-dissociated NPCs were plated on poly-D-lysine-coated 24-well plates in NPIM for 24 hours. Cells were then changed to serum-free Neurobasal medium (Gibco BRL) supplemented with B27 (NB27 medium, Gibco BRL) and glutamine (Sigma-Aldrich). Cells were subsequently collected for RNA or protein analyses,

or fixed for immunocytochemistry after neuronal differentiation for specific days as indicated in the figure legends.

siRNA silencing of GLS1

siRNA silencing of GLS1 in NPCs was performed according to the standard protocol as previously described [162]. Briefly, siRNA targeting GLS1 (ID# s5840) was purchased from Applied Biosystems Inc. (Foster City, CA, USA). Before plated-NPCs were changed into serum-free Neurobasal medium for neuronal differentiation, cells were transfected by 100 nM siRNA duplexes for 24 hours with the presence of siIMPORTER (Upstate Cell Signaling Solutions, Charlottesville, VA) according to the manufacturer's instructions. Non-specific control siRNA from Applied Biosystems Inc. (ID# AM4635) was transfected with the same concentration as controls to GLS1 siRNA.

Protein extraction and Western blot

Cells were rinsed twice with 1 X PBS and subsequently lysed by M-PER Protein Extraction Buffer (Pierce, Rockford, IL) containing 1× protease inhibitor cocktail (Roche). Protein concentrations were determined by the BCA Protein Assay Kit (Pierce). Proteins (20-30 μg) from cell lysates were separated by sodium dodecyl sulfate-polyacrylamide gel electrophoresis (SDS-PAGE). After being electrophoreticly transferred to the polyvinyldifluoridene (PVDF) membranes (Millipore and Bio-Rad), proteins were incubated with purified primary antibodies for MAP-2 (mouse, cat#MAB3418, Millipore, 1:1000), KGA (rabbit, Dr. N. Curthoys, Colorado State University, Fort Collins, CO, 1:1000), GAC (rabbit, Dr. N. Curthoys, Colorado State University, 1:500), GAD67

(mouse, cat#MAB5406, Millipore, 1:500), PARP (rabbit, cat# 9542s, Cell Signaling Technologies, Beverly, MA, 1:1000), or β-actin (Sigma-Aldrich) overnight at 4 ^{o}C followed by a horseradish peroxidase-linked secondary anti-rabbit or anti-mouse antibody (Cell Signaling Technologies, 1:10,000). Antigen-antibody complexes were visualized by Pierce ECL Western Blotting Substrate (Pierce). For data quantification, films were scanned with a CanonScan 9950F scanner; the acquired images were then analyzed on a Macintosh computer using the public domain NIH Image J program (at http://rsb.info.nih.gov/nih-image/).

RNA extraction and TaqMan real-time quantitative RT-PCR

RNA was extracted with TRIzol Reagent (Invitrogen Corp, Carlsbad, CA, USA) and RNeasy Kit according to the manufacturer's protocol (Qiagen Inc., Valencia, CA, USA). Primers used for real-time reverse-transcription polymerase chain reaction (real-time RT-PCR) were KGA (ID# 489954: forward sequence 5-CGAAGATTTGCTTTGTCAGCTATGG-3, reverse sequence 5-CTCTGCAGCAGCTACATGGA-3, probe sequence 5-CAGCGGGACTATGATTC-3), GAC (ID# 528445: forward sequence 5-TATGGAAAAAAGTGTCACCTGAGTCA-3, reverse sequence 5-GCTTTTCTCTCCCAGACTTTCCATT-3, probe sequence 5'-AATGAGGACATCTCTACAACTGTA-3), microtubule-associated protein 2 (MAP-2) (ID# hs00258900) and GAPDH (ID# 4310884E) were commercially available at Applied Biosystems Inc. Real-time RT-PCR was completed using the One-step quantitative TaqMan assay in a StepOne^{TM} Real-Time PCR

system (Applied Biosystems Inc.). Relative MAP-2, KGA and GAC mRNA levels were determined and standardized with a GAPDH internal control using the comparative ΔΔCT method. All primers used in the study were previously tested for amplification efficiencies and the results were confirmed similar.

Immunocytochemistry

Cells were fixed in 4% PFA and washed in PBS as previously described [161]. Cells were subsequently incubated overnight at 4 ^{o}C with primary antibodies, followed by goat anti-mouse IgG Alexa Fluor 488 secondary antibodies (Molecular Probes, Eugene, OR, 1:1000) for 1 hour at room temperature. Primary antibodies included mouse MAP-2 (Millipore, 1:500), rabbit GFAP (Dako, Carpinteria CA, 1: 2000) and mouse anti-Ki67 (BD Biosciences, San Diego, CA, 1:500). All of the antibodies were diluted in in PBS containing 0.1% Triton X-100 and 2% BSA. Cells were counterstained with DAPI (Sigma-Aldrich, 1:1000) to identify the nuclei. Morphological changes of cells were visualized and captured with a Nikon Eclipse E800 microscope equipped with a digital imaging system, or a Zeiss META 510 confocal microscope (Carl Zeiss MicroImaging, LLC). Images were imported into Image-Pro Plus, version 7.0 (Media Cybernetics, Sliver Spring, MD) for quantification purpose. A total of 500-1000 immunostained cells from 10 random fields per well were manually counted using magnifications of 20X objective lens.

Glutamate analyses

The glutamate levels in the cells were determined using the Amplex Red Glutamic acid / Gutamate oxidase Assay Kit (invitrogen) based on the

manufacturer's instruction. Cell lysates were diluted to the same protein concentration before starting the assay.

In situ TUNNEL assay

Primary human NPCs were transfected by control siRNA or GLS1 siRNA. Three days after transfection, cells were fixed and stained with an *in situ* TUNEL assay (Roche Diagnostics, Indianapolis, IN). TUNEL positive NPCs and total cell numbers were counted after acquiring 10 random images from immunostained fields using a Nikon Eclipse TE2000E microscope. A minimum of 10 fields was counted for each group of treatment.

Statistical analyses

Data were shown as means ± SEM and analyzed. The data were evaluated statistically by the analysis of variance (ANOVA) followed by Tukey-test for pairewise comparisons. Two-tailed Student's t test was used to compare means of two treatment groups. Significance was considered when $P < 0.05$. All experiments were performed with at least three donors to account for any individual-specific differences. Assays were performed at least three times in triplicate or quadruplicate.

4.4 Results

GLS1 variants KGA and GAC are upregulated after neuronal differentiation

Human NPC were differentiated to neurons in adherent cultures for 2 weeks. Total protein and RNA were extracted at multiple time points, including day 0, 4, 7 and 13 after differentiation. The mRNA levels of the neuronal marker MAP-2 continued to increase throughout this period of time (Figure 4.1A), suggesting successful and continuous neuronal differentiation of the cultured cells. Interestingly, the mRNA levels of both KGA and GAC were upregulated during neuronal differentiation (Figure 4.1B-C). The mRNA levels of KGA were positively correlated with the MAP-2 levels (Figure 4.1D). Similarly, there were significant correlation between the mRNA levels of GAC and MAP-2 (Figure 4.1E).

In parallel to mRNA levels, the protein levels of MAP-2 continuously increased throughout the period of neuronal differentiation, confirming successful ongoing neuronal differentiation of the cultured cells (Figure 4.2A-B). Likewise, both KGA and GAC were upregulated during neuronal differentiation (Figure 4.2A, C-D). KGA protein had 3-fold and 4.5-fold upregulation at 7 days and 13 days after differentiation, respectively (Figure 4.2C). Similarly, GAC protein had 2-fold and 3.5-fold upregulation at 4 days and 7 days after differentiation, respectively (Figure 4.2D). The protein levels of KGA were positively correlated with the MAP-2 levels (Figure 4.2E). Similarly, there were significant positive correlation between the protein levels of GAC and MAP-2

(Figure 4.2F). Together, the upregulation of KGA and GAC and their correlation with MAP-2 during neuronal differentiation suggests that KGA and GAC may be required for NPC to differentiate into neurons.

siRNA silencing of GLS1 impairs neuronal differentiation

To test whether KGA and GAC were required for neuronal differentiation, we used siRNA to specifically silence GLS1 expression in NPC. The GLS1 siRNA-transfected NPCs were induced to differentiate in neuronal media for 6 days. The knockdown of GLS1 was confirmed firstly through Real-time PCR, which demonstrated significant decreases of the mRNA levels of both KGA (Figure 4.3A) and GAC (Figure 4.3B) compared with the control siRNA group. The knockdown was further confirmed by Western blot as the protein levels of both KGA (Figure 4.4A-B) and GAC (Figure 4.4A, C) were significantly decreased in siGLS1 group. In addition, the glutamate levels were also found reduced in siGLS1 groups (Figure 4.4D). After siRNA knockdown of GLS1, MAP-2 mRNA and protein levels were reduced to greater than 50% of that in control siRNA-transfected cells (Figure 4.3C, Figure 4.4E). The reduction of the mature neuronal marker MAP-2 in GLS1-deficient cells indicates that GLS1 is required for neuronal differentiation.

To further characterize the morphological changes of neurons transfected by GLS1 siRNA, we labeled MAP-2 in the differentiated cultures through immunocytochemistry (Figure 4.5A). Human NPCs transfected with random control siRNA had approximately 70% of the cells positive for MAP-2 (Figure 4.5B) at 6 days after differentiation. However, NPCs transfected with siRNA

targeting GLS1 had significantly lower percentage (40%) of cells positive for MAP-2 (Figure 4.5B). The impairment was specific to neuronal differentiation because the astrocytes differentiation, as determined by GFAP immunostaining, did not appear to alter after GLS1 knockdown when compared with control siRNA group (Figure 4.5C). These data suggest that GLS1 is required for the formation of mature neurons.

siRNA silencing of GLS1 impairs NPC proliferation

NPC proliferation is also a key step of neurogenesis. To determine whether deficiency of GLS1 affected NPC proliferation, we transfected NPCs with siRNA targeting GLS1 and kept the culture in NPIM for 3 days. The decreases of KGA and GAC mRNA levels by GLS1 siRNA transfection in NPCs were confirmed by Real-time RT-PCR (Figure. 4.6A-B). Via immunocytochemistry that labeled the $Ki67^{+}$ cells, we were able to determine the levels of NPC proliferation in the culture. The percentage of Ki67-positive cells was significantly decreased when GLS1 was knocked down (Figure 4.6C-D). This suggests a critical role of GLS1 in the NPC pool expansion.

siRNA silencing of GLS1 impairs NPC survival

Next, we determined NPC survival after GLS1 was knocked down by siRNA. The levels of apoptosis were identified by Terminal deoxynucleotidyl transferase dUTP nick end labeling (TUNEL) assay. DNA fragmentation was detected by TUNEL through the labeling of the terminal end of nucleic acids. We applied TUNEL assay to undifferentiated NPCs kept in NPIM. siGLS1 significantly increased the percentage of TUNEL positive cells in the human

NPC culture, compared with siRNA control group (Figure 4.7A-B). Therefore, the TUNEL assay identified the existence of more cellular apoptosis when GLS1 was deficient. To further confirm the apoptosis, we examined poly ADP ribose polymerase (PARP) cleavage in the NPCs that are GLS1-deficient. PARP is deactivated and cleaved by activated caspase 3 (cleaved caspase 3) in the apoptosis cascade, thus cleaved PARP represents ongoing apoptosis. Western blot analysis revealed the presence of cleaved PARP in both control and GLS1 siRNA groups. However, Cleaved PARP was apparently at higher levels in GSL1 siRNA group compared with control siRNA group (Figure 4.7C-D). These data demonstrate the occurrence of cellular apoptosis after GLS1 was knocked down.

4.5 Discussion

Neurogenesis is a finely tuned and highly orchestrated process that includes maintaining and expansing the pool of neural stem/progenitor cells (NPC), migration of NPC, differentiation of NPC to neurons, neuronal survival and integration of newly-born neurons to the existing synaptic networks [145]. As a result, hindered or impaired neurogenesis often causes malformations of brain, disruptions of neural signal transduction, difficulties and deterioration of cognitive functions, as reviewed by Jessel and Sanes [141] [145-147]. Given the fundamental importance of neurogenesis to human health and diseases, factors involved in this process remain to be further illustrated. In the present study of this chapter, we show that GLS1 isoforms were upregulated and correlated with MAP-2 during neuronal differentiation (Figures 4.1-4.2). siRNA silencing of GLS1 in NPCs impaired their subsequent neuronal differentiation, suggesting GLS1 is critical for neuronal differentiation (Figures 4.3-4.5). Furthermore, we show reduced proliferation and increased apoptosis in GLS1-deficient cells, suggesting that GLS1 is required for NPC proliferation and survival (Figures 4.6-4.7). Collectively, we characterized GLS1 regulation in NPCs and identified GLS1 as a one of the essential factors for neurogenesis. Therefore, globally knocking down GLS1 is not applicable. The initial hypothesis that by knocking down GLS1 in brain will we be able to reduce brain inflammation and neurotoxicity relating to HAND needs even more detailed and comprehensive examinations.

GLS1 is an important mitochondrial enzyme for cell metabolism. Its expression increases during mammalian neural development and remains high in postnatal CNS, implying an essential role of GLS1 for neurogenesis. We report for the first time that deficiency of GLS1 leads to hindered NPC differentiation, impaired proliferation and undermined survival. This finding cross confirms the function of glutaminase on neurogenesis with the report that GLS2 contributes to neuronal differentiation [163]. Due to the fact that GLS1 is the dominant glutaminase isoform expressed in mammalian CNS compared with GLS2, tight-regulation of GLS1 is of critical importance to brain development.

The identification of GLS1's involvement in neurogenesis has an important clinical implication. GLS1, especially the GAC variant, has been revealed to regulate oncogenic transformation [164-166] or the progressions of excitotoxicity in HIV-1-associated neurocognitive disorders [84]. Therefore, inhibiting GLS1 may serve for therapeutic purpose in cancer treatment or neurodegenerative diseases. Indeed, inhibition of GLS1 by either a potent small-molecule pharmacological inhibitor or by siRNA knockdown slowed the growth of glioma cells [166], or prevented the oncogenic transformation of human breast cancer cells and B lymphoma cells [165]. Lack of one copy of *Gls1* has blunted the tumorigenesis in an immune-competent mouse model of hepatocellular carcinoma [167]. Also, knocking down GAC in HIV-infected microglia or macrophages alleviated the damage to neurons co-cultured [84]. However, although knocking down GLS1 by siRNA apparently provides benefits in cancer or neurodegerative diseases' therapies, our studies with NPC suggest

that it may have unintended consequences on neurogenesis and brain development as the properties and functions of NPCs were altered or impaired when GLS1 was deficient. Therefore, directing the GLS1 inhibitors or siRNA to the right area and specific cell type, and applying the inhibitors with right dose is of critical importance and requires further investigation. Moreover, *Gls1* KO mice were lethal at postnatal day 1 due to glutamatergic synaptic transmission disruptions [168], and *Gls1*$^{+/-}$ mice exhibited reduced hippocampal activity and developed schizophrenia-like symptoms [169]. These studies on GLS1 knockout (*Gls1* KO) mice are in agreement with our evaluation of the critical role of GLS1 on neurogenesis, particularly on the formation of neuronal maturation and neural connections.

Neuronal differentiation, NPC proliferation, and NPC survival, are three components of neurogenesis examined in the study of this chapter. How GLS1 functions to affect each of those components is currently unclear. However, there are some potential underlying pathways that GLS1 may take to assert its influential role. First, the product of GLS1-mediated deamination of glutamine, glutamate, is known to regulate neurogenesis. Interestingly, glutamate has been shown to possess dichotomous effects on neurogenesis, depending on its concentrations. Low-to-moderate concentrations of exogenous glutamate (10 μM) introduced to cell or brain slice culture led to increased NPC proliferation and neurogenic potentials [156-158], whereas high concentrations of exogenous glutamate (300 μM) introduction to culture resulted in impeded DNA synthesis and reduced cellular proliferation [170]. Second, excess glutamate has a direct

toxic effect on mature neurons [171-174]. Excess glutamate produced by immune-ativated macrophages and microglia has been documented in several neurodegenerative diseases, including Parkinson's disease, Alzheimer's disease, stroke, and HIV-associated neurocognitive dementia [84, 90]. Third, glutamate can serve as an alternative energy substrate for the TCA cycle. Therefore, GLS1 deficiency might have led NPC into a starvation-like state under which the normal activities like cellular proliferation and differentiation are weakened. In addition, cells lacking energy are known to switch to the apoptosis signaling cascade. It is likely that more than one pathway cross talks and plays out in the NPCs that are deficient of GLS1. More studies on glutamate signaling pathways leading to the impairment of NPC functions are needed.

In summary, our study demonstrated that GLS1 is essential for neurogenesis *in vitro*. These data suggest that globally knocking down GLS1 is not application and great caution should be taken when targeting GLS1 in cancer or neurogenerative disease therapy.

4.6 Figures

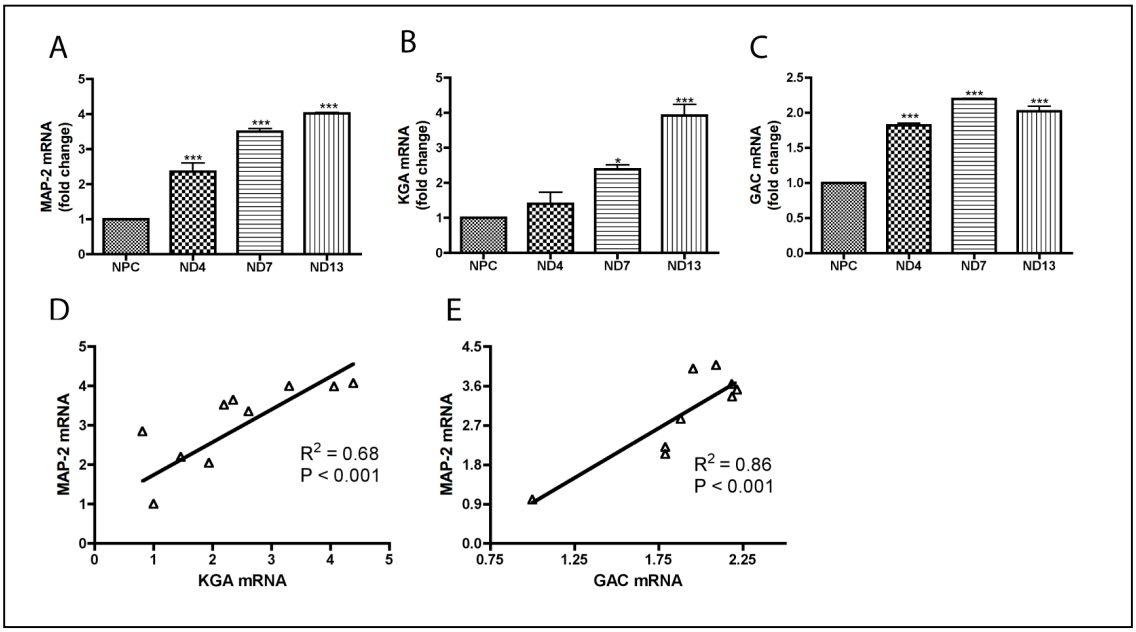

Figure 4.1 Transcript levels of GLS1 isoforms, KGA and GAC, were upregulated during NPC differentiation to neurons. (A-C) Human NPCs were exposed to neuron differentiation medium for differentiation. At 0, 4, 7, and 13 days after differentiation, mRNA was collected and expressions of MAP-2 (A), KGA (B), and GAC (C) were analyzed using Real-time RT-PCR. Data were normalized to GAPDH and presented as fold change compared to NPC. Data are shown as the means ± SEM of three independent experiments with three different donors. (D-E) Correlation of the gene mRNA levels of KGA (D) and GAC (E) with MAP-2 was determined by Spearman correlation. * denotes $P < 0.05$, *** denotes $P < 0.001$ compared with NPC, N = 3.

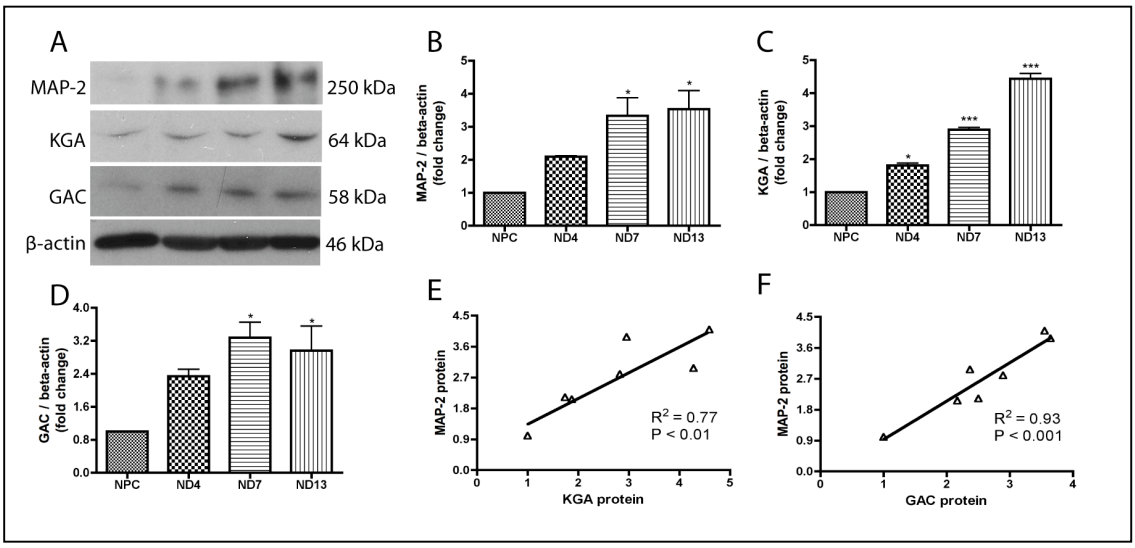

Figure 4.2 Protein levels of GLS1 isoforms, KGA and GAC, were upregulated during NPC differentiation to neurons. (A-D) Human NPCs were exposed to neuron differentiation medium for differentiation. At 0, 4, 7, and 13 days after differentiation, protein was extracted and expressions of MAP-2 (A-B), KGA (D), and GAC (D) were analyzed using Western blot. Data were normalized to beta-actin and presented as fold change compared to NPC. Data are shown as the means ± SEM of three independent experiments with three different donors. (E-F) Correlation of the protein levels of KGA (E) and GAC (F) with MAP-2 was determined by Spearman correlation. * denotes $P < 0.05$, *** denotes $P < 0.001$ compared with NPC, N = 3.

Figure 4.3 Lack of GLS1 impaired the expression of MAP-2 mRNA during neuronal differentiation. (A-C) Human NPCs were transfected by control siRNA or GLS1 siRNA and then exposed to neuron differentiation medium for 4 days and 6 days. mRNA was collected and the expressions of KGA at 4 days and 6 days (A), GAC at 4 days and 6 days (B), and MAP-2 at 4 days and 6 days (C) were analyzed using Real-time RT-PCR. Data were normalized to GAPDH and presented as fold changes. Data are shown as the means ± SEM of three different donors. * $P < 0.05$, ** $P < 0.01$, *** $P < 0.001$, compared with control siRNA group, N = 3.

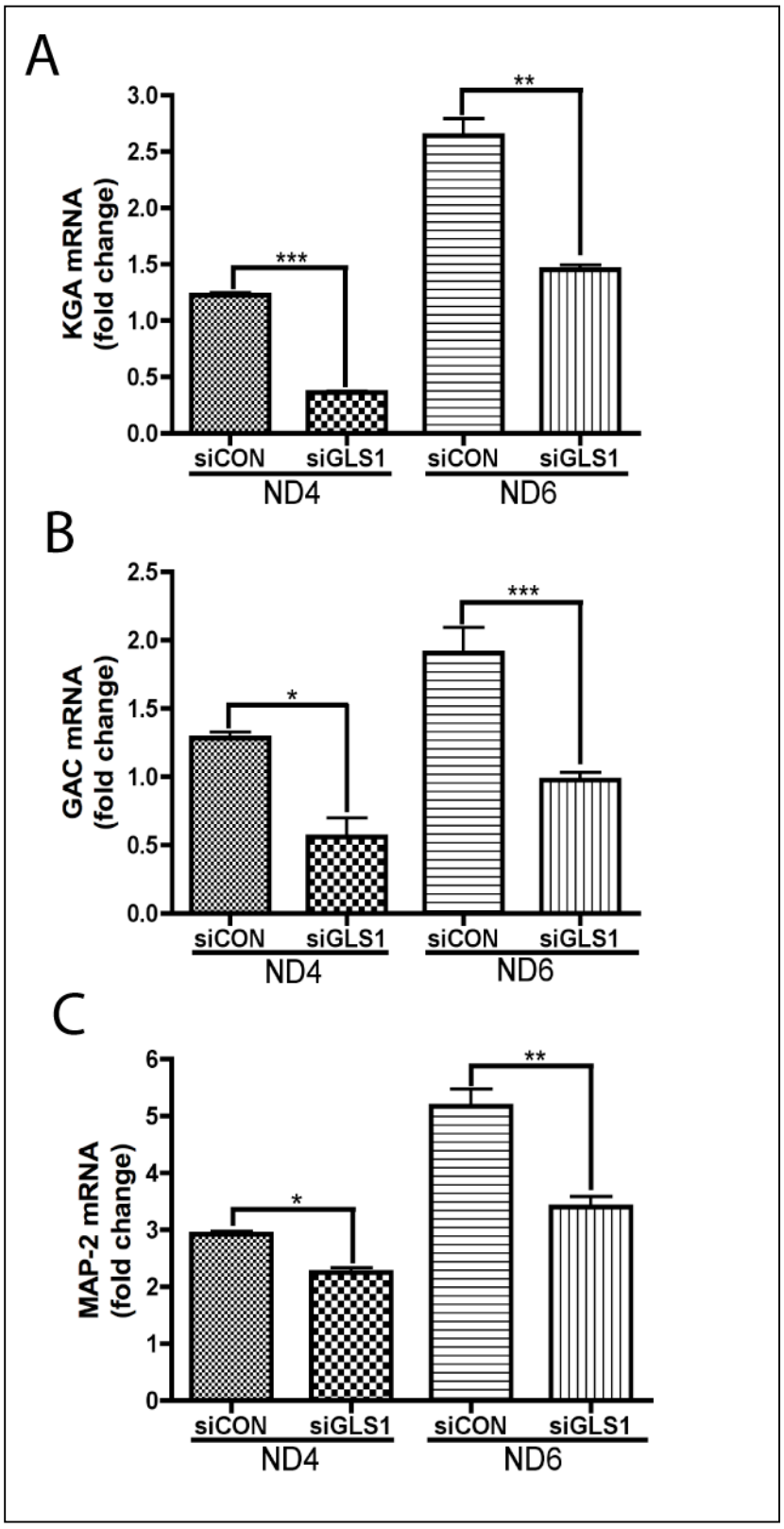
A
KGA mRNA (fold change)
3.0
2.5
2.0
1.5
1.0
0.5
0.0
***
**
siCON
siGLS1
siCON
siGLS1
ND4
ND6
B
GAC mRNA (fold change)
2.5
2.0
1.5
1.0
0.5
0.0
*
***
siCON
siGLS1
siCON
siGLS1
ND4
ND6
C
MAP-2 mRNA (fold change)
6
5
4
3
2
1
0
*
**
siCON
siGLS1
siCON
siGLS1
ND4
ND6

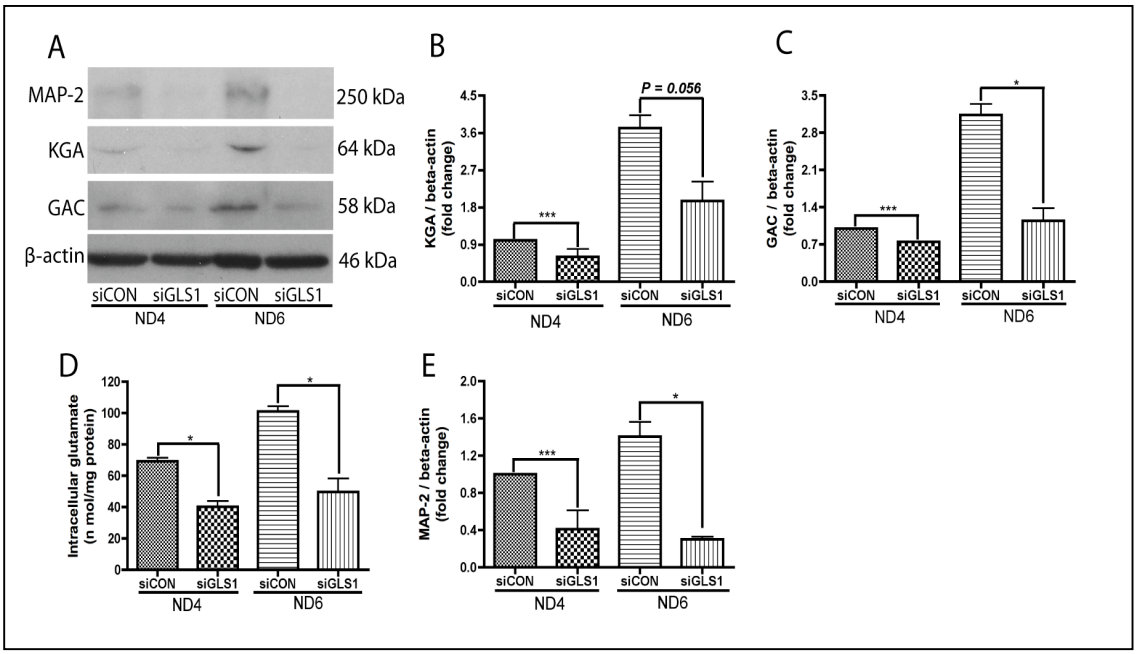

Figure 4.4 Lack of GLS1 impaired the expression of MAP-2 protein during neuronal differentiation. (A-E) Human NPCs were transfected by control siRNA or GLS1 siRNA and then exposed to neuron differentiation medium for 4 days and 6 days. Total protein was collected and the expressions of KGA at 4 days and 6 days (A-B), GAC at 4 days and 6 days (A, C), and MAP-2 at 4 days and 6 days (A, D) were analyzed using Western blot. Data were normalized to beta-actin and presented as fold changes. Intracellular glutamate levels were tested using the Amplex Red Glutamic acid / Gutamate oxidase Assay Kit (E). Data are shown as the means ± SEM of three different donors. * $P < 0.05$, ** $P < 0.01$, *** $P < 0.001$, compared with control siRNA group, N = 3.

Figure 4.5 Lack of GLS1 impaired neuronal differentiation. Human NPCs were transfected by control siRNA or GLS1 siRNA and then exposed to neuron differentiation medium for 6 days. The cultured cells were fixed and stained with MAP-2 to determine the levels of neuronal differentiation. (A) Representative pictures of MAP-2^+ (green) and $GFAP^+$ (red) were shown. Nuclei were labeled with DAPI (blue). (B-C) The percentages of MAP-2^+ cells (B) and $GFAP^+$ cells (C) were determined by counting the number of MAP-2^+ or $GFAP^+$ cells over the number of $DAPI^+$ cells in each microscopic field. Images were acquired from a Zeiss META 510 confocal microscope. Magnifications: 20X objective lens. Scale bar = 50 μm. Data are shown as means ± SEM of 10 fields in each experimental group for the three donors. *** $P < 0.001$, compared with control siRNA group, N = 3.

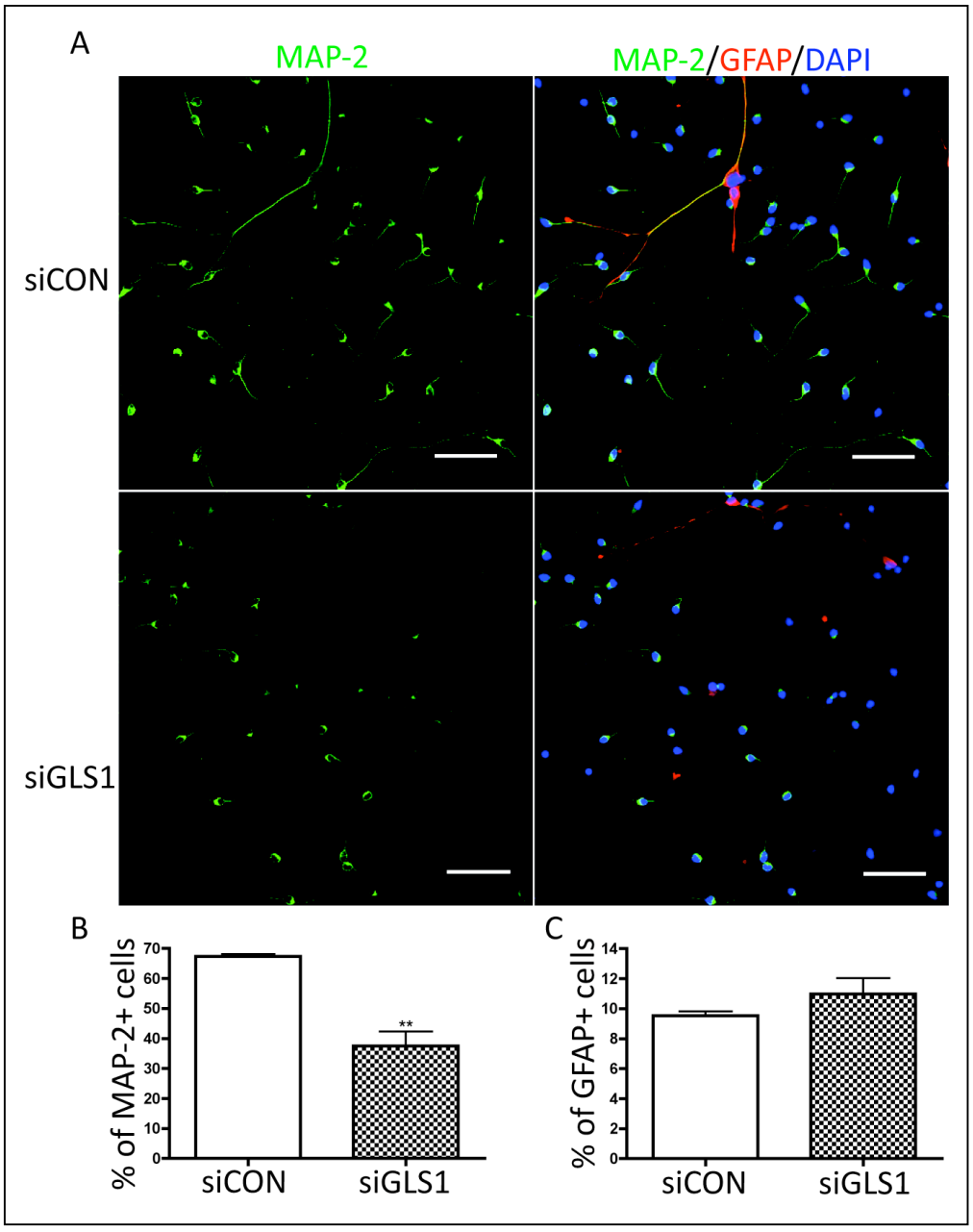
A
MAP-2
MAP-2/GFAP/DAPI
siCON
siGLS1
B
% of MAP-2+ cells
70
60
50
40
30
20
10
0
**
siCON
siGLS1
C
% of GFAP+ cells
14
12
10
8
6
4
2
0
siCON
siGLS1

Figure 4.6 GLS1 silencing reduced NPC proliferation. Human NPCs were transfected by control siRNA or GLS1 siRNA, then kept in NPIM for 3 days. NPC proliferation was determined by immuno-labeling the Ki67 of proliferating cells in each culture. (A-B) KGA and GAC mRNA levels were confirmed to be reduced in NPCs transfected by siGLS1 kept in NPIM. (C) Representative pictures of $Ki67^+$ (green) cells in control siRNA- and siGLS1-transfected NPC cultures were shown. Nestin (red) was used to label NPCs. Nuclei (blue) were labeled with DAPI. (D) The percentage of $Ki67^+$ cells was determined by counting the number of $Ki67^+$ cells over the number of $DAPI^+$ cells in each microscope field. Images were acquired from a Nikon Eclipse TE2000E fluorescent microscope. Magnifications: 20X objective lens. Scale bar = 50 μm. Data are shown as means ± SEM of 10 fields in each experimental group for the three donors. * $P < 0.05$, ** $P < 0.01$, *** $P < 0.001$, compared with control siRNA group, N = 3.

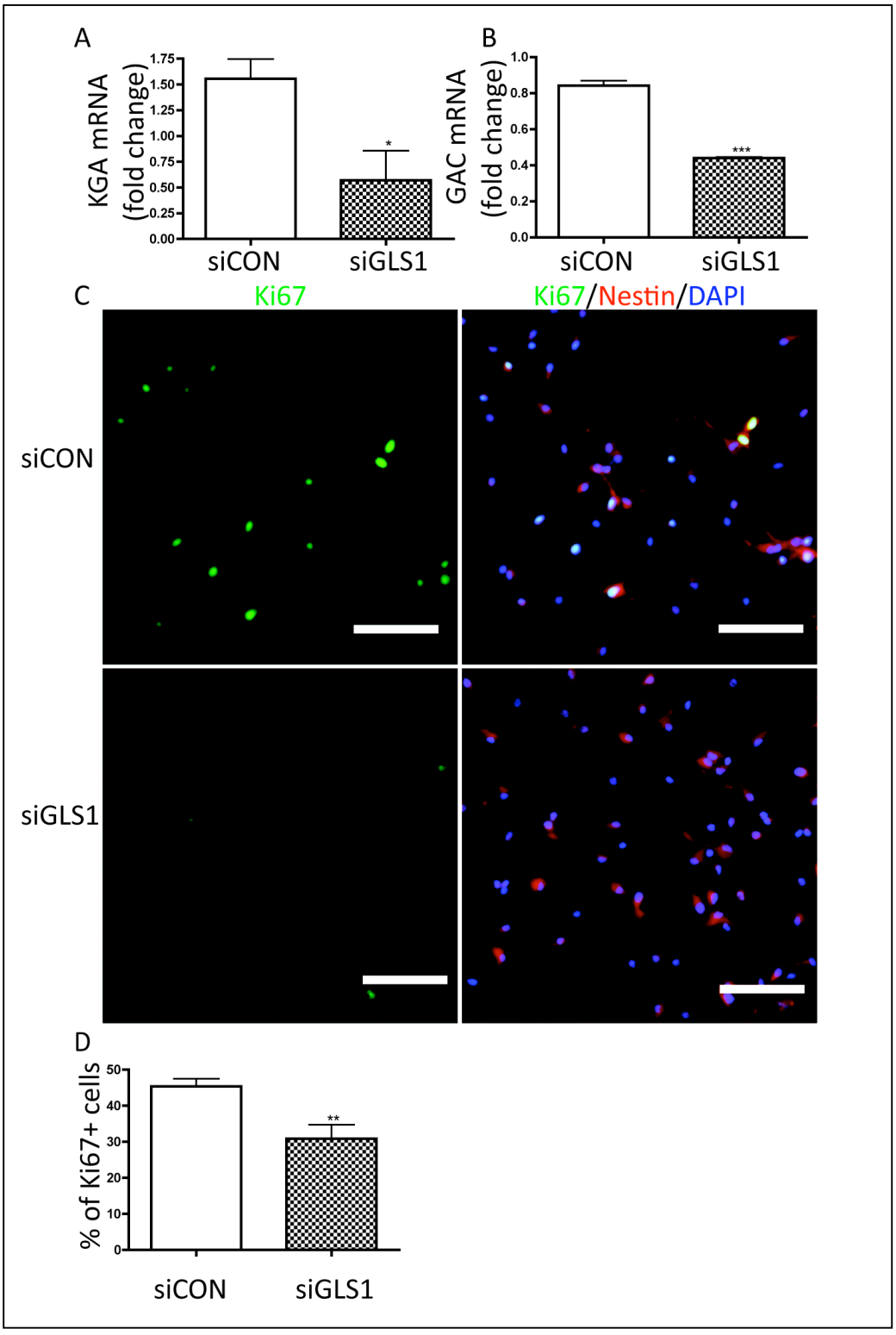
A
KGA mRNA (fold change)
1.75
1.50
1.25
1.00
0.75
0.50
0.25
0.00
*
siCON
siGLS1
B
GAC mRNA (fold change)
1.0
0.8
0.6
0.4
0.2
0.0
***
siCON
siGLS1
C
Ki67
Ki67/Nestin/DAPI
siCON
siGLS1
D
% of Ki67+ cells
50
40
30
20
10
0
**
siCON
siGLS1

Figure 4.7 GLS1 silencing increased NPC apoptosis. Human NPCs were transfected by control siRNA or GLS1 siRNA, then kept in growth media for 3 days. NPC apoptosis was determined by TUNEL assay and PARP cleavage. (A) Representative pictures of $TUNEL^+$ (green) cells in control siRNA- and siGLS1-transfected NPC cultures were shown. Nestin (red) was used to label NPCs. Nuclei (blue) were labeled with DAPI. (B) The percentage of $TUNEL^+$ cells was determined by counting the number of $TUNEL^+$ cells over the number of $DAPI^+$ cells in each microscope field. (C) Whole cell lysates were collected and NPC apoptosis was analyzed by Western blot for PARP cleavage. Beta-actin was used as loading control. (D) PARP cleavage levels were normalized as a ratio of cleaved PARP to actin after densitometric quantification of panel C and shown as fold change relative to control siRNA group. Images were acquired from a Nikon Eclipse TE2000E fluorescent microscope. Magnifications: 20X objective lens. Scale bar = 50 μm. Data are shown as means ± SEM of 10 fields in each experimental group for the three donors. * $P < 0.05$, compared with control siRNA group, N = 3.

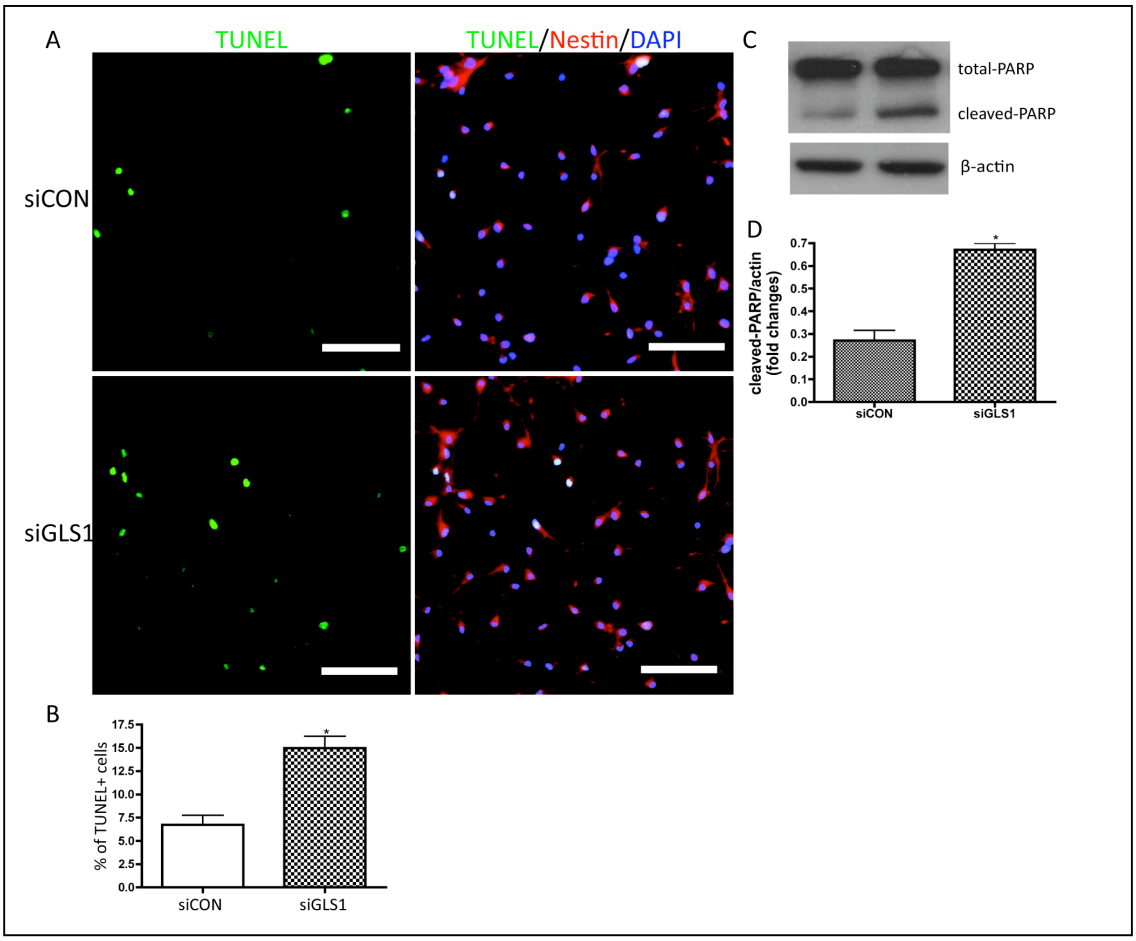
A
TUNEL
TUNEL/Nestin/DAPI
siCON
siGLS1
B
% of TUNEL+ cells
17.5
15.0
12.5
10.0
7.5
5.0
2.5
0.0
siCON
siGLS1
C
total-PARP
cleaved-PARP
β-actin
D
cleaved-PARP/actin (fold changes)
0.7
0.6
0.5
0.4
0.3
0.2
0.1
0.0
siCON
siGLS1

Chapter 5

General Summary and Future Directions

5.1 Summary and General Discussion

Cognitive impairment in HAND is a consequence of synaptic network damage in basal ganglia, cerebral cortex and hippocampus of HAND patients. Chronic neuroinflammation is a hallmark of HAND and a constitutive component of the pathogenesis of various neurodegenerative diseases including HAND. HIV-infected and immune-activated microglia and macrophages instigate brain inflammation and induce neuronal injury [27, 175, 176] through the production and release of various soluble neurotoxic factors including glutamate [30, 32, 37, 40-52]. Excess glutamate has the potential to induce extensive neuronal injury. Apart from microglial and macrophages, neurons play a critical role in the progression of brain inflammation as well. Proinflammatory cytokines TNF-α and IL-1β, which are typically elevated during neurodegenerative diseases, induced neuronal loss via the production and release of excess glutamate from neurons treated by the inflammatory cytokines [53]. Therefore, apart from the macrophage- and microglial-neuronal interaction, the neuronal-neuronal interaction has a major pathogenic role in the progressions of excitotoxicity and neuroinflammation through excess glutamate.

Our central objective focuses on the *in vivo* investigations of the primary glutamate-producing enzyme in CNS, GLS1, in the neuropathogenesis of HAND. Our laboratory has documented the abberant upregulation of GLS1 as a key pathogenic event in excess glutamate production and augmentation of brain inflammation and neurotoxicity in macrophages, microglia, and inflammatory neurons *in vitro* [50, 86, 90] [53]. This suggests that GLS1 may be a novel

therapeutic target for treating HAND. In order to further determine the pathogenic role of dysregulated GLS1, we have utilized integral animal models.

Our endeavor towads the central objective started with investigations of the regulation of GLS1 in the CNS of HAND murine models. Based on the revelation of elevated glutamate in the plasma and CSF of HIV-1-infected individuals, and the finding of the isoform-specific upregulation of GAC in postmortem brain tissues of HAND patients from previous studies, we hypothesize that there is strong association between GLS1 dysregulation with brain inflammation and cognitive impairment of HAND animals. In chapter 2, we show indeed that the GLS1 isoforms KGA and GAC were upregulated in the whole brain tissues of HIV-Tat Tg mouse and in the neuroinflammatory areas of HIVE-SCID mouse brains. Both HIV-Tat Tg mouse and HIVE-SCID mouse exhibited impairment in spatial learning and memory as revealed by MWM test. Importantly, the elevated GLS1 expression levels were significantly correlated with the increased CNS reactive astrogliosis and impaired spatial learning and memory of HIV-Tat Tg mouse. These data support our central hypothesis that there is strong association between GLS1 dysregulation with CNS inflammation and cognitive impariment of HAND mouse, suggesting that GLS1 dysregulation might contribute to HAND pathogenesis via mediating brain inflammation and excitotoxicity.

But whether there is a causal-effect relationship between GLS1 dysregulation and CNS disorder in HAND remains unclear. Therefore, we next investigate whether the brain-specific overexpression of GLS1 will have a causal

effect on neurotoxicity and synaptic damage leading to cognitive deteriorations in relevance to HAND pathogenesis. In chapter 3, we have generated the Nestin-GAC mouse which has the overexpression of GAC specific to brain. By characterizing the pathology and behaviors of Nestin-GAC mouse, we report that the brain-specific overexpression of GAC leads to hippocampal and cortical synaptic network damage, increased apoptosis and reactive astrogliosis in the hippocampi and cortices of mice. Importantly, we have found impairment of LTP in Nestin-GAC mice, further demonstrating the synaptic damage in hippocampi of these animals. Together, these results indicate for the first time that the overexpressed GAC in brain has a causal-effect relationship with prolonged brain inflammation and increased apoptosis, leading to neural network damage and finally resulting in the impairment of cognitive functions of animals. Many of these pathological changes including reactive astrogliosis, neuronal injury, and cognitive impairment of learning and memory are in parallel to those seen in HIV-Tat Tg mouse.

There are two major issues of the CNS pathological profiles of Nestin-GAC mouse remainning to be addressed. First, the regulation of glutamate receptors in Nestin-GAC mouse brains is an interesting and important question to be answered. Excitotoxicity is a commonplace in various neurodegenerative diseases including HAND. Overactivation of NMDA receptors is a major component of excitotoxicity. High-affinity NMDA receptor antagonist MK801 has blocked the toxicity from neurons treated by inflammatory cytokines TNF-α and IL-1β [53]. And more importantly, a low-to-moderate-affinity NMDA receptor

antagonist memantine has substantially abrogated neurotoxicity and largely mitigated the impairment of synaptic transmission and LTP [111]. Determining whether or not the neurotoxicity observed in Nestin-GAC mouse brains is via the overactivation of NMDA receptors will greatly facilitate our endeavor to further validate the resemblance of Nestin-GAC mouse as a novel HAND murine model.

Apart from the alterations of glutamate receptors, to study whether there are dysregulations or dysfunctions of glutamate transporters in Nestin-GAC mouse is of equal importance. Glutamate transporters are crucial for glutamate uptake and regulating glutamate homeostasis [135]. Therefore, they are important for buffering against excess glutamate-mediated excitotoxicity in the brain. Previous studies have revealed that deregulation or loss of function of glutamate transporters EAAT1 and EAAT2 on astrocytes are involved in neural inflammation and neurotoxicity [91, 136, 137]. EAAT2 expression levels were largely reduced on inflammatory cytokines-treated astrocytes via the upregulation of EAAT2 repressors by astrocyte-elevated gene 1 (AEG-1) [91]. Importantly, by enhancing EAAT1 activity the investigators are able to diminish neural damage and recover cognitive impairment [138, 139]. Therefore, we speculate that there can be dysregulations or loss-of-function of certain important glutamate transporters in Nestin-GAC mouse brain and the dysfunction of glutamate transporters exaggerate neuroinflammation and neuronal injury.

At current stage, we have determined the aberrant upregulation of GLS1 isoforms KGA and GAC in the whole brain tissues of HIV-Tat Tg mice, and we have found causality between GLS1 dysreulgation and neurotoxicity. One important question to be answered next is to document the expression profiles of KGA and GAC in different areas of HIV-Tat Tg mice brains. Unlike HIVE-SCID mice which have the HIV-1-infected MDM injected into the basil ganglia thus displaying most of the neuroinflammatory and neurotoxic responses there, HIV-Tat Tg mice carry the expression of Tat almost globally in CNS [96, 97]. Therefore, the spatial profile of GLS1 dysregulation in HIV-Tat Tg mouse CNS is expected to be discrepant from that in HIVE-SCID mouse CNS. Our previous data revealed that the majority of GLS1 aberrant upregulation in HIVE-SCID mouse CNS was found in neurons of the inflammatory area [53]. Studies on the brain areas that display most extensive and severe neural injury revealed that the neuronal damage is largely localized in the cerebellum and cortex of HIV-Tat Tg mouse [101]. Besides, relatively subtle neural damages including reductions in spine density and malformations of dendrites of neurons were found in the whole brain of HIV-Tat Tg mouse [106]. In consideration of developing GLS1 inhibitors for therapeutic purpose, it is important to locate the specific cell type and possibly the specific brain area that has the majority of GLS1 dysregulation in HIV-Tat Tg mouse.

Besides the spatial profile of GLS1 dysregulation, to know the temporal regulation profile of GLS1 in HIV-Tat Tg mouse is equally important. This will help to determine the sequence of inflammatory and neurotoxic events occuring

in HIV-Tat Tg mouse brain. It is interesting to dissect the effect of GLS1 dysregulation on brain excitotoxcity during different life stage. To achieve this, a tamoxifen-controlled temporal Tg mouse model is of great help.

Taken together, these results so far demonstrate the pathogenic role of the aberrantly-overexpressed brain GLS1 *in vivo* and suggest that dysregulated GLS1 under pathological conditions can be a novel therapeutic target for slowing or reversing HAND progressions and diminishing HAND-related complications. Because of that, to develop glutaminase inhibitors that target specific isoform of the enzyme and target specific cell types are one of the promising approaches for next step. Likewise, genetic approaches aiming to knock down the expression levels of glutaminase in specific types of cells have also been proposed as a promising therapeutic approach. However, great caution should be taken when targeting GLS1 in HAND therapy by genetical methods as we have identified an essential role of GLS1 in NPC functions. In chapter 4, we show that GLS1 isoforms were upregulated and correlated with MAP-2 during neuronal differentiation. siRNA silencing of GLS1 in NPCs impaired their subsequent neuronal differentiation. And we report reduced proliferation and increased apoptosis in GLS1-deficient cells. These results suggest that GLS1 is essential for the differentiation, proliferation and survival of NPC. Therefore, knocking down GLS1 globally in the brain is not applicable for therapeutic purpose. We will need to develop conditional knockout (cKO) mouse model with the expression of GLS1 temporally controlled in specific cell types.

5.2 Future directions

First, a lack of GLS1 cKO murine model has hindered further investigations of GLS1 functions in disease and in adult CNS due to early lethality of GLS1 KO mouse on the first day after birth. To establish GLS1 as a therapeutic target in HAND and further elucidate the underlying mechanisms, we will generate GLS1 cKO mouse with tamoxifen-inducible temporal control and GLS1 specifically deleted in macrophages and microglia by crossing the GLS1-floxed mice with Csf1R-CreER mice. The resulting Csf1R-GLS1$^{-/-}$ mouse will have GLS1 knocked out only in macrophages and microglia with the temporal control of tamoxifen. To investigate whether the deletion of GLS1 in macrophages and microglia can diminish or reverse the destructive effects of HIV-Tat expression in mouse brain, we will cross the Csf1R-GLS1$^{-/-}$ mouse with HIV-Tat Tg mouse. Behavioral assessment will be performed and subsequent pathological and electrophysiological characterizations will be done.

Second, we will evaluate the neuroprotective effect of GLS1 inhibitors in the HIV-Tat Tg mouse and GLS1-overexpression Tg mouse. Immediately after the induction of Tat or the GLS1 overexpression, GLS1 inhibitors will be continuously administered via intraperitoneal injection daily. Behavioral evaluations will be performed. Subsequently, brain tissues of HIV-Tat Tg mice or GLS1-overexpression Tg mice will be collected for pathological or physiological characterizations.

Third, we will carry out the genomic and proteomic analyses of regulations on glutamate transporters and the subunits of glutamate receptors in

our GLS1-overexpression Tg mouse and compare with that in HIV-Tat Tg mouse. Although NMDA receptors are known to be the major player in excitotoxicity and the resultant neurological disorders, alterations in glutamate transporters and other glutamate receptors also clearly have a role in it [91, 136, 137] [138, 139]. This will be of great help to expand the regulation profiles of key molecules involved in HAND progressions and identify new potential therapeutic targets apart from GLS1 itself and NMDA receptors. And next to that, the effort will be put on the evaluations of the neuroprotective potential by normalizing these newly-defined dysregulated molecuels.

5.3 Figures

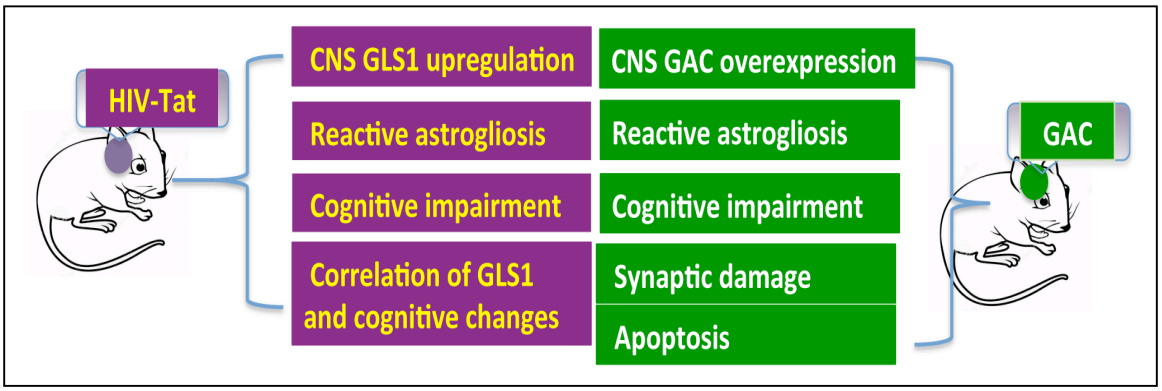

Figure 5.1 Summary of the pathogenic role of GLS1 dysregulation in HAND. GLS1 isoforms KGA and GAC were upregulated in the whole brain tissues of HIV-Tat Tg mouse. HIV-Tat Tg mouse exhibited impairment in spatial learning and memory as revealed by MWM test. Importantly, the elevated GLS1 expression levels were significantly correlated with the increased CNS reactive astrogliosis and impaired spatial learning and memory of HIV-Tat Tg mouse. Brain-specific overexpression of GAC leads to hippocampal and cortical synaptic network damage, increased apoptosis and reactive astrogliosis in the hippocampi and cortices of mice. We have found impairment of LTP in Nestin-GAC mice, further demonstrating the synaptic damage in hippocampi of these animals.

Acknowledgments

Sincerely, I would like to thank my advisor Dr. Jialin Zheng. Over the 5 years of PhD study, I have learned a lot from him. Without the generous support and encouraging guidance from him, I can hardly imagine the completion of my study or any possible achievement. He has helped me to cope numerous obstacles and difficulties during these years. His enthusiam, generosity, and perseverance have inspired me to not giving up and keep trying toward my goal. Specially, I would like to thank the direct supervisor of my projects, Dr. Yunlong Huang. Dr. Huang has provided me with terrific scientific guidance in every project of my study and has spent a great deal of time teaching me important technology or trouble shooting of problems. And I want to give thanks to Dr. Anna Dunaevsky, Dr. Jyothi Arikkath, Dr. Huangui Xiong and Dr. Wallace Thoreson for their valuable suggestions and continuous support to my carrer development.

Special thanks go to our collaborators. Dr. Norman Curthoys, Dr. Kurt Hauser and Dr. Yong Zhao have given us great suggestions and provided us with critical research tools. Their expertise are of great value to me and other members of our lab.

Many thanks go to current and former lab members of Zheng laboratory. Special thanks to Yuju Li and Dr. Lixia Zhao for being the first teachers when I started my lab work. They helped me from basic techniques, literature selection to presentation and writing skills. Many thanks to Dr. Qiang Chen, Dr. Yongxiang Wang, Dr. Hui Peng, Dr. Changhai Tian, Dr. Dongsheng Xu, Beiqing

Wu, Dr. Zenghan Tong, Runze Zhao, Miao He, Fang Liu, Dr. Dapeng Chen, Dr. Bing Zhu and Dr. Kangmu Ma for giving me good suggestions. We have had a lot of fun together and helped each other through these years.

I woule like to thank UNMC Advanced-Microscope Core, UNMC Mouse Genome Engineering Core and UNMC Comparative Medicine for providing fantastic technical support. And many thanks go to the Department of Pharmacology and Experimental Neuroscience, the China Scholarship Council, and the Asia Pacific Rim Development Program. Without their support, I would not be able to pursue my goal and complete my PhD study in UNMC.

Finally, I would like to thank my family, particularly to my beloved husband Xiaohuan Xia,. We were classmates in college and went to UNMC together five years ago. Life will be much harder if without his love and support. Also, I want to give thanks to my family in China, for their unconditional support through all these years. I do wish they could come to join my graduation ceremony.

Reference

1. Tan, I.L., et al., *HIV-associated opportunistic infections of the CNS*. Lancet Neurol, 2012. **11**(7): p. 605-17.
2. Antinori, A., et al., *Updated research nosology for HIV-associated neurocognitive disorders*. Neurology, 2007. **69**(18): p. 1789-99.
3. McArthur, J.C., B.J. Brew, and A. Nath, *Neurological complications of HIV infection*. Lancet Neurol, 2005. **4**(9): p. 543-55.
4. McArthur, J.C., et al., *Human immunodeficiency virus-associated dementia: an evolving disease*. J Neurovirol, 2003. **9**(2): p. 205-21.
5. McArthur, J.C., et al., *Human immunodeficiency virus-associated neurocognitive disorders: Mind the gap*. Ann Neurol, 2010. **67**(6): p. 699-714.
6. Letendre, S., et al., *Neurologic complications of HIV disease and their treatment*. Top HIV Med, 2007. **15**(2): p. 32-9.
7. Boisse, L., M.J. Gill, and C. Power, *HIV infection of the central nervous system: clinical features and neuropathogenesis*. Neurol Clin, 2008. **26**(3): p. 799-819, x.
8. Michaud, V., et al., *The dual role of pharmacogenetics in HIV treatment: mutations and polymorphisms regulating antiretroviral drug resistance and disposition*. Pharmacol Rev, 2012. **64**(3): p. 803-33.
9. Roquebert, B., et al., *Role of HIV-1 minority populations on resistance mutational pattern evolution and susceptibility to protease inhibitors*. AIDS, 2006. **20**(2): p. 287-9.

10. Varatharajan, L. and S.A. Thomas, *The transport of anti-HIV drugs across blood-CNS interfaces: summary of current knowledge and recommendations for further research*. Antiviral Res, 2009. **82**(2): p. A99-109.

11. Persidsky, Y. and L. Poluektova, *Immune privilege and HIV-1 persistence in the CNS*. Immunol Rev, 2006. **213**: p. 180-94.

12. Sharer, L.R., E.S. Cho, and L.G. Epstein, *Multinucleated giant cells and HTLV-III in AIDS encephalopathy*. Hum Pathol, 1985. **16**(8): p. 760.

13. Budka, H., *Multinucleated giant cells in brain: a hallmark of the acquired immune deficiency syndrome (AIDS)*. Acta Neuropathol, 1986. **69**(3-4): p. 253-8.

14. Masliah, E., et al., *Spectrum of human immunodeficiency virus-associated neocortical damage*. Ann Neurol, 1992. **32**(3): p. 321-9.

15. Persidsky, Y., et al., *An analysis of HIV-1-associated inflammatory products in brain tissue of humans and SCID mice with HIV-1 encephalitis*. J Neurovirol, 1997. **3**(6): p. 401-16.

16. Zink, W.E., et al., *Impaired spatial cognition and synaptic potentiation in a murine model of human immunodeficiency virus type 1 encephalitis*. J Neurosci, 2002. **22**(6): p. 2096-105.

17. Ketzler, S., et al., *Loss of neurons in the frontal cortex in AIDS brains*. Acta Neuropathol, 1990. **80**(1): p. 92-4.

18. Masliah, E., et al., *Selective neuronal vulnerability in HIV encephalitis*. J Neuropathol Exp Neurol, 1992. **51**(6): p. 585-93.

19. Williams, K., X. Alvarez, and A.A. Lackner, *Central nervous system perivascular cells are immunoregulatory cells that connect the CNS with the peripheral immune system*. Glia, 2001. **36**(2): p. 156-64.

20. Takahashi, K., et al., *Localization of HIV-1 in human brain using polymerase chain reaction/in situ hybridization and immunocytochemistry*. Ann Neurol, 1996. **39**(6): p. 705-11.

21. Thompson, K.A., et al., *Astrocyte specific viral strains in HIV dementia*. Ann Neurol, 2004. **56**(6): p. 873-7.

22. Ma, M., J.D. Geiger, and A. Nath, *Characterization of a novel binding site for the human immunodeficiency virus type 1 envelope protein gp120 on human fetal astrocytes*. J Virol, 1994. **68**(10): p. 6824-8.

23. Di Rienzo, A.M., et al., *Virological and molecular parameters of HIV-1 infection of human embryonic astrocytes*. Arch Virol, 1998. **143**(8): p. 1599-615.

24. Tornatore, C., et al., *HIV-1 infection of subcortical astrocytes in the pediatric central nervous system*. Neurology, 1994. **44**(3 Pt 1): p. 481-7.

25. Conant, K., et al., *In vivo and in vitro infection of the astrocyte by HIV-1*. Adv Neuroimmunol, 1994. **4**(3): p. 287-9.

26. Koenig, S., et al., *Detection of AIDS virus in macrophages in brain tissue from AIDS patients with encephalopathy*. Science, 1986. **233**(4768): p. 1089-93.

27. Gendelman, H.E., et al., *The neuropathogenesis of the AIDS dementia complex*. AIDS, 1997. **11 Suppl A**: p. S35-45.

28. Nath, A. and J. Geiger, *Neurobiological aspects of human immunodeficiency virus infection: neurotoxic mechanisms*. Prog Neurobiol, 1998. **54**(1): p. 19-33.

29. Zheng, J. and H.E. Gendelman, *The HIV-1 associated dementia complex: a metabolic encephalopathy fueled by viral replication in mononuclear phagocytes*. Curr Opin Neurol, 1997. **10**(4): p. 319-25.

30. Li, W., et al., *NMDA receptor activation by HIV-Tat protein is clade dependent*. J Neurosci, 2008. **28**(47): p. 12190-8.

31. Conant, K., et al., *Induction of monocyte chemoattractant protein-1 in HIV-1 Tat-stimulated astrocytes and elevation in AIDS dementia*. Proc Natl Acad Sci U S A, 1998. **95**(6): p. 3117-21.

32. Giulian, D., et al., *The envelope glycoprotein of human immunodeficiency virus type 1 stimulates release of neurotoxins from monocytes*. Proc Natl Acad Sci U S A, 1993. **90**(7): p. 2769-73.

33. Huang, Y., et al., *The role of TNF related apoptosis-inducing ligand in neurodegenerative diseases*. Cell Mol Immunol, 2005. **2**(2): p. 113-22.

34. Viviani, B., et al., *Cytokines role in neurodegenerative events*. Toxicol Lett, 2004. **149**(1-3): p. 85-9.

35. Smith, J.A., et al., *Role of pro-inflammatory cytokines released from microglia in neurodegenerative diseases*. Brain Res Bull, 2012. **87**(1): p. 10-20.

36. Takikita, S., et al., *Neuronal apoptosis mediated by IL-1 beta expression in viral encephalitis caused by a neuroadapted strain of the mumps virus (Kilham Strain) in hamsters*. Exp Neurol, 2001. **172**(1): p. 47-59.

37. Sui, Z., et al., *Functional synergy between CD40 ligand and HIV-1 Tat contributes to inflammation: implications in HIV type 1 dementia*. J Immunol, 2007. **178**(5): p. 3226-36.

38. Glass, J.D. and R.T. Johnson, *Human immunodeficiency virus and the brain*. Annu Rev Neurosci, 1996. **19**: p. 1-26.

39. Boutin, H., et al., *Role of IL-1alpha and IL-1beta in ischemic brain damage*. J Neurosci, 2001. **21**(15): p. 5528-34.

40. Eggert, D., et al., *Development of a platelet-activating factor antagonist for HIV-1 associated neurocognitive disorders*. J Neuroimmunol, 2009. **213**(1-2): p. 47-59.

41. Perry, S.W., et al., *Platelet-activating factor receptor activation. An initiator step in HIV-1 neuropathogenesis*. J Biol Chem, 1998. **273**(28): p. 17660-4.

42. Tong, N., et al., *Activation of glycogen synthase kinase 3 beta (GSK-3beta) by platelet activating factor mediates migration and cell death in cerebellar granule neurons*. Eur J Neurosci, 2001. **13**(10): p. 1913-22.

43. Nishida, K., et al., *Increased brain levels of platelet-activating factor in a murine acquired immune deficiency syndrome are NMDA receptor-mediated*. J Neurochem, 1996. **66**(1): p. 433-5.

44. Matusevicius, D., et al., *Multiple sclerosis: the proinflammatory cytokines lymphotoxin-alpha and tumour necrosis factor-alpha are upregulated in cerebrospinal fluid mononuclear cells*. J Neuroimmunol, 1996. **66**(1-2): p. 115-23.

45. Navikas, V., et al., *Increased interleukin-6 mRNA expression in blood and cerebrospinal fluid mononuclear cells in multiple sclerosis*. J Neuroimmunol, 1996. **64**(1): p. 63-9.

46. Meda, L., et al., *Proinflammatory profile of cytokine production by human monocytes and murine microglia stimulated with beta-amyloid[25-35]*. J Neuroimmunol, 1999. **93**(1-2): p. 45-52.

47. Genis, P., et al., *Cytokines and arachidonic metabolites produced during human immunodeficiency virus (HIV)-infected macrophage-astroglia interactions: implications for the neuropathogenesis of HIV disease*. J Exp Med, 1992. **176**(6): p. 1703-18.

48. Dawson, V.L. and T.M. Dawson, *Nitric oxide in neurodegeneration*. Prog Brain Res, 1998. **118**: p. 215-29.

49. Adamson, D.C., et al., *Immunologic NO synthase: elevation in severe AIDS dementia and induction by HIV-1 gp41*. Science, 1996. **274**(5294): p. 1917-21.

50. Zhao, J., et al., *Mitochondrial glutaminase enhances extracellular glutamate production in HIV-1-infected macrophages: linkage to HIV-1 associated dementia*. J Neurochem, 2004. **88**(1): p. 169-80.

51. Giulian, D., K. Vaca, and C.A. Noonan, *Secretion of neurotoxins by mononuclear phagocytes infected with HIV-1*. Science, 1990. **250**(4987): p. 1593-6.

52. Kaul, M., G.A. Garden, and S.A. Lipton, *Pathways to neuronal injury and apoptosis in HIV-associated dementia*. Nature, 2001. **410**(6831): p. 988-94.

53. Ye, L., et al., *IL-1beta and TNF-alpha induce neurotoxicity through glutamate production: a potential role for neuronal glutaminase*. J Neurochem, 2013. **125**(6): p. 897-908.

54. Erecinska, M. and I.A. Silver, *Metabolism and role of glutamate in mammalian brain*. Prog Neurobiol, 1990. **35**(4): p. 245-96.

55. Komuro, H. and P. Rakic, *Intracellular Ca2+ fluctuations modulate the rate of neuronal migration*. Neuron, 1996. **17**(2): p. 275-85.

56. LoTurco, J.J., M.G. Blanton, and A.R. Kriegstein, *Initial expression and endogenous activation of NMDA channels in early neocortical development*. J Neurosci, 1991. **11**(3): p. 792-9.

57. McEntee, W.J. and T.H. Crook, *Glutamate: its role in learning, memory, and the aging brain*. Psychopharmacology (Berl), 1993. **111**(4): p. 391-401.

58. Lipton, S.A., M. Yeh, and E.B. Dreyer, *Update on current models of HIV-related neuronal injury: platelet-activating factor, arachidonic acid and nitric oxide*. Adv Neuroimmunol, 1994. **4**(3): p. 181-8.

59. Haughey, N.J. and M.P. Mattson, *Calcium dysregulation and neuronal apoptosis by the HIV-1 proteins Tat and gp120*. J Acquir Immune Defic Syndr, 2002. **31 Suppl 2**: p. S55-61.

60. Foga, I.O., et al., *Antioxidants and dipyridamole inhibit HIV-1 gp120-induced free radical-based oxidative damage to human monocytoid cells*. J Acquir Immune Defic Syndr Hum Retrovirol, 1997. **16**(4): p. 223-9.

61. Haughey, N.J., et al., *Perturbation of sphingolipid metabolism and ceramide production in HIV-dementia*. Ann Neurol, 2004. **55**(2): p. 257-67.

62. Lipton, S.A., *Memantine prevents HIV coat protein-induced neuronal injury in vitro*. Neurology, 1992. **42**(7): p. 1403-5.

63. Muller, W.E., et al., *gp120 of HIV-1 induces apoptosis in rat cortical cell cultures: prevention by memantine*. Eur J Pharmacol, 1992. **226**(3): p. 209-14.

64. Nath, A., et al., *Synergistic neurotoxicity by human immunodeficiency virus proteins Tat and gp120: protection by memantine*. Ann Neurol, 2000. **47**(2): p. 186-94.

65. Rao, V.L., et al., *Traumatic brain injury down-regulates glial glutamate transporter (GLT-1 and GLAST) proteins in rat brain*. J Neurochem, 1998. **70**(5): p. 2020-7.

66. Benveniste, H., *Glutamate, microdialysis, and cerebral ischemia: lost in translation?* Anesthesiology, 2009. **110**(2): p. 422-5.

67. Xu, G.Y., et al., *Concentrations of glutamate released following spinal cord injury kill oligodendrocytes in the spinal cord*. Exp Neurol, 2004. **187**(2): p. 329-36.

68. Kanellopoulos, G.K., et al., *White matter injury in spinal cord ischemia: protection by AMPA/kainate glutamate receptor antagonism*. Stroke, 2000. **31**(8): p. 1945-52.

69. Zoia, C.P., et al., *Fibroblast glutamate transport in aging and in AD: correlations with disease severity*. Neurobiol Aging, 2005. **26**(6): p. 825-32.

70. Killestein, J., N.F. Kalkers, and C.H. Polman, *Glutamate inhibition in MS: the neuroprotective properties of riluzole*. J Neurol Sci, 2005. **233**(1-2): p. 113-5.

71. Holcomb, T., et al., *Isolation, characterization and expression of a human brain mitochondrial glutaminase cDNA*. Brain Res Mol Brain Res, 2000. **76**(1): p. 56-63.

72. Marquez, J., et al., *Mammalian glutaminase isozymes in brain*. Metab Brain Dis, 2013. **28**(2): p. 133-7.

73. Erdmann, N.B., N.P. Whitney, and J. Zheng, *Potentiation of Excitotoxicity in HIV-1 Associated Dementia and the Significance of Glutaminase*. Clin Neurosci Res, 2006. **6**(5): p. 315-328.

74. Mock, B., et al., *A glutaminase (gis) gene maps to mouse chromosome 1, rat chromosome 9, and human chromosome 2*. Genomics, 1989. **5**(2): p. 291-7.

75. Elgadi, K.M., et al., *Cloning and analysis of unique human glutaminase isoforms generated by tissue-specific alternative splicing*. Physiol Genomics, 1999. **1**(2): p. 51-62.

76. Porter, L.D., et al., *Complexity and species variation of the kidney-type glutaminase gene*. Physiol Genomics, 2002. **9**(3): p. 157-66.

77. Chua, J.J., et al., *The architecture of an excitatory synapse*. J Cell Sci, 2010. **123**(Pt 6): p. 819-23.

78. Boyken, J., et al., *Molecular profiling of synaptic vesicle docking sites reveals novel proteins but few differences between glutamatergic and GABAergic synapses*. Neuron, 2013. **78**(2): p. 285-97.

79. Karakas, E., M.C. Regan, and H. Furukawa, *Emerging structural insights into the function of ionotropic glutamate receptors*. Trends Biochem Sci, 2015. **40**(6): p. 328-337.

80. Golubeva, A.V., et al., *Metabotropic Glutamate Receptors in Central Nervous System Diseases*. Curr Drug Targets, 2015.

81. Gegelashvili, G. and A. Schousboe, *Cellular distribution and kinetic properties of high-affinity glutamate transporters*. Brain Res Bull, 1998. **45**(3): p. 233-8.

82. Rose, C.F., A. Verkhratsky, and V. Parpura, *Astrocyte glutamine synthetase: pivotal in health and disease*. Biochem Soc Trans, 2013. **41**(6): p. 1518-24.

83. Chaudhry, F.A., et al., *Glutamine uptake by neurons: interaction of protons with system a transporters*. J Neurosci, 2002. **22**(1): p. 62-72.

84. Huang, Y., et al., *Glutaminase dysregulation in HIV-1-infected human microglia mediates neurotoxicity: relevant to HIV-1-associated neurocognitive disorders*. J Neurosci, 2011. **31**(42): p. 15195-204.

85. Tian, C., et al., *Mitochondrial glutaminase release contributes to glutamate-mediated neurotoxicity during human immunodeficiency virus-1 infection*. J Neuroimmune Pharmacol, 2012. **7**(3): p. 619-28.

86. Tian, C., et al., *HIV-infected macrophages mediate neuronal apoptosis through mitochondrial glutaminase*. J Neurochem, 2008. **105**(3): p. 994-1005.

87. Zhao, L., et al., *Interferon-alpha regulates glutaminase 1 promoter through STAT1 phosphorylation: relevance to HIV-1 associated neurocognitive disorders*. PLoS One, 2012. **7**(3): p. e32995.

88. Zhao, L., Y. Huang, and J. Zheng, *STAT1 regulates human glutaminase 1 promoter activity through multiple binding sites in HIV-1 infected macrophages*. PLoS One, 2013. **8**(9): p. e76581.

89. Murry, C.E. and G. Keller, *Differentiation of embryonic stem cells to clinically relevant populations: lessons from embryonic development*. Cell, 2008. **132**(4): p. 661-80.

90. Erdmann, N., et al., *In vitro glutaminase regulation and mechanisms of glutamate generation in HIV-1-infected macrophage*. J Neurochem, 2009. **109**(2): p. 551-61.

91. Vartak-Sharma, N., et al., *Astrocyte elevated gene-1 is a novel modulator of HIV-1-associated neuroinflammation via regulation of nuclear factor-kappaB signaling and excitatory amino acid transporter-2 repression*. J Biol Chem, 2014. **289**(28): p. 19599-612.

92. Emdad, L., et al., *Astrocyte elevated gene-1: recent insights into a novel gene involved in tumor progression, metastasis and neurodegeneration*. Pharmacol Ther, 2007. **114**(2): p. 155-70.

93. Aoyama, K. and T. Nakaki, *Neuroprotective properties of the excitatory amino acid carrier 1 (EAAC1)*. Amino Acids, 2013. **45**(1): p. 133-42.

94. Jaeger, L.B. and A. Nath, *Modeling HIV-associated neurocognitive disorders in mice: new approaches in the changing face of HIV neuropathogenesis*. Dis Model Mech, 2012. **5**(3): p. 313-22.

95. Johnson, T.P., et al., *Induction of IL-17 and nonclassical T-cell activation by HIV-Tat protein*. Proc Natl Acad Sci U S A, 2013. **110**(33): p. 13588-93.

96. Fitting, S., et al., *Synaptic dysfunction in the hippocampus accompanies learning and memory deficits in human immunodeficiency virus type-1 Tat transgenic mice*. Biol Psychiatry, 2013. **73**(5): p. 443-53.

97. Bruce-Keller, A.J., et al., *Morphine causes rapid increases in glial activation and neuronal injury in the striatum of inducible HIV-1 Tat transgenic mice*. Glia, 2008. **56**(13): p. 1414-27.

98. Schneider, J., et al., *Shedding and interspecies type sero-reactivity of the envelope glycopolypeptide gp120 of the human immunodeficiency virus*. J Gen Virol, 1986. **67 (Pt 11)**: p. 2533-8.

99. Garza, H.H., Jr., O. Prakash, and D.J. Carr, *Aberrant regulation of cytokines in HIV-1 TAT72-transgenic mice*. J Immunol, 1996. **156**(10): p. 3631-7.

100. Choi, J., et al., *Molecular mechanism of decreased glutathione content in human immunodeficiency virus type 1 Tat-transgenic mice*. J Biol Chem, 2000. **275**(5): p. 3693-8.

101. Kim, B.O., et al., *Neuropathologies in transgenic mice expressing human immunodeficiency virus type 1 Tat protein under the regulation of the astrocyte-specific glial fibrillary acidic protein promoter and doxycycline*. Am J Pathol, 2003. **162**(5): p. 1693-707.

102. Eggert, D., et al., *Neuroprotective activities of CEP-1347 in models of neuroAIDS*. J Immunol, 2010. **184**(2): p. 746-56.

103. Persidsky, Y., et al., *Human immunodeficiency virus encephalitis in SCID mice*. Am J Pathol, 1996. **149**(3): p. 1027-53.

104. Gendelman, H.E., et al., *Efficient isolation and propagation of human immunodeficiency virus on recombinant colony-stimulating factor 1-treated monocytes*. J Exp Med, 1988. **167**(4): p. 1428-41.

105. Ferrarese, C., et al., *Increased glutamate in CSF and plasma of patients with HIV dementia*. Neurology, 2001. **57**(4): p. 671-5.

106. Fitting, S., et al., *Interactive comorbidity between opioid drug abuse and HIV-1 Tat: chronic exposure augments spine loss and sublethal dendritic pathology in striatal neurons*. Am J Pathol, 2010. **177**(3): p. 1397-410.

107. Kraft-Terry, S.D., et al., *A coat of many colors: neuroimmune crosstalk in human immunodeficiency virus infection*. Neuron, 2009. **64**(1): p. 133-45.

108. Jiang, Z.G., et al., *Glutamate is a mediator of neurotoxicity in secretions of activated HIV-1-infected macrophages*. J Neuroimmunol, 2001. **117**(1-2): p. 97-107.

109. Lin, T., et al., *A central nervous system specific mouse model for thanatophoric dysplasia type II*. Hum Mol Genet, 2003. **12**(21): p. 2863-71.

110. Zhu, B., et al., *CXCL12 enhances human neural progenitor cell survival through a CXCR7- and CXCR4-mediated endocytotic signaling pathway*. Stem Cells, 2012. **30**(11): p. 2571-83.

111. Anderson, E.R., H.E. Gendelman, and H. Xiong, *Memantine protects hippocampal neuronal function in murine human immunodeficiency virus type 1 encephalitis*. J Neurosci, 2004. **24**(32): p. 7194-8.

112. Anderson, E.R., et al., *Hippocampal synaptic dysfunction in a murine model of human immunodeficiency virus type 1 encephalitis*. Neuroscience, 2003. **118**(2): p. 359-69.

113. Lesburgueres, E., et al., *Early tagging of cortical networks is required for the formation of enduring associative memory*. Science, 2011. **331**(6019): p. 924-8.

114. Kingwell, K., *Memory: Tagging in the cortex*. Nat Rev Neurosci, 2011. **12**(4): p. 188.

115. Frey, U. and R.G. Morris, *Synaptic tagging: implications for late maintenance of hippocampal long-term potentiation*. Trends Neurosci, 1998. **21**(5): p. 181-8.

116. Frey, U. and R.G. Morris, *Synaptic tagging and long-term potentiation*. Nature, 1997. **385**(6616): p. 533-6.

117. Ross, R.S. and H. Eichenbaum, *Dynamics of hippocampal and cortical activation during consolidation of a nonspatial memory*. J Neurosci, 2006. **26**(18): p. 4852-9.

118. Clark, R.E., et al., *Anterograde amnesia and temporally graded retrograde amnesia for a nonspatial memory task after lesions of hippocampus and subiculum*. J Neurosci, 2002. **22**(11): p. 4663-9.

119. Alvarez, P., et al., *Differential effects of damage within the hippocampal region on memory for a natural, nonspatial Odor-Odor Association*. Learn Mem, 2001. **8**(2): p. 79-86.

120. Sweatt, J.D., *Neuroscience. Creating stable memories*. Science, 2011. **331**(6019): p. 869-70.

121. Yeckel, M.F. and T.W. Berger, *Spatial distribution of potentiated synapses in hippocampus: dependence on cellular mechanisms and network properties*. J Neurosci, 1998. **18**(1): p. 438-50.

122. O'Mara, S.M., S. Commins, and M. Anderson, *Synaptic plasticity in the hippocampal area CA1-subiculum projection: implications for theories of memory*. Hippocampus, 2000. **10**(4): p. 447-56.

123. Song, D., et al., *Nonlinear dynamic modeling of spike train transformations for hippocampal-cortical prostheses*. IEEE Trans Biomed Eng, 2007. **54**(6 Pt 1): p. 1053-66.

124. Kobayashi, M., et al., *Hippocalcin-deficient mice display a defect in cAMP response element-binding protein activation associated with impaired spatial and associative memory*. Neuroscience, 2005. **133**(2): p. 471-84.

125. Zelcer, I., et al., *A cellular correlate of learning-induced metaplasticity in the hippocampus*. Cereb Cortex, 2006. **16**(4): p. 460-8.

126. Zhao, M.G., et al., *Deficits in trace fear memory and long-term potentiation in a mouse model for fragile X syndrome*. J Neurosci, 2005. **25**(32): p. 7385-92.

127. Delint-Ramirez, I., P. Salcedo-Tello, and F. Bermudez-Rattoni, *Spatial memory formation induces recruitment of NMDA receptor and PSD-95 to synaptic lipid rafts*. J Neurochem, 2008. **106**(4): p. 1658-68.

128. Zhang, Z., et al., *Bell-shaped D-serine actions on hippocampal long-term depression and spatial memory retrieval*. Cereb Cortex, 2008. **18**(10): p. 2391-401.

129. Nakashiba, T., et al., *Transgenic inhibition of synaptic transmission reveals role of CA3 output in hippocampal learning*. Science, 2008. **319**(5867): p. 1260-4.

130. Magnusson, K.R., et al., *Age-related declines in a two-day reference memory task are associated with changes in NMDA receptor subunits in mice*. BMC Neurosci, 2007. **8**: p. 43.

131. Rolls, E.T., *Hippocampo-cortical and cortico-cortical backprojections*. Hippocampus, 2000. **10**(4): p. 380-8.

132. Naie, K. and D. Manahan-Vaughan, *Regulation by metabotropic glutamate receptor 5 of LTP in the dentate gyrus of freely moving rats: relevance for learning and memory formation*. Cereb Cortex, 2004. **14**(2): p. 189-98.

133. Manahan-Vaughan, D. and K.H. Braunewell, *The metabotropic glutamate receptor, mGluR5, is a key determinant of good and bad spatial learning performance and hippocampal synaptic plasticity*. Cereb Cortex, 2005. **15**(11): p. 1703-13.

134. Brim, B.L., et al., *Memory in aged mice is rescued by enhanced expression of the GluN2B subunit of the NMDA receptor*. Behav Brain Res, 2013. **238**: p. 211-26.

135. Tzingounis, A.V. and J.I. Wadiche, *Glutamate transporters: confining runaway excitation by shaping synaptic transmission*. Nat Rev Neurosci, 2007. **8**(12): p. 935-47.

136. Masliah, E., et al., *Deficient glutamate transport is associated with neurodegeneration in Alzheimer's disease*. Ann Neurol, 1996. **40**(5): p. 759-66.

137. Blasco, H., et al., *The glutamate hypothesis in ALS: pathophysiology and drug development*. Curr Med Chem, 2014. **21**(31): p. 3551-75.

138. Liang, J., et al., *Excitatory amino acid transporter expression by astrocytes is neuroprotective against microglial excitotoxicity*. Brain Res, 2008. **1210**: p. 11-9.

139. Sulkowski, G., et al., *Modulation of glutamate transport and receptor binding by glutamate receptor antagonists in EAE rat brain*. PLoS One, 2014. **9**(11): p. e113954.

140. McKay, R., *Stem cells in the central nervous system*. Science, 1997. **276**(5309): p. 66-71.

141. Jessell, T.M. and J.R. Sanes, *Development. The decade of the developing brain*. Curr Opin Neurobiol, 2000. **10**(5): p. 599-611.

142. Kintner, C., *Neurogenesis in embryos and in adult neural stem cells*. J Neurosci, 2002. **22**(3): p. 639-43.

143. Lie, D.C., et al., *Neurogenesis in the adult brain: new strategies for central nervous system diseases*. Annu Rev Pharmacol Toxicol, 2004. **44**: p. 399-421.

144. Alvarez-Buylla, A., B. Seri, and F. Doetsch, *Identification of neural stem cells in the adult vertebrate brain*. Brain Res Bull, 2002. **57**(6): p. 751-8.

145. Bergstrom, T. and K. Forsberg-Nilsson, *Neural stem cells: brain building blocks and beyond*. Ups J Med Sci, 2012. **117**(2): p. 132-42.

146. Nogues, X., et al., *Functions for adult neurogenesis in memory: an introduction to the neurocomputational approach and to its contribution*. Behav Brain Res, 2012. **227**(2): p. 418-25.

147. Ming, G.L. and H. Song, *Adult neurogenesis in the mammalian central nervous system*. Annu Rev Neurosci, 2005. **28**: p. 223-50.

148. Parent, J.M., *Injury-induced neurogenesis in the adult mammalian brain*. Neuroscientist, 2003. **9**(4): p. 261-72.

149. Arvidsson, A., et al., *Neuronal replacement from endogenous precursors in the adult brain after stroke*. Nat Med, 2002. **8**(9): p. 963-70.

150. Nakatomi, H., et al., *Regeneration of hippocampal pyramidal neurons after ischemic brain injury by recruitment of endogenous neural progenitors*. Cell, 2002. **110**(4): p. 429-41.

151. Whitney, N.P., et al., *Inflammation mediates varying effects in neurogenesis: relevance to the pathogenesis of brain injury and neurodegenerative disorders*. J Neurochem, 2009. **108**(6): p. 1343-59.

152. Doetsch, F. and C. Scharff, *Challenges for brain repair: insights from adult neurogenesis in birds and mammals*. Brain Behav Evol, 2001. **58**(5): p. 306-22.

153. Limke, T.L. and M.S. Rao, *Neural stem cells in aging and disease*. J Cell Mol Med, 2002. **6**(4): p. 475-96.

154. Kvamme, E., B. Roberg, and I.A. Torgner, *Phosphate-activated glutaminase and mitochondrial glutamine transport in the brain*. Neurochem Res, 2000. **25**(9-10): p. 1407-19.

155. Schlett, K., *Glutamate as a modulator of embryonic and adult neurogenesis*. Curr Top Med Chem, 2006. **6**(10): p. 949-60.

156. Suzuki, M., et al., *Glutamate enhances proliferation and neurogenesis in human neural progenitor cell cultures derived from the fetal cortex*. Eur J Neurosci, 2006. **24**(3): p. 645-53.

157. Whitney, N.P., et al., *Calcium-permeable AMPA receptors containing Q/R-unedited GluR2 direct human neural progenitor cell differentiation to neurons*. FASEB J, 2008. **22**(8): p. 2888-900.

158. Luk, K.C., T.E. Kennedy, and A.F. Sadikot, *Glutamate promotes proliferation of striatal neuronal progenitors by an NMDA receptor-mediated mechanism*. J Neurosci, 2003. **23**(6): p. 2239-50.

159. Cameron, H.A., B.S. McEwen, and E. Gould, *Regulation of adult neurogenesis by excitatory input and NMDA receptor activation in the dentate gyrus*. J Neurosci, 1995. **15**(6): p. 4687-92.

160. Haydar, T.F., et al., *Differential modulation of proliferation in the neocortical ventricular and subventricular zones*. J Neurosci, 2000. **20**(15): p. 5764-74.

161. Peng, H., et al., *Stromal cell-derived factor 1-mediated CXCR4 signaling in rat and human cortical neural progenitor cells*. J Neurosci Res, 2004. **76**(1): p. 35-50.

162. Peng, H., et al., *HIV-1-infected and/or immune activated macrophages regulate astrocyte SDF-1 production through IL-1beta*. Glia, 2006. **54**(6): p. 619-29.

163. Velletri, T., et al., *GLS2 is transcriptionally regulated by p73 and contributes to neuronal differentiation*. Cell Cycle, 2013. **12**(22): p. 3564-73.

164. Erickson, J.W. and R.A. Cerione, *Glutaminase: a hot spot for regulation of cancer cell metabolism?* Oncotarget, 2010. **1**(8): p. 734-40.

165. Wang, J.B., et al., *Targeting mitochondrial glutaminase activity inhibits oncogenic transformation*. Cancer Cell, 2010. **18**(3): p. 207-19.

166. Seltzer, M.J., et al., *Inhibition of glutaminase preferentially slows growth of glioma cells with mutant IDH1*. Cancer Res, 2010. **70**(22): p. 8981-7.

167. Xiang, Y., et al., *Targeted inhibition of tumor-specific glutaminase diminishes cell-autonomous tumorigenesis*. J Clin Invest, 2015. **125**(6): p. 2293-306.

168. Masson, J., et al., *Mice lacking brain/kidney phosphate-activated glutaminase have impaired glutamatergic synaptic transmission, altered breathing,*

disorganized goal-directed behavior and die shortly after birth. J Neurosci, 2006. **26**(17): p. 4660-71.

169. Gaisler-Salomon, I., et al., *Glutaminase-deficient mice display hippocampal hypoactivity, insensitivity to pro-psychotic drugs and potentiated latent inhibition: relevance to schizophrenia*. Neuropsychopharmacology, 2009. **34**(10): p. 2305-22.

170. LoTurco, J.J., et al., *GABA and glutamate depolarize cortical progenitor cells and inhibit DNA synthesis*. Neuron, 1995. **15**(6): p. 1287-98.

171. Olney, J.W., *Glutamate-induced neuronal necrosis in the infant mouse hypothalamus. An electron microscopic study*. J Neuropathol Exp Neurol, 1971. **30**(1): p. 75-90.

172. Choi, D.W., *Glutamate neurotoxicity and diseases of the nervous system*. Neuron, 1988. **1**(8): p. 623-34.

173. McCall, A., et al., *Monosodium glutamate neurotoxicity, hyperosmolarity, and blood-brain barrier dysfunction*. Neurobehav Toxicol, 1979. **1**(4): p. 279-83.

174. Newcomb, R., et al., *Increased production of extracellular glutamate by the mitochondrial glutaminase following neuronal death*. J Biol Chem, 1997. **272**(17): p. 11276-82.

175. Bredesen, D.E., *Neural apoptosis*. Ann Neurol, 1995. **38**(6): p. 839-51.

176. Yuan, J. and B.A. Yankner, *Apoptosis in the nervous system*. Nature, 2000. **407**(6805): p. 802-9.